Application of an Energy Based Security Method to Voltage Instability in Electrical Power Systems

by

Thomas Jeffrey Overbye

A dissertation submitted in partial fulfillment

of the requirements for the degree of

Doctor of Philosophy

(Electrical and Computer Engineering)

at the

UNIVERSITY OF WISCONSIN - MADISON

1991

Application of an Energy Based Security Method to Voltage Instability in Electrical Power Systems

by

Thomas Jeffrey Overbye

A dissertation submitted in partial fulfillment

of the requirements for the degree of

Doctor of Philosophy

(Electrical and Computer Engineering)

at the

UNIVERSITY OF WISCONSIN - MADISON

1991

Abstract

This thesis proposes a method using an energy function approach to assess the vulnerability of an electrical power system to voltage collapse. This approach is based upon the use of Lyapunov's direct method, which provides a means for determining the stability of systems of nonlinear differential equations, such as the power system models employed here. A closed form energy function is first defined for a power system dynamic model, which includes voltage dependent reactive loads, reactive power limits on generators, and transmission line losses. The voltage stability of a particular portion of the power system is quantified by using this energy function to evaluate the difference between the system's normal operating point and one of the system unstable equilibrium points (UEPs). These UEPs correspond to the alternative solutions of the power flow equations. The energy difference associated with a UEP then provides a measure of the voltage security in particular areas of the system. Since in a large system there may be a number of separate areas simultaneously vulnerable to voltage collapse, separate voltage security measures would be needed for each.

The energy differences are shown to change in a manner proportional to changes in the power system operating point, and in particular do not exhibit discontinuities when generators reach their reactive power limits. At least one energy difference goes to zero as the system approaches the point of voltage collapse. Thus by monitoring the energy differences the system voltage security can be quantified. Additionally, a method for improving system voltage security is presented using the sensitivities of the closed form energy differences to various system controls. Lastly, an algorithm is presented for rapidly determining these alternative solutions with low associated energy differences, thus allowing for on-line use. Application of the method and its computational aspects are examined on systems of up to 415 buses.

Acknowledgements

I would first of all like to express my appreciation to Professor Christopher L. DeMarco for his help in all regards. I have been extremely fortunate to have had the opportunity to work with him. His help and understanding have not only made this thesis possible, but have also made my graduate studies here at the University of Wisconsin a very enjoyable experience.

I would also like to extend my appreciation to professors Dobson and Alvarado. Their suggestions and comments during the time spent researching and writing this thesis have been most helpful.

I would like to thank my fellow graduate students in the power and control groups for their help and assistance over the years. Studying and working with them has further helped to make my graduate studies both a beneficial and enjoyable experience.

I am grateful to Madison Gas and Electric company for employment over the last ten years, and to my colleagues there for both their friendship, and for their insights into the operation of an actual power system.

I would also like to extend my thanks to my other friends outside of school and work, and to my family. Last, but certainly not least, I extend my thanks to the Lord Jesus Christ for all things, and to whom all praise ultimately belongs.

Table of Contents

Chapter 1 - Introduction

1.1 Voltage Instability in Power Systems

The availability of reliable and economical electrical power is vitally important to the well being of major industrial economies. Over the last few decades electrical systems throughout the industrialized world have changed from relatively localized systems to large interconnected systems with tens or hundreds of millions of customers who often receive power from generators hundreds or even thousands of miles distant. This high degree of interconnection makes it essential that the high voltage transmission system, used to transmit this power, be operated in both a secure and economical manner. An operating point is classified as secure when the system can adequately supply the necessary power to all customers even in the event of statistically plausible contingencies (such as transmission line outages or loss of generators). The system security requirement, however, is often contradictory to economically optimal operation, which can require operation of the system near its limit in order to take advantage of distant, low cost generation.

Traditionally the balancing of system security with economical operation has presented utility operators and planners with the two problems of thermal loading and angular (or transient) stability. The

former problem requires that the electrical current on each individual transmission line or transformer be less than a limit derived from the thermal characteristics of the device and the ambient conditions. The latter problem requires that the system be able to return to a secure operating point following a large scale disturbance (e.g. loss of a generator). Many analysis techniques, such as optimal power flow and transient stability programs, have been developed to predict the impact of these problems. However over the last few years, as the operating conditions for large power systems have evolved, another type of problem has been observed with increasing frequency. This phenomena is often referred to as voltage instability or voltage collapse.

Voltage instability is characterized by the voltages throughout a large portion of the high voltage transmission system gradually declining over a period of minutes to hours. Eventually, if system loading continues to increase, the voltages suddenly collapse, resulting in either local or system-wide blackouts. To illustrate the basic mechanics of voltage collapse, consider the simple system shown in Figure 1-1. The region on the left represents an area of the power system with excess generation capacity, while the region on the right is characterized by high demand (load). Power is therefore transferred through the transmission lines connecting the regions. This system is a rough equivalent to many large power systems, which depend upon

distant generation to serve large urban loads. The voltage response of the system could be represented approximately by using a two bus radial system model consisting of a generator bus supplying a load bus through an equivalent transmission line. Figure 1-2 shows the voltage variation at the load bus for such a simple system as the amount of power transferred through the transmission line is increased. For low levels of interchange the sensitivity of the voltage to amount of power interchanged is rather low, resulting in little drop in voltage at the load end. However as the interchange is increased, the voltage sensitivity also increases, first gradually, but then with increasing rapidity. The net effect is an increasingly rapid drop in voltage. Eventually a critical power level is reached, characterized by an infinite voltage sensitivity. An attempt to transfer more than this critical amount of power results in loss of a stable operating point, and subsequent voltage collapse .

The voltage behavior of the two bus radial system has been analyzed by numerous authors [1], [8]. The two bus model is, however, inadequate for representing all but the simplest of electrical systems. The high degree of transmission system interconnections within modern electrical systems requires the modeling of meshed networks consisting often of thousands of buses. The analysis of the voltage stability, and the prevention of voltage collapse in such a large, meshed system is a much more challenging problem.

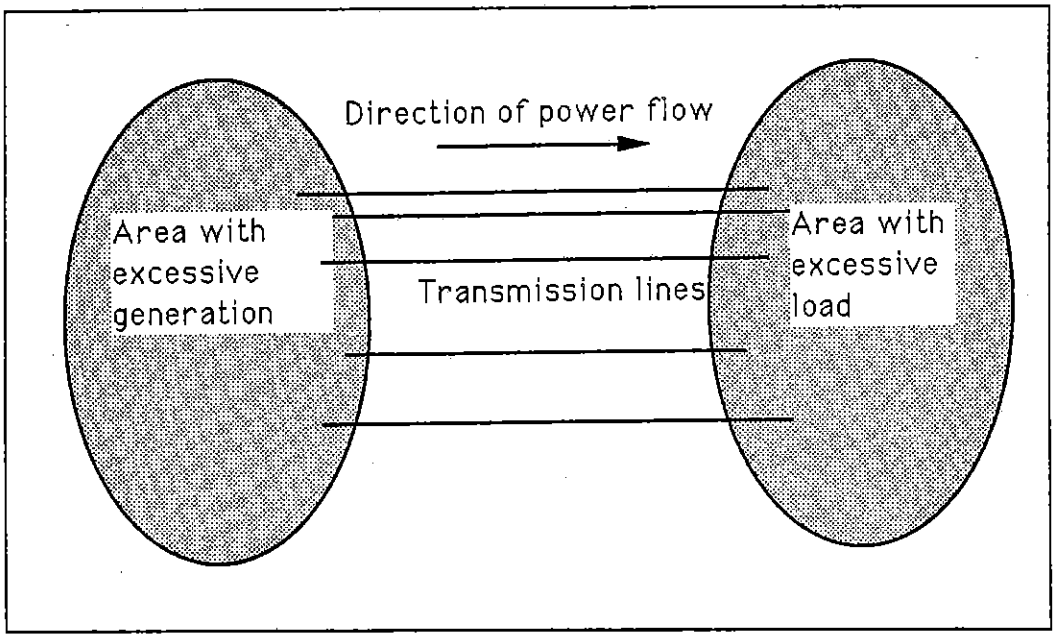

Figure 1-1 : Electric Power System Simplification

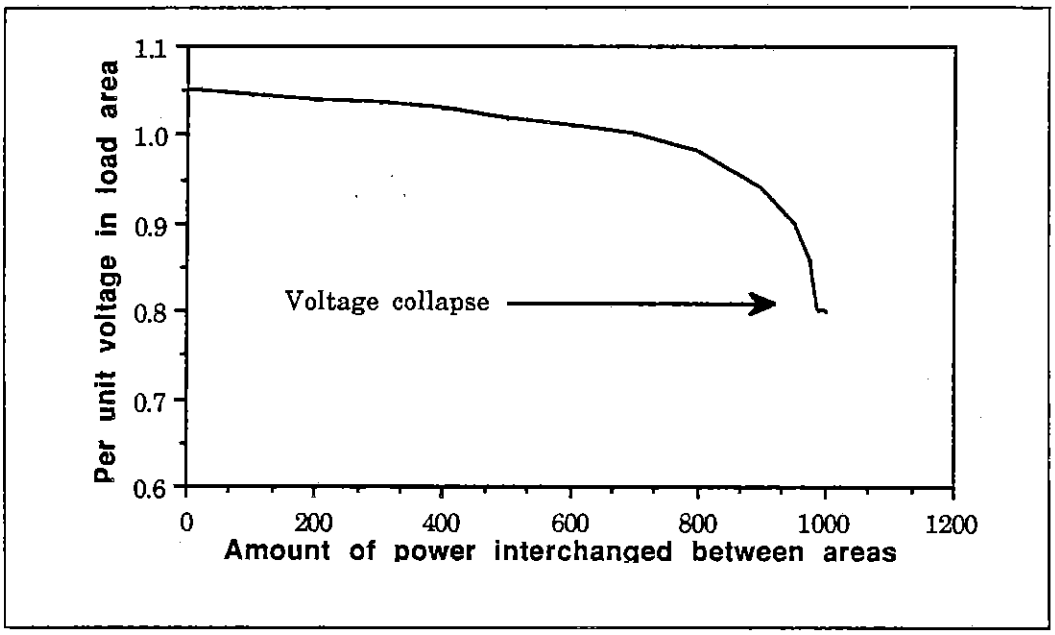

Figure 1-2 : Load Area Voltage as a Function of Power Transfer

An actual incident of a large scale voltage collapse induced blackout occurred in 1978 in France [2]. Over the course of 26 minutes, voltages throughout the entire French high voltage transmission system gradually declined from normal voltage of approximately 410KV to less than 340KV. The cause of this collapse was large power transfers between the French system and other European electric systems. A more recent incident occurred in Tokyo during the summer of 1987 [3]. There, high load demand and the necessity of importing power from distant generators caused a power outage of 8000 MW, affecting about 2.6 million people. Again the actual voltage collapse was preceded by about 20 minutes of gradually

declining voltages throughout a large portion of the Tokyo system. Domestically, near-record loads and high power transfers during 1987 caused voltages in the high voltage transmission system in Illinois and Indiana to decline by as much as 12% over the course of hours, although an actual voltage collapse did not occur [4]. Voltage security problems in this time frame have also occurred in the Northeastern U.S., with at least 8 incidents documented in 1988 [5].

Presently some utilities assess the security of their systems on-line via security-constrained optimal power flow (OPF) programs [6] (the term on-line is used to mean that the present state of the power system is being analyzed, with results of the analysis available within seconds to minutes). These programs try to optimize system operation by recommending various controller moves (such as changes in generator MW outputs, transformer tap positions, etc.) to minimize system operating cost while insuring that there are no security violations. Examples of security violations would include transmission line flows above some thermal limit, or bus voltage magnitudes below some limit. Typically limits are determined using assumed conditions in off-line studies. While this approach has proved useful in dealing with problems of a thermal overload nature, it is inadequate for a number of reasons in predicting the onset of voltage instability. First, voltage instability problems have been shown to occur in systems where voltage magnitudes never decline below levels that have

traditionally been deemed acceptable in off-line planning studies [7]. Thus since voltages never decline below their limits (until the system ultimately collapses), they never become active constraints in the OPF problem. Therefore no control action is initiated. Second, near the point of collapse, voltage variations can be extremely sensitive to changes in load and other system parameters [8]. Knowledge of the voltage level only at the current operating point may not be sufficient since a small change in the system operating point could cause a large voltage drop. Lastly, in order to avoid the high cost of constructing new lines, utilities would like to operate their systems in such a manner as to maximize the capacity from their existing transmission system. However to do this they need an indication of how close they are to the point of voltage collapse. Current OPF programs provide no such proximity indicator.

The absence of an easily computable proximity indicator to voltage collapse has meant that utilities must calculate system limits (such as maximum MW transfer) using off-line power flow programs. In [9] it is reported that engineers must run hundreds of power flow simulations daily using assumed future operating conditions in order to predict what these limits should be. An obvious difficulty of such an off-line approach lies in predicting the future conditions. Worst case scenarios are often assumed. This can result in either overly conservative limits, which prevent the utilities from taking advantage

of more economical but more distant generation, or blackouts when the actual conditions differ significantly from the assumed conditions. The magnitude of this problem can be seen in [9] where one of the larger utilities in the US reported that during 1987 they were not able to utilize their available generators as economically as possible 74% of the time, and that in approximately 96% of these instances the problem was due to reactive power and voltage limitations in the transmission system. Clearly a new approach to this problem is needed.

In this thesis a method based upon energy function techniques is developed, to accurately determine how close a power system is to the point of voltage collapse. This approach is based upon the use of Lyapunov's direct method, which provides a means for assessing the stability of systems of nonlinear differential equations, such as the power system models employed here. A closed form energy function is first defined for the power system dynamic model. The voltage stability of a particular section (or area) of the power system is then quantified by using this energy function to evaluate the difference between the system's normal operating point and one of the system unstable equilibrium points (UEPs). These UEPs are identified by the alternative solutions of the power flow equations. The energy difference associated with each UEP provides a measure of the voltage security in particular area of the system. Since in a large

system there may be a number of separate areas vulnerable to voltage collapse, separate voltage security measures would be needed for each.

As the system moves towards the point of voltage collapse, the energy differences tend to decrease in a manner proportional to changes in the system operating point, with one of them going to zero immediately before the system experiences voltage collapse. Thus the voltage security of the system could be assessed directly by determining the appropriate alternative power flow solutions, and their associated energy differences. It is shown that these solutions can be calculated with reasonable computational cost, allowing for on-line use.

1.2 Power system Stability

In order to motivate the use of energy function methods, the concepts of power system stability are briefly reviewed. Power systems are nonlinear, often with slowly varying inputs, and subject to a number of discrete disturbances. Such a system can be represented by the following set of differential and algebraic equations:

$$\begin{aligned} \dot{\mathbf{x}} &= \mathbf{f}(\mathbf{x}(t), \mathbf{y}(t), \mathbf{u}(t)) \\ \mathbf{0} &= \mathbf{g}(\mathbf{x}(t), \mathbf{y}(t), \mathbf{u}(t)) \end{aligned} \tag{1-1}$$

where

- **x** - state variables (e.g. bus voltage phase angles)
- **y** - algebraic variables (e.g. bus voltage magnitudes)
- **u** - input variables (which includes the changing load/generation injections and other disturbances)

A system of the form described by (1-1) is said to have an equilibrium point $\mathbf{x}_0$ at time $t_0 \in R_+$ if for a fixed known input, $\mathbf{u}(\bullet)$, $\mathbf{f}(\mathbf{x}(t),\mathbf{y}(t),\mathbf{u}(t)) = \mathbf{0}$, $\forall\ t \geq t_0$. Thus the mathematical definition requires that once the system reaches its equilibrium point $\mathbf{x}_0$ at time t_0 it remains there ad infinitum. However for realistic power systems this is never the case. The system state variables are subject to constant variation in response to both sporadic large disturbances to the system (e.g. loss of a large generator) along with the time variation in the loads of individual

customers. However, this load variation is usually of the form of a slowly varying average value (with its largest component normally having a 24 hour period) along with a small (a few percent) random variation about this average value. This random variation term typically displays much more rapid variation, on a time scale of seconds. Research into aggregate load models has suggested that such small random effects may be modeled by a white or colored noise term in the load [10]. Ignoring for the moment the infrequent large disturbances, we can express $\mathbf{u}(t)$ as

$$\mathbf{u}(t) = \mathbf{u}^{slow}(t) + \mathbf{u}^{small}(t)$$

where

$\mathbf{u}^{slow}$ - slowly varying average load component

$\mathbf{u}^{small}$ - zero mean, "small" magnitude load variation

If the time scale of the problem of interest is sufficiently short, relative to the variation in $\mathbf{u}^{slow}(t)$, stability studies often make the assumption that

$$\mathbf{u}^{slow}(t) = \hat{\mathbf{u}} \quad \text{(constant)}$$
$$\mathbf{u}^{small}(t) = \mathbf{0}$$

and we can therefore rewrite (1-1) as

$$\begin{aligned} \dot{\mathbf{x}} &= \mathbf{f}(\mathbf{x}(t), \mathbf{y}(t), \hat{\mathbf{u}}) = \hat{\mathbf{f}}(\hat{\mathbf{x}}, \hat{\mathbf{y}}) \\ 0 &= \mathbf{g}(\mathbf{x}(t), \mathbf{y}(t), \hat{\mathbf{u}}) = \hat{\mathbf{g}}(\hat{\mathbf{x}}, \hat{\mathbf{y}}) \end{aligned} \tag{1-2}$$

Since $\hat{\mathbf{u}}$ is now a constant, (1-2) is an autonomous system. Therefore if $[\hat{\mathbf{x}}_o, \hat{\mathbf{y}}_o]$ is an equilibrium point of (1-2) at some time t_o, we know that it is an equilibrium point at all time thereafter. Then if the true system has a solution $[\mathbf{x}(\bullet), \mathbf{y}(\bullet)]$ for some given $\mathbf{u}(\bullet)$, we would expect that for a given time $\hat{t}$ with an instantaneous input of $\mathbf{u}(\hat{t}) = \hat{\mathbf{u}}$, $\mathbf{x}(\hat{t})$ and $\mathbf{y}(\hat{t})$ from (1-1) should be "close" to $\hat{\mathbf{x}}(\hat{t})$ and $\hat{\mathbf{y}}(\hat{t})$ from (1-2). One approximates the actual time varying input $\mathbf{u}(\bullet)$ with a time invariant input by "freezing" $\mathbf{u}$ at a given time $\hat{t}$. We can then define a "frozen equilibrium" of (1-1) as $[\hat{\mathbf{x}}_o, \hat{\mathbf{y}}_o]$, and then determine the stability of the autonomous system relative to this equilibrium point. The approximation of the actual time varying system by a time invariant system is often the "hidden assumption" in most power system stability analysis. The validity of this assumption is dependent upon how fast the system inputs are changing relative to the dynamics of the system and the time scale of the problem. If the time variation in $\mathbf{u}^{slow}$ is truly "slow enough", relative to the dynamics of the system, and in the absence of any disturbances ($\mathbf{u}^{small} = \mathbf{0}$), the system state would sit in a negligibly small neighborhood of the frozen equilibrium point. This point would gradually change on the

time scale of $\mathbf{u}^{slow}$, and if the system is asymptotically stable, the state would track this slow variation.

As noted above, this is never precisely the case for an actual system since the state is constantly being perturbed away from this equilibrium point by various system disturbances. In addition to the time scale classification described above, one can also classify disturbances as either small disturbances (modeled by $\mathbf{u}^{small} \neq \mathbf{0}$) or large disturbances. By definition, a small disturbance is an event for which the system state remains in the neighborhood of the frozen equilibrium point and for which linearized models are accurate. These small magnitude random load variations add a small amount of "energy" to the system and thus are constantly perturbing the state away from its equilibrium point. This energy is normally dissipated through damping in the system. The classification of system stability related to small scale disturbances is known as small disturbance stability [11].

Steady-state stability is typically determined by linearizing the system about the equilibrium point of interest and then requiring that all eigenvalues have strictly negative real parts. For an actual system at its normal operating point, this is a minimal requirement. Once this eigenvalue requirement is satisfied, the effects of these small random variations are usually considered negligible and are typically ignored

in normal power system analysis. In contrast, large disturbances are events which suddenly drive the state far away from its equilibrium point, and/or change the equilibrium by changing the system structure. Examples of large scale disturbances are loss of generators, loss of a transmission line, or other faults on the system. Following such an event the question to be answered is whether the system will return to a frozen equilibrium point (which may be different from the pre-disturbance equilibrium point). This classification of stability is known as transient stability. For $t < t^d$ (time when disturbance is applied to the system) the system equations are assumed to be the following:

$$\begin{aligned} \dot{\mathbf{x}} &= \mathbf{f}(\mathbf{x}(t), \mathbf{y}(t), \hat{\mathbf{u}}) = \mathbf{0} \\ \mathbf{0} &= \mathbf{g}(\mathbf{x}(t), \mathbf{y}(t), \hat{\mathbf{u}}) \end{aligned}$$

where $\hat{\mathbf{u}}$ is a constant and the system is assumed to have reached its frozen equilibrium. At $t = t^d$ the disturbance is applied to the system, possibly changing $\hat{\mathbf{u}}$, $\mathbf{f}(\bullet)$, and $\mathbf{g}(\bullet)$. For $t \geq t^d$ the new equations are

$$\begin{aligned} \dot{\mathbf{x}} &= \mathbf{f}^d(\mathbf{x}(t), \mathbf{y}(t), \hat{\mathbf{u}}^d) \\ \mathbf{0} &= \mathbf{g}^d(\mathbf{x}(t), \mathbf{y}(t), \hat{\mathbf{u}}^d) \end{aligned}$$

Note that in the general case, a number of individual disturbances could be applied to the system at separate discrete times (to model, for

example, the action of line reclosures or protective relays actions). Since $\mathbf{u}^d$ is modeled as a constant during the time period between disturbances, the system is considered time invariant during each time segment. The assumption that $\mathbf{u}^{slow}(t)$ = constant and $\mathbf{u}^{small}(t) = \mathbf{0}$ is typically valid since the time frame during which the system either reaches a stable equilibrium point, or loses synchronism (unstable) is seldom more than a few seconds. Thus the ultimate determination of whether a system is transiently stable is a function of the pre-disturbance operating point and which large disturbances we choose to apply to the system. From a more formal mathematical viewpoint, steady state stability implies the equilibrium of interest is asymptotically stable. A system is transiently stable for a disturbance if the initial state "resulting" from the disturbance is inside the post-disturbance equilibrium's region of attraction. Clearly any system can be considered to be transiently unstable if the disturbance is large enough (consider the disturbance defined to be the loss of a significant portion of total system generation). Normally a system is called transiently stable if it can return to a stable equilibrium point following any credible disturbance. However the key point is that, except for a small number of discrete disturbances, a time invariant $\mathbf{u}$ is assumed throughout the problem.

Returning again to the problem of voltage instability, we first note that most reports of voltage collapse seem to indicate that it was not

directly caused by a large disturbance in the system. This is one of the features that distinguishes voltage collapse from transient stability. Instead the system operating point is moving (on a time scale of minutes to hours), usually with gradually increasing loads, from a state of relative security to one of vulnerability. Since voltage instability is driven by the time variation in $\mathbf{u}(t)$, clearly the earlier assumption of a time invariant system is no longer possible. However this future variation in $\mathbf{u}(t)$ is known only approximately at best. Additionally, as the system state evolves in response to $\mathbf{u}(t)$, various automatic control systems (e.g. load tap changing [LTC] transformers and generator reactive power outputs) will act upon the system, trying to hold their control values close to their setpoints. Thus the determination of a system's voltage stability involves prediction of behavior in a nonlinear, time varying system whose input function is only approximately known.

1.3 Existing Voltage Security Measures

As was mentioned earlier, utilities are continually confronted with the problem of how to operate their systems in both a secure and economical manner. In order to solve this problem, the typical utility must determine the settings of a few hundred controllers (e.g. MW output of a generator, MW transactions with other utilities, voltage

setpoint of a generator, transformer tap position, etc.) in order to supply power to hundreds or thousands of time varying aggregate loads (with each load normally representing hundreds or thousands of customers) so that economy is maximized and security is maintained. In order to assess system security, it is necessary that the utility have some measure to determine how close the system is to voltage collapse. This section reviews the various methods appearing in the literature and in standard industry practice of assessing this voltage security.

Intuitively, the problem of determining proximity to voltage collapse can best be explained by the well established concept of security regions [12], [13], [14], [15] [19]. To illustrate this concept in two dimensions, refer to Figure 1-3. The current stable, frozen equilibrium of the power system can be thought of as being located at point **u** within a region called the feasible space. The dimensions of this space are the set of inputs. Each point in the feasible space corresponds to a set of inputs for which a stable operating point exists. In actual practice the size of the feasible space would be further reduced due to other operational constraints, such transformer, generator and transmission lines limits. To simplify the intuitive development of the voltage security measures, other operational constraints are not yet considered; these constraints will be included in Chapter 5. As $\mathbf{u}^{slow}$ varies with time (both through customers

changing their loads and through actions of the controllers mentioned in the previous paragraph), the location of $\mathbf{u}$ within the feasible space also varies. Surrounding the feasible space is the infeasible space, which is defined as those values of $\mathbf{u}$ which do not possess a stable operating point. If we assume that $\mathbf{u}^{small} = \mathbf{0}$ and that the variation in $\mathbf{u}^{slow}$ is very much slower than the dynamics of the system, then the boundary between these two regions is quite distinct. This is never completely true in practice. Therefore we have some points in the feasible region close to the boundary that have corresponding operating points that are "small disturbance" stable, but are not secure because small perturbations of the form $\mathbf{u}^{small}$ can cause the state to move out of the region of attraction for the equilibrium. However, the assumption used for power systems is that the width of the "band" about the boundary containing these marginally stable points is small compared to the variation in $\mathbf{u}$ caused by $\mathbf{u}^{slow}$.

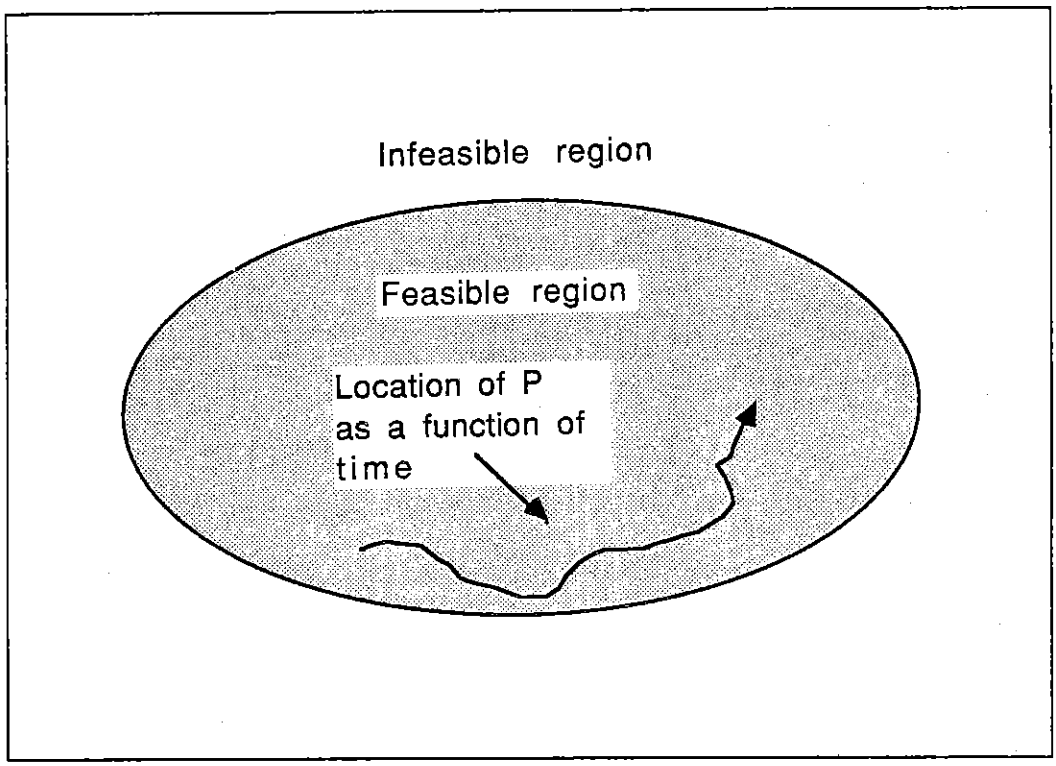

Figure 1-3 : Time Variation in Power System Operating Point

Determining the voltage security of any operating point is then reduced to the problem of determining how close its corresponding **u** is to the feasibility boundary. However two problems arise. First, calculating the entire set of points comprising the feasibility boundary is computationally prohibitive for all but the simplest systems (this boundary is calculated in Chapter 2 for a very simple system). Second, even if the boundary could be identified, one must determine which portion of the boundary should be used when determining the proximity of **u** to that boundary. Intuitively one might think that the

closest boundary point (in a Euclidean sense) would be appropriate. The applicability of this approach depends on the relative correlation and the individual variation in the elements of **u**, and on the shape of the boundary. For example consider the simple case with the input subspace considered consisting of the real power injections at buses i and j, $\mathbf{u} = [P_i\ P_j]$, with the feasible region defined $||\mathbf{u}||_\infty \leq 1.0$. Assume that the output of P_i is free to vary, but the output of P_j is fixed at 0.95 (e.g. P_i represents a load bus and P_j represents a base load generator). Since P_j is constant, only the portion of the boundary in the P_i dimension is of interest. In calculating the system security measure, the distance from **u** to the P_i boundary should be used, rather than the distance to a closest boundary point. In a higher dimensional system, where the individual elements of **u** could be relatively uncorrelated, a number of different security measures may be needed. With this context in mind, several of the techniques of determining proximity to voltage collapse are examined.

Probably the most common technique used by utilities today to maintain voltage security is the use of various operational guidelines and/or heuristic rules of thumb. These are based both upon studies performed days or months earlier using assumed system conditions, and the individual operator's best judgement. On-line power flow studies may also be used to augment these guidelines [16]. Examples of operational guidelines are limiting the amount of power

interchanged with neighboring utilities when various units are out of service, and maintaining transmission system voltages above certain levels. While these guidelines have certainly proved useful in preventing some system problems, they have a number of fundamental weaknesses. The main problem is that the guidelines have been derived based on assumed conditions which never completely match the actual operating state. For example transmission lines or generators might be out of service, load distribution might not match what was anticipated, or neighboring utilities may be operating their systems in an unanticipated manner. Thus it is up to the system operator to determine how the limits in the guideline should be interpolated based upon actual conditions. Second, the guidelines often do not provide reliable quantitative indication of how close the system is to the voltage feasibility boundary. Thus the operator does not have a good idea of direction in which the state is moving, and how control actions are affecting the voltage security of the system. This information is particularly useful when unexpected operating states are encountered. The lack of a quantitative measure of voltage security has meant the existing security enhancement software (such as the linear programming technique from [6] or the Newton's method optimization from [17]) must try to assess the system voltage security indirectly by looking at bus voltages and transmission system flows.

A number of techniques have been developed which attempt to quantify how close the system is to the point of voltage collapse. These proximity indicators can be broken down into two groups: those that determine system voltage security by making assumptions about the future system trajectory from the present state, and those that use only information about the present state of the system.

The most straightforward of the former techniques is to simply make an assumption about how the system inputs will change with time and then solve the power flow problem at a number of discrete timesteps until the simulated system loses its steady state solution (failure of a Newton-Raphson iteration is often used an indication that no solution exists). In essence a single point on the boundary of the feasible space is determined by making an estimate at the current time = t_0 of the trajectory $\mathbf{u}(t)$ for $t > t_0$. The proximity to voltage collapse is then based upon the value $\mathbf{u}(T)$ when the critical point on the boundary is reached.

In normal circumstances utilities often have fairly good estimates of how some of the components of $\mathbf{u}(t)$ will vary over the next few hours. In particular, their own generation dispatch, their interchange with other companies and their customer load distribution are usually known. However there is often less certainty concerning the future variation of the generation, interchange, and load of their neighboring

utilities (with whom they may have a competitive relationship). Additionally voltage collapse often occurs under abnormal circumstances (such as under extremely high loads). In such situations the utility has little historical data upon which to base a prediction of future variations in **u**(t).

A problem with developing a proximity indicator based upon assumed future changes in **u** is that the indicator could be highly sensitive to the accuracy of this prediction of this trajectory. For example, consider the case where the current operating point is close to the voltage stability boundary. If the assumed **u**(t) for $t > t_o$ moves the system state in a direction parallel to, or away from this boundary, the current operating point could be judged as quite secure. However, if the actual system moves in only a slightly different direction, the system could experience a voltage collapse. Additionally, since the calculation of this indicator requires a time simulation, it would be difficult to calculate the effects of controller changes upon the proximity indicator without repeating the entire simulation from the new assumed operating point. This not only introduces additional inaccuracies due to again using an assumed **u**(t), but may be computationally prohibitive since each proposed controller change could require solving a series of power flow solutions.

A number of improvements on this approach have appeared in recent literature. In [18] and [19] the computational burden is reduced by recognizing that since the critical point of voltage collapse is characterized by singularity of the Jacobian, a point of the boundary surface can be determined by solving the power flow equations with the explicit requirement of singularity of the Jacobian matrix. This bifurcation calculation has become known as the Point of Collapse method in the power system literature. The method works by parameterizing **u** as a function of an arbitrary scalar t and then solving directly for the value of t which results in a singular Jacobian. The computational requirements of this method are on the order of a few power flow solutions. Additionally, the results of various automatic control actions (such as transformer tap movement and generator reactive output variation), along with their limits can be handled directly during the iterative solution. The boundary point determined is dependent upon the parameterization of **u** chosen. The closest point on the boundary (in terms of Euclidean distance) can also be determined using either an iterative method [20] or directly [21]. These methods exploit the observation that the normal to the closest boundary point can be computed using the left eigenvalue method from [20].

An approach is presented in [22] which attempts to determine the closest point on the feasibility boundary through an iterative process,

where each successive value of $\mathbf{u}(t)$ is determined by moving in the direction of the gradient of the determinant of the power flow Jacobian. The boundary is assumed to be reached when the value of the determinant is sufficiently small. By providing a result based upon the distance to the closest boundary point, the technique is not dependent upon an assumed $\mathbf{u}(t)$. However, the authors state that the calculation of $\nabla|J|$ is very time consuming, with the computational cost greater than $O(n^3)$ (where n is the number of buses in the power system model). In [23] the distance to voltage collapse is determined not by solving a series of power flows, but rather through a series of linearized approximations. Thus this technique also results in reduced computational costs. Automatic control actions which would occur along the simulated trajectory are also taken into account. However as with the earlier methods, the resultant accuracy of both these techniques depends upon the appropriateness of the assumed trajectory.

The second major group of methods for assessing proximity to voltage instability are those techniques which only use information about the present state of the electrical system. In contrast to the previously discussed methods, they make no assumptions about future system trajectories. In [24] and [25] the use of the smallest singular value of the Jacobian of the power flow equations, denoted by σ_{min}, is recommended as a proximity indicator. The singular value of the

Jacobian matrix **J** may be obtained as the square root of the smallest eigenvalue of $(\mathbf{J}^T\mathbf{J})$. As the system moves towards the point of voltage collapse, σ_{min} decreases, eventually reaching zero when **J** becomes singular. The advantage of this approach is that it is not necessary to make predictions about future changes in the system trajectory. The proximity indicator is solely based upon the current operating point. In [24] it is shown that σ_{min} can be calculated quite quickly, and decreases as the system moves towards voltage collapse. However its decrease is not smooth with respect to variations in the system state; it can exhibit large discontinuities when the generators hit their reactive power limits. These discontinuities could cause problems as a system gradually approaches the point of voltage collapse, since σ_{min} might vary slowly initially, giving the operator a false sense of security. The value could then suddenly jump downwards as generators hit their reactive limits, notifying the operator too late to take preventative controller actions.

The proposed method of enhancing system security in [25] is to move controllers so that σ_{min} is maximized while maintaining feasibility. In order to perform this optimization, it is necessary to calculate the sensitivity of σ_{min} to each of the system controllers. This is done using a singular value decomposition of the Jacobian matrix. The disadvantage of the method, aside from using σ_{min} as security measure, it that the computational cost of computing the singular

value decomposition of the Jacobian matrix is $O(n^3)$. Therefore it is computationally prohibitive for a large system, at least on a serial machine. In [26] a singular value decomposition algorithm is presented using large arrays of parallel processors. Whether such an approach is workable in a utility control center has yet to be determined.

A different type of indicator, which is also only based upon the current operating state, is presented in [27]. The proposed qualitative measure varies from 0 (for a system with no load) to 1 for a system experiencing voltage collapse. The measure is calculated by partitioning the bus admittance matrix based upon load and generator buses. Then a partial inversion of the matrix is performed in order to calculate the load bus voltages as a linear function of their currents and the generator bus voltages. A security measure L_j is then calculated for each bus based upon these linearizations. The system security indicator is the maximum of the L_j's. This indicator has the advantage that it can be obtained with reasonable computational effort and can be extended to large systems. One of the difficulties with the approach is that since only current operating point information is used, the nonlinear effects of generators and transformers can not be included unless the devices have already hit their limits at the current operating point. Also it appears that it would be difficult to derive the

effects of controller actions on the measure in order to improve system voltage security.

A variation of the use of Jacobian singularity to determine proximity to voltage collapse is presented in [28] and [29]. Rather than using the least singular value of the Jacobian, three security measures are calculated. First, an estimate of the eigenvalue of the portion of the Jacobian matrix associated with the reactive power equations at the load buses is calculated. This eigenvalue estimate is based upon the flows in the system, and measures the reactive power surplus or deficit of the transmission system. For a secure system the eigenvalue is very large, becoming smaller as the system load is increased. Second, the ability of the voltage control devices in a portion of the system to maintain a type of steady state "voltage controllability" is determined. A system has voltage controllability if it is possible to both raise the voltage at the load buses by increasing the generator voltage set points, and if decreasing the reactive load causes an increase in the bus voltages. These sensitivity values are based upon selective values of the inverse of the Jacobian matrix. Once all the voltage control devices within an area have reached their limits, the area no longer has voltage controllability. The third security criteria is based upon the amount of reactive power which can be imported into an area with a reactive deficiency. This value is a measure of the

reactive transmission reserve on the boundary of the voltage vulnerable area.

A third major grouping of voltage collapse proximity indicators are the methods based upon multiple solutions of the system equations. As will be shown in later sections, these methods can be thought of as a hybrid between the methods which dependent explicitly upon an assumed future system trajectory, and those that use only current system state information. Techniques utilizing multiple solutions include the energy based approach, which the author will present in this thesis[30], [31], [32]; and the methods presented in [33] and [34]. The latter methods are based upon calculating a scalar index which can be interpreted as the "angle" between two of the vector solutions of (1-2).

As has been shown, a number of different approaches have been put forth to determine the voltage vulnerability of power systems. While many of these approaches have provided insight into the voltage stability problem, no technique to date has provided the electric utilities with an easily computable, accurate measure which can be used both to determine how close a system is to voltage instability, and to identify feasible control actions that best increase the system voltage security. In this thesis a method based upon energy function techniques is developed to solve these problems.

Chapter 2 - Application of Energy Function Methods to Voltage Collapse

2.1 Energy Function Methods Introduced

Insight into the problem of voltage instability may be gained by the study of the region of attraction of an asymptotically stable equilibrium for the power system model. One tool which has proved useful in analyzing the region of attraction of such systems is Lyapunov's direct method. Consider a set of differential equations of the form

$$\dot{\mathbf{x}} = f(x) \tag{2-1}$$

Comparing this equation with (1-1) we note that $\mathbf{u}(\bullet)$ is no longer explicitly identified, and that the algebraic variables have been eliminated. This is not to say that $\mathbf{u}(\bullet)$ is longer present, but rather that it is modeled as a fixed known input. The idea behind the use of Lyapunov's direct method is that for a time invariant system of this form, the relative stability of a stable equilibrium point $\mathbf{x}^s$ can be quantified if it is possible to define a scalar function ϑ with certain properties. Typical requirements on such a function are that $\vartheta(\mathbf{x}^s) = 0$ and that ϑ is a locally positive definite function (l.p.d.f.) about the

stable equilibrium over some region Ω. Additionally, the system dynamics must be such that the energy derivative along trajectories of the system, defined as

$$\dot{\vartheta}(\mathbf{x}) = \nabla\vartheta(\mathbf{x})\, \mathbf{f}(\mathbf{x}(t)) \tag{2-2}$$

is always less than or equal to zero for all $\mathbf{x} \in \Omega$. If these properties hold, the function ϑ is known formally as a Lyapunov function (it is also referred to as an energy function, since it is in some sense analogous to the "energy" of the system). The existence of ϑ can provide sufficient conditions for the asymptotic stability of $\mathbf{x}^s$. Additionally, Ω is contained within the region of attraction of $\mathbf{x}^s$. These results can be stated formally as LaSalle's theorem [35]:

LaSalle's Theorem For the system from (2-1), let $\vartheta: R^n \rightarrow R$ be a continuously differentiable l.p.d.f., and suppose that for some $\vartheta^{cr} > 0$, the set

$$\Omega_c = \text{component of } \{\mathbf{x} \in R^n : \vartheta(\mathbf{x}) \leq \vartheta^{cr}\} \text{ containing } \mathbf{x}^s$$

is bounded. Suppose ϑ is bounded below on Ω_c, that $\dot{\vartheta}(\mathbf{x}) \leq 0$ $\forall \mathbf{x} \in \Omega$, and that the set

$$S = \{\mathbf{x} \in \Omega_c : \dot{\vartheta}(\mathbf{x}) = 0\}$$

contains no trajectories of (2-1) other than the trivial trajectory $\mathbf{x}(t) \equiv \mathbf{x}^s$. Then the equilibrium point $\mathbf{x}^s$ of (2-1) is asymptotically stable (proof is given in [35]).

Therefore the relative stability of $\mathbf{x}^s$ can be quantified based upon the value of ϑ^{cr}. The region Ω can be thought of as defining an energy "well" contained in the region of attraction. Unless the system receives a disturbance that pushes the state $\mathbf{x}$ to a point with energy greater than ϑ^{cr}, the state can not escape the well and will eventually return asymptotically to $\mathbf{x}^s$.

The method can be illustrated with the example of a ball in a two dimensional well shown in Figure 2-1. The well has an asymptotically stable equilibrium point (SEP) $\mathbf{x}^s$ at the local minimum of the function in the center, and an unstable equilibrium point (UEP) $\mathbf{x}^u$ at the local maximum on the right. Assume the ball is initially at $\mathbf{x}^s$, and then is subsequently displaced from the SEP by some type of disturbance. The problem then is to determine whether following this disturbance the ball will eventually return to the SEP; that is, to quantify the security of the SEP. To solve this problem using Lyapunov's direct method, a Lyapunov function ϑ is needed. For a general system of the form of (2-1) this is far from trivial. However for this simple example system, a suitable ϑ is the total potential and kinetic energy of the ball with $\vartheta(\mathbf{x}^s)$ defined as zero. Then to

determine whether the ball will escape the well, we note that since due to friction the ball's total energy following the disturbance is non-increasing with time (and that there are no nontrivial trajectories where $\dot{\vartheta}(\mathbf{x}) \equiv 0$), we can guarantee that the ball will return asymptotically to $\mathbf{x}^s$, provided its initial energy following the disturbance is less than the potential energy associated with $\mathbf{x}^u$ ($\vartheta[\mathbf{x}^u] = \vartheta^{cr}$). Thus the value of $\vartheta(\mathbf{x}^u)$ can be thought of as providing a quantitative measure of the security of $\mathbf{x}^s$.

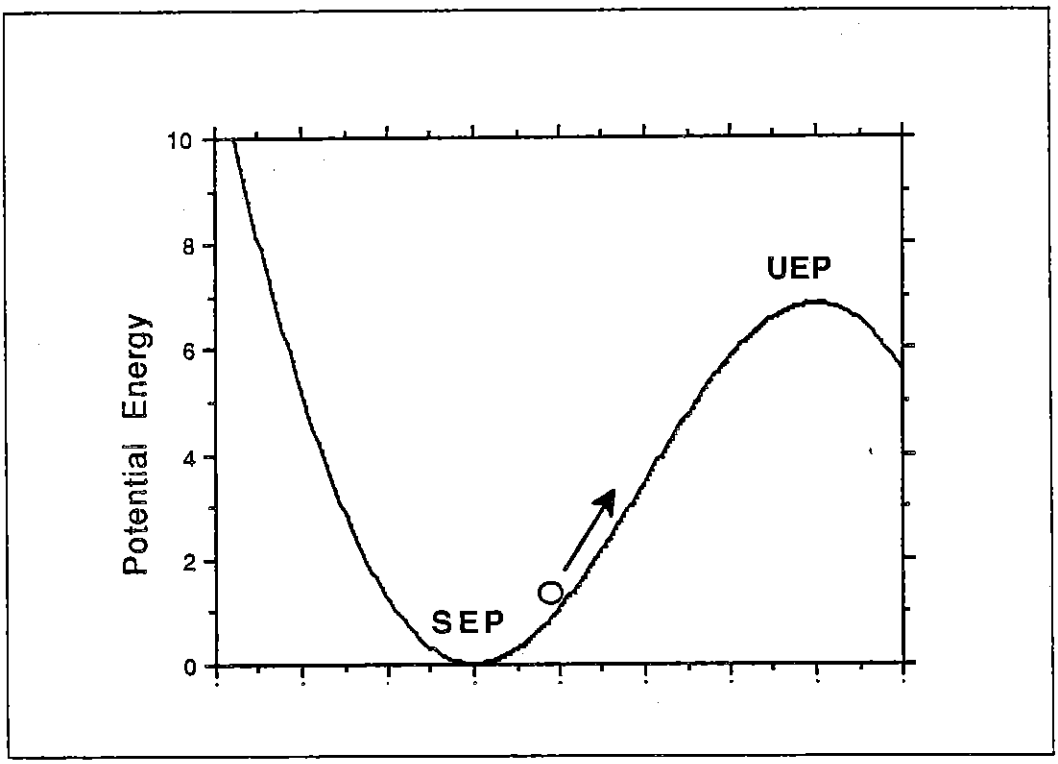

Figure 2-1 : Ball in Well Example

LaSalle's theorem can be applied to power systems by first assuming that the system is time invariant. This corresponds to freezing $\mathbf{u}^{slow}(t) = \hat{\mathbf{u}}$ (constant) and setting $\mathbf{u}^{small} \equiv 0$. Then, assuming that a suitable ϑ function can be defined, we can think of the stable operating point of the system as being close to the bottom of a time invariant energy well with the "depth" of the well determined by both $\hat{\mathbf{u}}$ and the system equations. The depth of the well then gives some indication of the security of the current operating point since the greater the depth, the larger the disturbance needed to escape the well. This depth can be measured by calculating the energy associated with the lowest point(s) on the boundary of the well. A necessary condition for such a saddle point is that $\nabla\vartheta(\mathbf{x}) = \mathbf{0}$; it will be shown later that for the function used here these saddle points in energy correspond to the unstable equilibrium points (UEPs) of (2-1).

The use of energy functions has proved quite useful in determination of system transient stability [36]. In that context, a large disturbance is first applied to the system, which, in essence, gives the system some initial "energy". Following the disturbance, a time invariant system model is assumed, so the existence of a time invariant energy well follows. Using the simplest Lyapunov based criterion, if the initial energy following the disturbance is less than that of the post-fault system's UEP with the lowest energy, the system will return

asymptotically to its post-fault equilibrium point. Other more sophisticated criterion make use of such concepts as the "controlling UEP" or "potential energy boundary surface." These approaches recognize that a fault which yields a system trajectory passing exactly through the lowest saddle point on the boundary of the energy well is a rare, worst case scenario.

In contrast, for the voltage security problem considered here the system has either not been subject to a large disturbance, or has seemingly "settled down" following the disturbance. Rather the system is subject to a time varying input $\mathbf{u}(\bullet)$ with a time scale of minutes to hours which is not a known fixed function. Therefore the operating point of the system is moving in a "quasi-static" manner, with the "frozen" equilibrium point approximating the true state of the system. At any fixed time $\hat{t}$ the shape and boundary saddle points of the energy well about the frozen equilibrium point could be determined. However this energy well is also a function of time, since its boundaries are at least partially a function of the operating point. As the system changes with time, so does the boundary of the energy well. Thus by monitoring the changes in the energy of the boundary saddle points, the security of the system could be tracked over time. As the system moves closer to the point of voltage collapse one would expect the depth of the energy well to decrease. This will be shown to

be the case in later sections. Eventually at the point of voltage collapse, where a stable solution no longer exists, the depth of the well goes to zero. Thus while the system has always remained close to the bottom of the well (i.e. close to its frozen equilibrium point), the shape of the well has changed with time so that at voltage collapse the energy function about this point is no longer locally positive definite. In actuality, however, shortly before this point, the random load variations, which have little effect on a normal, robust operating point, will dominate and cause the state to escape from the now shallow well. Once the state leaves the potential well about the operating point, the deterministic dynamics drive a very rapid decline in voltage magnitudes until either the problematic portion of the system is isolated by protective relaying actions, or the entire system collapses.

2.2 Derivation of Energy Function for Voltage Stability Assessment

The application of energy function methods to the problem of power system voltage stability is more challenging than was the case for the simple "ball in a well" example. In this section, the energy function method is developed. First, consider the static power balance equations for the two bus system shown in Figure 2-2. For simplicity the transmission line will be assumed to be lossless, so that the real

power injection at bus 1 must equal the real load at bus 2. Furthermore assume that the load attached at bus 2 is represented by a constant P-Q demand. The resulting power balance equations at bus 2 are:

$$P_L + B_{12}V\sin(\alpha) = 0 \quad (2\text{-}3)$$

$$Q_L - B_{22}V^2 - B_{12}V\cos(\alpha) \quad (2\text{-}4)$$

where

V := bus voltage magnitude at bus 2

$\alpha := \delta_2 - \delta_1$ phase angle difference between buses 2 and 1

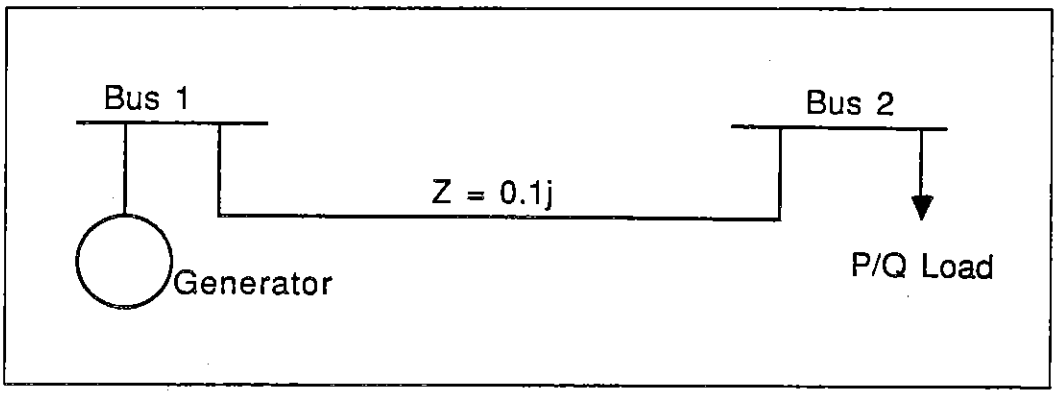

Figure 2-2: One-line Diagram of Two Bus System

For $B_{12} = -B_{22} = 10.0$, the locus of points in the α-V space satisfying these constraints for a range of P and Q values are shown in Figure 2-3. A radial line with a fixed sending voltage typically has two solutions for receiving end voltage. This is reflected in Figure 2-3 by

the fact that the P and Q constraints typically have two intersections, each corresponding to a power flow solution. However, as shown in Figure 2-3, for certain critical values of P and Q, the two constraint curves become tangent, with only one resultant solution. At this point the Jacobian of the two power balance equations must be singular. If either P or Q is increased further, the power flow equations no longer have a solution.

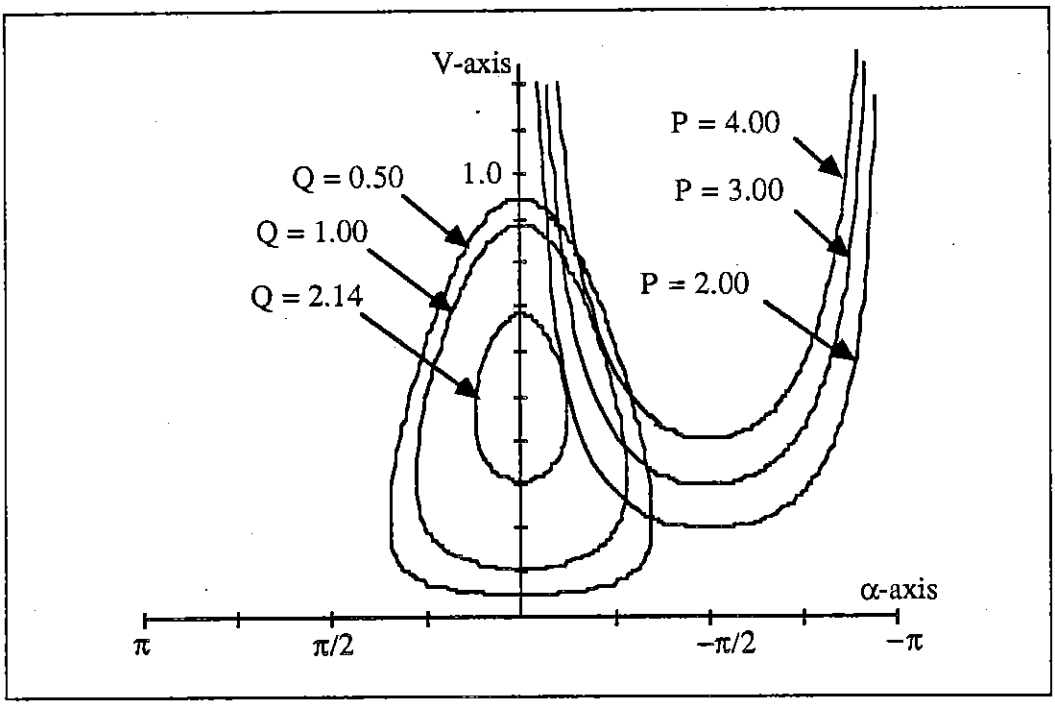

Figure 2-3 : Power Balance Constraints in α-V Plane

In order to develop the energy function approach, it is useful to also introduce dynamics to augment the algebraic power flow equations.

Note that the dynamics in this example do not represent the most general models that can be accommodated by the method. The goal here is to illustrate the basic methodology; the range of allowable models will be discussed later. First assume that the real power demand at bus 2 is a constant plus a linear term dependent on bus frequency. This follows the structure preserving model introduced for transient stability analysis in [37]. Using the classical model for the generator, the system equations are then given by:

$$M_g \dot{\omega} + D_g \omega - B_{12}V\sin(\delta_1-\delta_2) - P_M = 0$$

$$-(P_L + D_l \dot{\delta}_2) = B_{12}V\sin(\delta_2-\delta_1)$$

$$-Q_L = -B_{22}V2 - B_{21}V\cos(\delta_2-\delta_1)$$

Under the assumptions that $|P_M| = |P_L|$ (generator mechanical power matches active load demand) and $B_{12} = B_{21}$, and recalling the definition of α as the angle difference across the line, these equations may be rewritten as:

$$\dot{\omega} = - M_g^{-1} D_g \omega - M_g^{-1} f(\alpha,V) \qquad (2\text{-}5a)$$

$$\dot{\alpha} = -D_l^{-1} f(\alpha,V) + \omega \qquad (2\text{-}5b)$$

$$0 = V^{-1} g(\alpha,V) \qquad (2\text{-}5c)$$

where

M_g = Inertia constant of the generator

D_l, D_g = Damping of load and generator

$f(\alpha,V) = P_L + B_{12}V\sin(\alpha)$

$g(\alpha,V) = Q_L - B_{12}V\cos(\alpha) - B_{22}V^2$

$\omega = \dot{\delta}_1$

Note that multiplication by V^{-1} in (2-5c) does not affect the desired solutions because voltage magnitudes are always restricted to be strictly positive. The equilibrium of (2-5) are the (α,V) intersection points pictured in Figure 2-3, in the $\omega=0$ plane.

The mixed system of differential and algebraic constraints in (2-5) is not guaranteed to define a globally well posed dynamical system; that is, for some feasible initial conditions trajectories cannot be continued for all time, particularly when the voltage magnitudes are very low [38]. However, using the technique from [38] the algebraic equation is singularly perturbed to form a differential equation whose equilibrium is the solution of the original equation. For (2-5c), this becomes

$$\varepsilon\dot{V} = -V^{-1}g(\alpha,V) \qquad (2\text{-}5d)$$

where ε is a small positive parameter that controls the speed with which trajectories of voltage magnitude move towards values satisfying the reactive power balance. It is shown later that the

model's ability to predict voltage collapse is independent of the choice of this parameter. From an engineering standpoint, 2-5d may be interpreted as follows. The load demand is taken as an "independent input", and the voltage magnitude responds to this input to maintain reactive power balance. The right-hand side of 2-5d is the difference between the reactive power absorbed by the load and the reactive power delivered to the load. When the load instantaneously demands more reactive power than the system is supplying, (2-5d) predicts that the bus voltage drops until power balance is re-established. The rate of this change is dependent upon ε; for ε sufficiently small it is essentially instantaneous and the behavior is nearly identical to the original algebraic equation. Note that the use of ε is not advocated for simulating system trajectories since this would create an unnecessarily stiff set of differential equations to be solved. The point of introducing (2-5d) is to obtain a single model that is physically reasonable over a wide operating range of voltage, thereby facilitating the energy function analysis.

In order to develop the energy function for the system of equations given by (2-5a), (2-5b) and (2-5d), they are first written in matrix form as

$$\begin{bmatrix} \dot{\omega} \\ \dot{\alpha} \\ \dot{V} \end{bmatrix} = \begin{bmatrix} -M_g^{-1}D_gM_g^{-1} & -M_g^{-1} & 0 \\ M_g^{-1} & -D_l^{-1} & 0 \\ 0 & 0 & -\frac{1}{\varepsilon} \end{bmatrix} \begin{bmatrix} M_g\omega \\ f(\alpha,V) \\ V^{-1}g(\alpha,V) \end{bmatrix} \quad (2\text{-}6)$$

with M_g, D_l, D_g and ε assumed to be strictly positive.

Defining **A** as the 3 by 3 matrix from the right hand side of (2-6), $\mathbf{x} = [\omega\ \alpha\ V]^T$, $\phi(\mathbf{x}) = [M_g\omega\ \ f(\alpha,V)\ \ V^{-1}g(\alpha,V)]^T$, and letting $\theta(\mathbf{x})$ be defined as the vector function of the right-hand sides of equations (2-5a), (2-5b) and (2-5d), we can derive a Lyapunov function for this system using the following theorem:

Theorem 2.1 [39]

Suppose the system of the form $\dot{\mathbf{x}} = \theta(\mathbf{x})$ has a strictly stable linearization at the equilibrium point $\mathbf{x}^s$. Further suppose that there exists a constant matrix $\mathbf{A} \in \mathbf{R}^{nxn}$ satisfying

a) $\det(\mathbf{A}) \neq 0$;

b) $(\mathbf{A}+\mathbf{A}^T) \leq 0$, i.e., $(\mathbf{A}+\mathbf{A}^T)$ is negative semi-definite;

c) $\mathbf{A}^{-1}\theta(\mathbf{x}) = \phi(\mathbf{x})$ is a gradient function, or equivalently,

$$\mathbf{A}^{-1}\frac{\partial\theta(\mathbf{x})}{\partial\mathbf{x}} = \frac{\partial\phi(\mathbf{x})}{\partial\mathbf{x}} \text{ is symmetric.}$$

Under these conditions the integral

$$\vartheta(\mathbf{x}) = \int_{\mathbf{x}^s}^{\mathbf{x}} [\mathbf{A}^{-1}\theta(\mathbf{x})]^T d\mathbf{x} = \int_{\mathbf{x}^s}^{\mathbf{x}} [\phi(\mathbf{x})]^T d\mathbf{x} \qquad (2\text{-}7)$$

defines a Lyapunov function for the system of (2-1), that is $\vartheta(\mathbf{x})$ is locally positive definite about $\mathbf{x}^s$, and

$$\dot{\vartheta}(\mathbf{x}) = [\nabla\vartheta(\mathbf{x})]^T \theta(\mathbf{x}) = \frac{1}{2} [\nabla\vartheta(\mathbf{x})]^T (\mathbf{A}+\mathbf{A}^T)\nabla\vartheta(\mathbf{x}) \leq 0.$$

For the power system under consideration, the initial stipulation that (2-6) have a strictly stable linearization at the equilibrium point $\mathbf{x}^s$ is met by definition because only systems which have steady state stability are studied. The first requirement that $\det(\mathbf{A}) \neq 0$ can be shown to be true by straightforward calculation. Second, $(\mathbf{A}+\mathbf{A}^T)$ can be shown to be negative semi-definite by noting that it is a diagonal matrix whose diagonals are all less than zero. Lastly,

$$\mathbf{A}^{-1}\frac{\partial\theta(\mathbf{x})}{\partial\mathbf{x}} = \frac{\partial\phi(\mathbf{x})}{\partial\mathbf{x}} = \begin{bmatrix} M_g & 0 & 0 \\ 0 & B_{12}V\cos(\alpha) & B_{12}\sin(\alpha) \\ 0 & B_{12}\sin(\alpha) & -\frac{Q_L}{V^2} - B_{22} \end{bmatrix}$$

is a symmetric matrix, implying that $\mathbf{A}^{-1}\theta(\mathbf{x})$ is a gradient function. Therefore it is possible to define $\vartheta(\mathbf{x})$ by (2-7). Additionally, $\nabla\vartheta(\mathbf{x}) \equiv \phi(\mathbf{x})$ since

$$\nabla\vartheta(\mathbf{x}) = \nabla\int_{\mathbf{x}^s}^{\mathbf{x}} [\mathbf{A}^{-1}\theta(\mathbf{x})]^T d\mathbf{x}$$

$$= \nabla\int_{\mathbf{x}^s}^{\mathbf{x}} [\phi(\mathbf{x})]^T d\mathbf{x} = \phi(\mathbf{x}) - \phi(\mathbf{x}^s) = \phi(\mathbf{x})$$

From (2-7) it can be seen that $\vartheta(\mathbf{x})$ is the vector integral of $\phi(\mathbf{x})$ from $\mathbf{x}^s$ to $\mathbf{x}$, thus being dependent not only upon $\mathbf{x}$ but also upon $\mathbf{x}^s$; it can be characterized as an "energy difference" between the two states. However since the power systems under consideration here are assumed to have only a single stable equilibrium point of interest (the normal operating state of the system), for notational simplicity this dependence on $\mathbf{x}^s$ will be made to be implicit.

Formally, the previous definition of the Lyapunov function $\vartheta(\mathbf{x})$ is sufficient to show stability of $\mathbf{x}^s$ in the sense of Lyapunov, but not asymptotic stability. This is because we have not precluded the set

$$\Omega_c = \text{component of } \{\mathbf{x} \in \mathbf{R}^n : \vartheta(\mathbf{x}) \leq \vartheta^{cr}\} \text{ containing } \mathbf{x}^s$$

from containing trajectories of (2-1) where $\dot{\vartheta}(\mathbf{x}) \equiv \mathbf{0}$. If such a trajectory were to exist (other than the trivial trajectory $\mathbf{x}(t) \equiv \mathbf{x}^s$), the

value of $\vartheta(\mathbf{x})$ would never decrease, indicating that $\mathbf{x}$ is not converging to $\mathbf{x}^s$. However if $(\mathbf{A}+\mathbf{A}^T)$ is negative definite then Ω_C does not contain any trajectories where $\dot{\vartheta}(\mathbf{x}) \equiv \mathbf{0}$ (again other than the trivial trajectory $\mathbf{x}(t) \equiv \mathbf{x}^s$), and asymptotic stability can be shown by LaSalle's theorem. This would be the case in a physical system where all the diagonal elements of $\mathbf{A}$ are strictly less than zero.

For the two bus system under consideration here, with an equilibrium point $(0,\alpha^s,V^s)$, the Lyapunov function $\vartheta(\omega,\alpha,V)$ is given in closed form by:

$$\vartheta(\omega,\alpha,V) := \frac{1}{2} M_g\omega^2 - B_{12}V\cos(\alpha) + B_{12}V^s\cos(\alpha^s)$$
$$- \frac{1}{2}B_{22}V^2 + \frac{1}{2}B_{22}(V^s)^2 + P_L(\alpha-\alpha^s) + Q_L\ln\left(\frac{V}{V^s}\right) \qquad (2\text{-}8)$$

The function $\vartheta(\omega,\alpha,V)$ can be thought of as representing the energy of the system, with the first term representing the "kinetic energy" term, and the remaining terms representing the "potential energy" term. Using (2-8) it is possible to calculate the energy difference between any point in the (ω,α,V) space and the stable equilibrium point $\mathbf{x}^s$. For example, if we let P = 200MW and Q = 100MVAR, the per unit stable equilibrium point (i.e. the standard power flow solution) is (0,-13.52°,0.855). This solution can be verified by straightforward substitution into (2-6); note that the equilibrium point is independent

of the values of elements of **A**. Figure 2-4 plots the contours of this energy difference in the $\omega = 0$ plane. Since when $\omega = 0$ the system kinetic energy is zero, Figure 2-4 shows the potential energy well for the system at the specified values of P and Q.

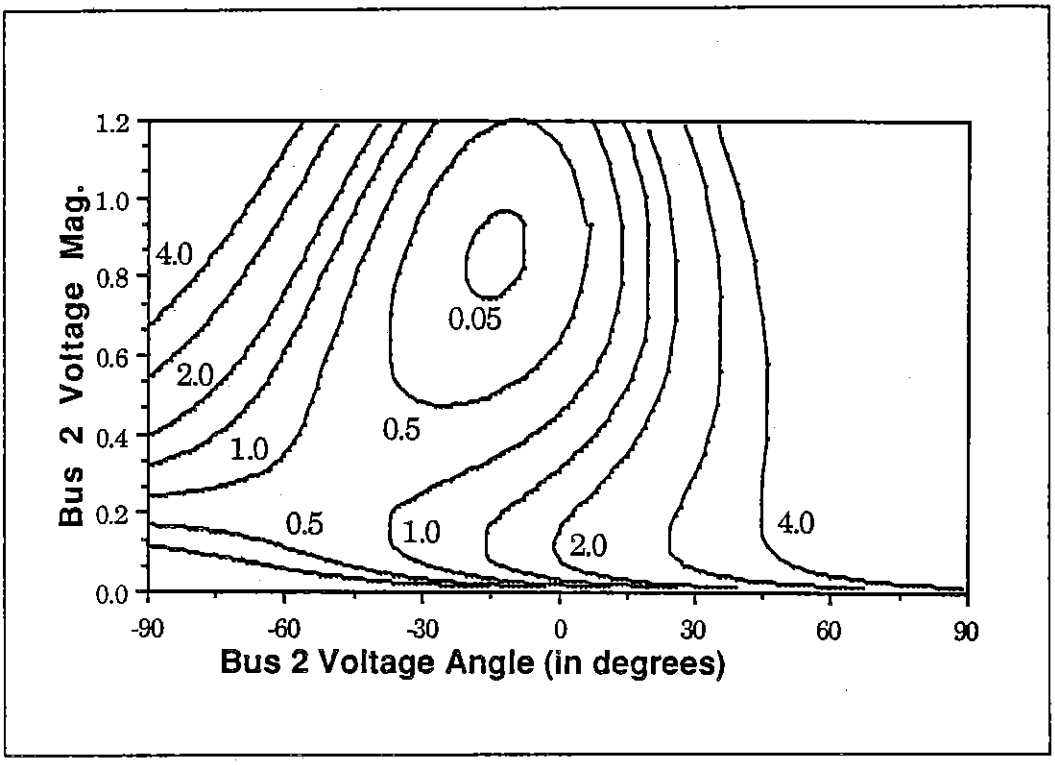

Figure 2-4 : Contours of Energy Function ϑ in α-V Space

To determine the depth of the energy well, it is necessary to calculate the value of the "nearest" saddle point, where $\nabla\vartheta(\mathbf{x}) = \mathbf{0}$. Geometrically, this is the first point $\mathbf{x}$, satisfying $\nabla\vartheta(\mathbf{x}) = \mathbf{0}$, encountered by expanding constant contours of ϑ from $\mathbf{x}^s$. Since **A** is

nonsingular, the only points where $\nabla\vartheta(\mathbf{x})$ is equal to zero are the equilibrium points of (2-6), where $\phi(\mathbf{x})$ is equal to zero. For the simple two bus system under consideration here, it is shown in [62] that such a system only has at most two equilibrium points and at most one saddle point. The equilibrium points correspond to the intersection of the two constraints shown in Figure 2-3. For the example loads of the previous paragraph, this second equilibrium is at (0, -49.91°, 0.261). The energy difference for this system can be found using (2-8) to be 0.8608. This value then provides a measure of the system security; it will be referred to as the energy measure.

The steady-state stability of each of these equilibrium points can be calculated by linearizing the system about each point and then determining the eigenvalues. The linearized equations are given by

$$\begin{bmatrix} \Delta\dot{\omega} \\ \Delta\dot{\alpha} \\ \Delta\dot{V} \end{bmatrix} = \begin{bmatrix} -M_g^{-1}D_g & -M_g^{-1}J_1 & -M_g^{-1}J_2 \\ 1 & -D_1^{-1}J_1 & -D_1^{-1}J_2 \\ 0 & -\frac{1}{\varepsilon}V^{-1}J_3 & -\frac{1}{\varepsilon}V^{-1}J_4 \end{bmatrix} \begin{bmatrix} \Delta\omega \\ \Delta\alpha \\ \Delta V \end{bmatrix} \quad (2\text{-}9)$$

with

$$J_1 = \frac{\partial f(\alpha,V)}{\partial \alpha}$$

$$J_2 = \frac{\partial f(\alpha,V)}{\partial V}$$

$$J_3 = \frac{\partial g(\alpha,V)}{\partial \alpha}$$

$$J_4 = \frac{\partial g(\alpha,V)}{\partial V}$$

Note that at an equilibrium point, where $g(\alpha,V) = 0$ by definition, we have

$$\frac{\partial [V^{-1} g(\alpha,V)]}{\partial V} = V^{-1} \frac{\partial g(\alpha,V)}{\partial V}$$

Define the 3 by 3 matrix from (2-9) as **B**. The stability of an equilibrium point could then be determined numerically by calculating the eigenvalues of **B**. An analytic calculation of the individual eigenvalues of the above system could, however, be quite difficult. Nevertheless, a number of properties concerning the stability of the above system can be determined analytically. Throughout the following analysis it will be assumed that M_g, D_g, D_l and ε are all strictly positive. The requirement that the generator inertia and damping constants, M_g and D_g, are strictly positive is satisfied for realistic generator models. The requirement that the load parameters, D_l and ε, are also strictly positive is based upon realistic load models and is normally satisfied in practice.

Define the determinant of the Jacobian of (2-3) and (2-4) (i.e. the power flow Jacobian):

$$J_{pf} = J_1 J_4 - J_2 J_3$$

Note that the definition of the power flow determinant, J_{pf}, assumes the elements of the power flow Jacobian are ordered so that the relationships between the state variables and the underlying state equations from (2-9) are maintained. Also define

$$c_1 = D_l^{-1} J_1 + (V\varepsilon)^{-1} J_4$$

$$c_2 = (M_g^{-1} D_g (D_l V\varepsilon)^{-1} + M_g^{-1} (V\varepsilon)^{-1})$$

The characteristic equation of **B** is then given by

$$\lambda^3 + (c_1 + M_g^{-1} D_g)\, \lambda^2 + (M_g^{-1} D_g c_1 +$$

$$(D_l V\varepsilon)^{-1} J_{pf} + M_g^{-1} J_1)\, \lambda + c_2 J_{pf} \qquad (2\text{-}9a)$$

The roots of the characteristic equation (2-9a) then determine the matrix's eigenvalues. The Routh-Hurwitz stability criterion can be used to determine the stability of the system [39]. Define the Routh array for (2-9) as

Column 1	Column 2
1	$(M_g^{-1}D_gc_1+M_g^{-1}J_1+(D_lV\varepsilon)^{-1}J_{pf})$
$(c_1+M_g^{-1}Dg)$	$c_2 J_{pf}$
$\dfrac{(M_g^{-1}D_gc_1+M_g^{-1}J_1)(c_1+M_g^{-1}D_g)+(c_1D_l^{-1}-M_g^{-1})(V\varepsilon)^{-1}J_{pf}}{c_1+M_g^{-1}D_g}$	0
c_2J_{pf}	0

The Routh-Hurwitz stability criterion then states that a necessary and sufficient condition for stability is that there are no sign changes in the first column of the array. Since the element in the first row of the above array is positive (it is equal to one), sufficient conditions for system stability could be developed by placing restrictions on the system parameters to insure that the remaining elements of the first column are positive.

Proposition (sufficient conditions for system stability)

The following are sufficient conditions for the stability of the system from (2-9):

1. M_g, D_g, D_l , V and ε are all strictly positive.

2. J_1 and J_4 positive
3. $J_2 * J_3$ non-negative
4. $J_{pf} > 0$

Proof

The first element in row 2 is positive by assumptions 1 and 2. This is because J_1, J_4, D_l , V and ε positive implies $c_1 > 0$. A sufficient condition for the first element in row 3 to be positive is that $J_2 * J_3$ be non-negative. The denominator is positive by the previous argument. The numerator can be rewritten as

$$(M_g^{-1} D_g c_1 + M_g^{-1} J_1)\, M_g^{-1} D_g + M_g^{-1} D_g c_1^2 + M_g^{-1} J_1 \; D_l^{-1} J_1$$

$$+ c_1 D_l^{-1} (V\varepsilon)^{-1} J_{pf} + M_g^{-1} (V\varepsilon)^{-1} J_1 J_4 \; - M_g^{-1} (V\varepsilon)^{-1} J_1 J_4$$

$$+ M_g^{-1} (V\varepsilon)^{-1} J_2 J_3$$

Canceling the second and third to last terms results in an expression with all terms strictly positive except for the last term, which is non-negative by assumption 3. The first element in row 4 is positive by assumptions 1 and 4. ♦

From (2-3) and (2-4) it can be seen that assumption 2 is satisfied if the angle across the transmission line is less than 90 degrees with B_{12}

positive and B_{22} negative. These assumptions are almost always satisfied in practice. Assumption 3 is always satisfied for the lossless case under consideration here because

$$\frac{\partial f(\alpha,V)}{\partial V} = V^{-1}\frac{\partial g(\alpha,V)}{\partial \alpha}$$

Therefore we can conclude that for a "normal" (as defined by assumptions 1 through 3) lossless two bus system, a sufficient condition for stability is that the determinant of the power flow Jacobian (as previously defined) is positive.

Proposition (sufficient conditions for system instability)

1. M_g, D_g, D_l , V and ε are all strictly positive.
2. $J_{pf} < 0$

Proof

By the Routh-Hurwitz stability criterion, the number of sign changes in elements of the first column of the Routh array determines the number of eigenvalues with strictly positive real parts. Since the first element in the first row is positive (it is equal to one), we only need show that at least one element in the first column is negative. Since $J_{pf} < 0$ by assumption 2 and $c_2 > 0$ by assumption 1, the first element in the last row is negative. ♦

Proposition System [2-9] can only lose stability by eigenvalues passing through the origin.

Provided M_g, D_g, D_l, V, and ε are all strictly positive, the system from (2-9) can not have purely imaginary eigenvalues (other than the trivial case of eigenvalues at the origin) when there are no other eigenvalues in the right half plane. Equivalently, the only way the system can lose stability is for an eigenvalue to pass from the left half plane through the origin into the right half plane. Similar results have previously been shown in [40] for the case of load buses modeled with fixed voltage magnitude (PV), and in [44] for the power system model considered here.

Proof

Assume the opposite, that the system loses stability by a pair of complex conjugate eigenvalues moving into the right half plane, not passing through the origin. At the point where they cross the imaginary axis, $|\mathbf{B}| \neq 0$ since $|\mathbf{B}|$ is equal to the product of the matrix's eigenvalues, and we have assumed that the system does not have a zero eigenvalue. However a necessary and sufficient condition for $|\mathbf{B}| \neq 0$ is that $J_{pf} \neq 0$ since

$$|\mathbf{B}| = -J_{pf}\left[M_g^{-1}D_g(D_1V\varepsilon)^{-1} + M_g^{-1}(V\varepsilon)^{-1}\right],$$

and all terms in parenthesis are assumed strictly positive.

However if $J_{pf} > 0$ all the eigenvalues have negative real parts, contradicting the original assumption that a pair of complex conjugate eigenvalues are on the imaginary axis. Conversely if $J_{pf} < 0$ the system has eigenvalues with strictly positive real part, contradicting the assumption that a stable system is losing stability with eigenvalues on the imaginary axis. Thus we've established a contradiction since we originally assumed that $J_{pf} \neq 0$. ♦

Therefore for the two bus lossless system, the stability of the equilibrium point can be determined by the sign of the determinant of the power flow Jacobian [41],[42]. For the second equilibrium point (0, -49.91°, 0.261) from above, the determinant of the Jacobian is -17.3, indicating it is unstable. Because the unstable equilibrium points are characterized by low voltage magnitudes, they will be referred to as "low voltage" solutions. The point (0, -49.91°, 0.261) is a saddle point, and hence can be used to measure the depth of the energy well.

The ability of the energy measure to predict vulnerability of a system to voltage collapse for the two bus system will be examined next. The problem to be solved is to quantify the voltage stability of a given system operating point, providing a measure of how far the system is from the point of voltage collapse. The system will lose its steady state stability, with subsequent voltage collapse, when the Jacobian of the two power flow equations is singular. Geometrically, this singular solution occurs when the active and reactive power constraint curves are tangent to one another. If either P or Q is increased further, the curves no longer intersect, and the power flow has no solution. For the two bus system it is straightforward to derive the algebraic expression describing the locus of point in the (P,Q) space where the Jacobian is singular. First observe that the Jacobian for the system is

$$\mathbf{J} = \begin{bmatrix} B_{12}V\cos(\alpha) & B_{12}V\sin(\alpha) \\ B_{12}V\sin(\alpha) & -2B_{22}V - B_{12}V\cos(\alpha) \end{bmatrix}$$

Points of singularity are identified by setting the determinant to zero, yielding the constraint

$$\det(J) = V\,(-2B_{12}B_{22}V\cos(\alpha) - (B_{12})^2) = 0$$

Ignoring the unrealistic case of V = 0, the determinant is zero for all (α,V) pairs satisfying

$$V\cos(\alpha) = \frac{-B_{12}}{2B_{22}}$$

Since from (2-3) and (2-4) each point in the (α,V) space maps to only one point in the (P,Q) space, the locus of points which satisfy the above equation can be plotted in the (P,Q) space. These points are shown in Figure 2-5. Note that the boundary between the feasible and infeasible regions is only a function of the system parameters B_{12} and B_{22}. Since the boundary is defined as the set of loads whose constraint curves are tangent, each point on the boundary has only a single power flow solution. Hence the energy measure associated with these points is identically zero since the upper and lower limits of the integral in (2-7) are identical. For each point contained within the feasible region an energy measure can be calculated by first determining both the normal operating point solution (i.e $\mathbf{x}^s$) and the low voltage solution (i.e. $\mathbf{x}^u$), and then calculating the energy measure using (2-7). The contours of these energy measures are shown in Figure 2-6. Since the points in the infeasible region do not have power flow solutions, their energy measures are not defined.

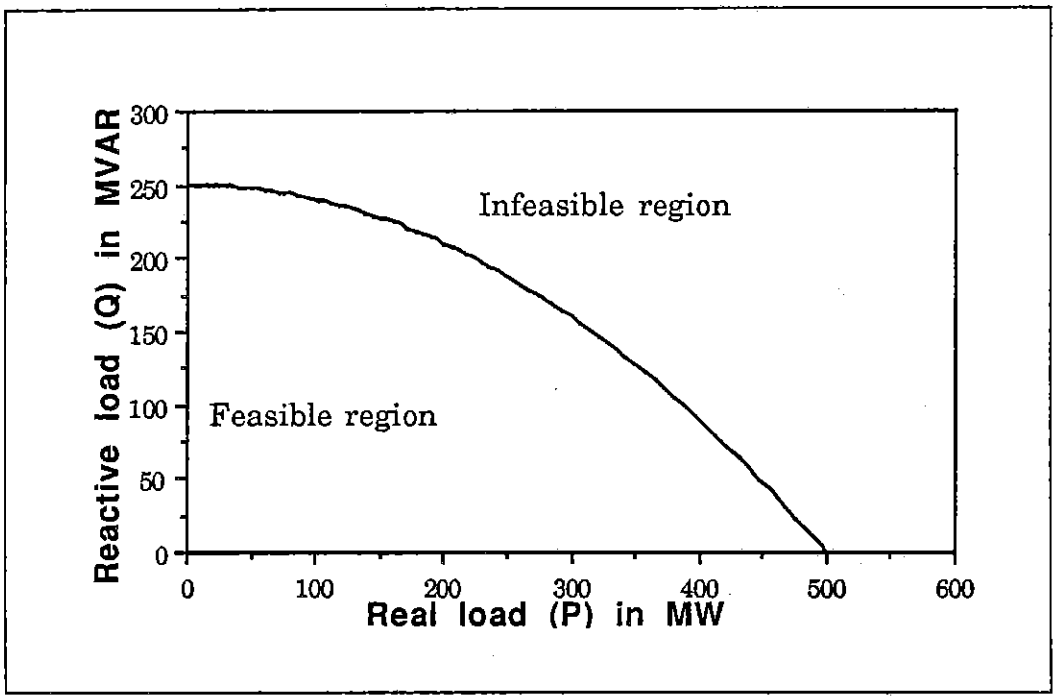

Figure 2-5 : Locus of Points where Power Flow Jacobian is Singular

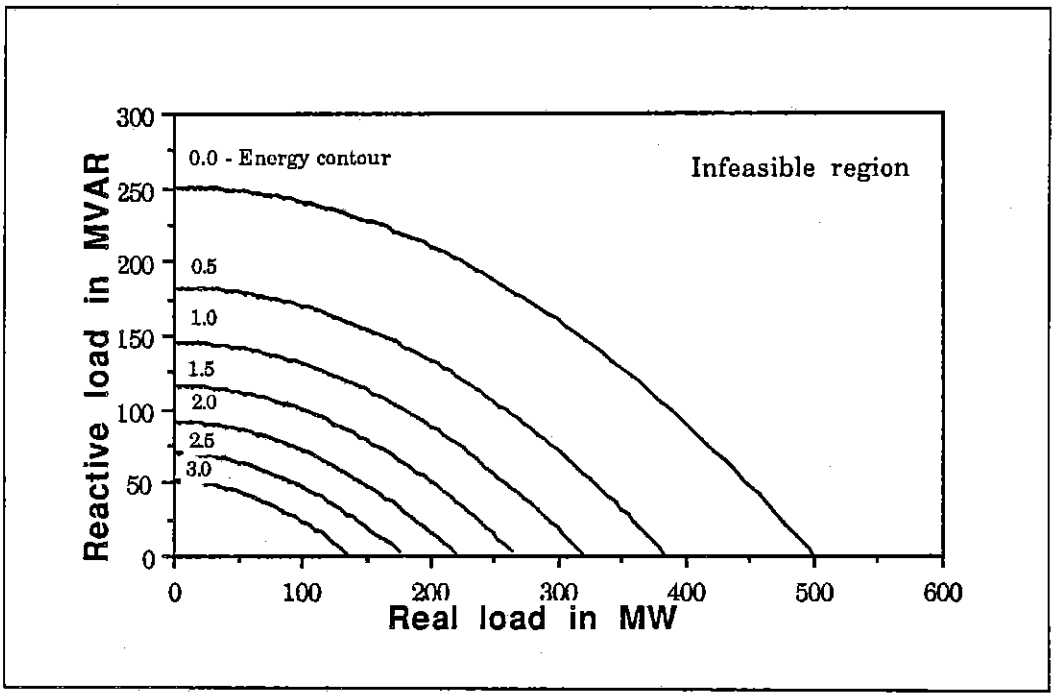

Figure 2-6 : Contours of Energy Function ϑ in P-Q Space

Interestingly, the energy contours in Figure 2-6 are both parallel to the feasible region boundary and fairly evenly spaced. Recognizing this, various frozen equilibrium points (operating states) could be ranked, according to their proximity to the feasible region boundary, by their energy measures. The usefulness of this method's ability to rank operating points is illustrated in the following example. Consider a fairly typical scenario where P(t) and Q(t) are slowly varying functions of time which are not known a priori. Also assume that the operating point is sampled at a rate so that relatively small variations in P and Q occur between sample periods. At each sample period

we'd like to calculate a proximity index which tells us how close the system is to voltage collapse so that corrective action can be taken if needed. For such an approach to provide useful results, a number of criteria should be satisfied by the proximity index.

First, we need to know beforehand what value of the index corresponds to voltage collapse. Therefore a simplistic approach of watching the voltage magnitude at the load bus would not work since we have no idea beforehand of the voltage magnitude at which voltage collapse will occur. The energy method provides this functionality since voltage collapse occurs by definition when the energy measure is zero. Second, in order for the proximity index to adequately predict how close a system is to voltage collapse, it must vary in a smooth, ideally linear, manner with respect to continuous changes in the system (i.e. does not exhibit discontinuous changes in value for small system changes). It can be seen that the energy method has this characteristic by noting that the contours in Figure 2-6 are fairly uniformly spaced. Third, the index should be relatively insensitive to the assumed path the system will take from the current operating point (for which the index is to be determined), and the point where the system is assumed to reach the feasible region boundary. This insensitivity is needed because future load variations are known only approximately at best. Strong dependence upon an assumed path could result in inaccurate rankings of various operating points.

Consider the case where the current operating point is close to the boundary, but the assumed path is parallel to, or away from, this boundary. The operating point would be ranked as quite secure, even though a slight variation in the actual path from the assumed path could result in loss of steady state stability. Since in the energy method no assumption is made about future system load variation, this criteria is also met. Lastly, the computational time to calculate the index must be suitable for on-line use. The scalar energy measure is determined by solving for the current operating point (α^s, V^s) and for the unstable equilibrium (α^u, V^u), and then simply calculating the energy difference.

Based on the insights gained from the lossless 2 bus system, the energy function approach appears to be a promising indicator of proximity to voltage collapse. Subsequent analysis and examples will show that its desirable properties also carry through to realistically sized networks. Completing the example from the penultimate paragraph, Figure 2-7 shows how the energy measures varies as the load at bus 2 is increased so that the P/Q ratio remains constant at 2. Recall that in the calculation of the energy measures for a given operating point, no assumptions are needed concerning the future variation in the load.

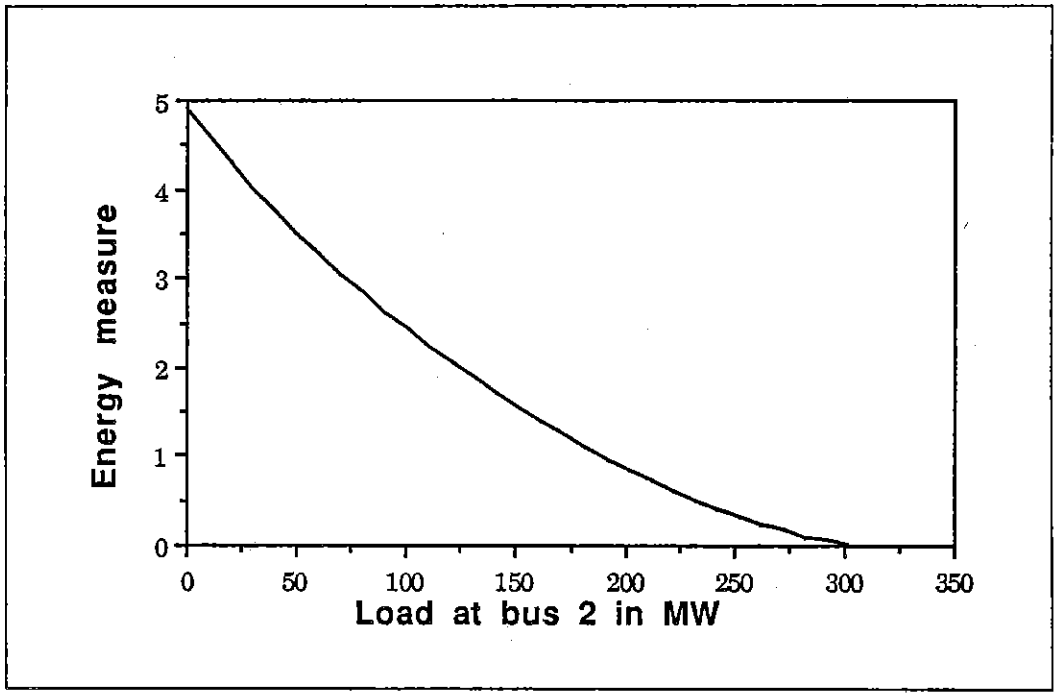

Figure 2-7 : Energy Measure versus Load Level for Two Bus System

For the lossless system previously studied it is possible to define an energy function which is truly a Lyapunov function. That is one in which energy is continuous and nonincreasing along all trajectories, and with the stable operating point as a local minimum of ϑ. This is no longer the case when losses are considered. Consider the realistic extension of (2-3) and (2-4) to include transmission line losses:

$$P_L + G_{11}V^2 + B_{12}V\sin(\alpha) + G_{12}V\cos(\alpha) = f_{lossy}(\alpha,V) = 0$$
$$Q_L - B_{22}V^2 - B_{12}V\cos(\alpha) + G_{12}V\sin(\alpha) = g_{lossy}(\alpha,V) = 0 \qquad (2\text{-}10)$$

Equation (2-6) could then be rewritten, substituting f_{lossy} and g_{lossy} for f and g respectively. In trying to derive a Lyapunov function for this system of equations, we note that Theorem 2.1 can no longer be applied to obtain a Lyapunov function because

$$\frac{\partial \phi(x)}{\partial x} = \begin{bmatrix} M_g & 0 & 0 \\ 0 & B_{12}V\cos(\alpha)-G_{12}V\sin(\alpha) & 2G_{11}V+B_{12}\sin(\alpha)+G_{12}\cos(\alpha) \\ 0 & B_{12}\sin(\alpha)+G_{12}\cos(\alpha) & -\frac{Q_L}{V^2} - B_{22} \end{bmatrix}$$

is no longer symmetric. In general for the case of a multimachine power system with losses, no global Lyapunov function has yet been found [43]. Instead the lossless Lyapunov function from (2-8) is used to approximate the behavior of the system. Since losses are included in system differential equations, but not in ϑ, the derivative of ϑ along all trajectories

$$\dot{\vartheta}(x) = \begin{bmatrix} M_g\omega & f(\alpha,V) & V^{-1}g(\alpha,V) \end{bmatrix} A \begin{bmatrix} M_g\omega \\ f_{lossy}(\alpha,V) \\ V^{-1}g_{lossy}(\alpha,V) \end{bmatrix}$$

can no longer be guaranteed to be non-positive. Therefore ϑ is no longer formally a Lyapunov function; for the remainder of this thesis the term energy function will be used instead. Also since analysis will focus on the value of ϑ at equilibrium points, where $\omega = 0$ by definition, ϑ will no longer be written as a function of ω.

Another consequence of including losses in the system model is that $\vartheta(\alpha^s,V^s)$ no longer defines a local minimum of the ϑ function as defined in (2-8). A necessary condition for a local minimum of ϑ at (α^s,V^s) is that $\nabla\vartheta(\alpha^s,V^s) = \mathbf{0}$. However

$$\nabla\vartheta(\alpha^s,V^s) = \begin{bmatrix} f(\alpha^s,V^s) \\ V^{-1}g(\alpha^s,V^s) \end{bmatrix}$$

$$= \begin{bmatrix} f_{lossy}(\alpha^s,V^s) \\ V^{-1}g_{lossy}(\alpha^s,V^s) \end{bmatrix} - \begin{bmatrix} G_{12}V\cos(\alpha) \\ V^{-1}G_{12}V\sin(\alpha) \end{bmatrix}$$

is no longer $\mathbf{0}$ since

$$\begin{bmatrix} f_{lossy}(\alpha^s,V^s) \\ g_{lossy}(\alpha^s,V^s) \end{bmatrix} = \mathbf{0}$$

by definition of an equilibrium point and $G_{12} \neq 0$ for a lossy system. This difficulty can be resolved in the neighborhood of the stable operating point (α^s, V^s) by redefining f and g used in (2-7) to be

$$\begin{aligned} P_L + B_{12}V\sin(\alpha) + G_{12}V^s\cos(\alpha^s) + G_{22}(V^s)^2 &= f(\alpha,V) \\ Q_L - B_{22}V^2 - B_{12}V\cos(\alpha) + G_{12}V^s\sin(\alpha^s) &= g(\alpha,V) \end{aligned} \tag{2-11}$$

Since the added terms in (2-11) are constants with respect to the variable of integration in (2-7), the vector function remains exactly integrable (i.e. no path dependence). With the addition of these constant offset terms, the gradient of the energy function at the stable equilibrium point is now identically zero. Note also that although the only explicit dependence of ϑ upon the system transfer conductances is through these offset terms, ϑ is implicitly dependent upon the transfer conductances since both of the limits of (2-7) reflect the influence of transfer conductances.

Using the redefined power balance equations (2-10), the revised energy function for the two bus system (2-8) is now

$$\begin{aligned} \vartheta(\omega,\alpha,V) := \; & \frac{1}{2}M_g\omega^2 - B_{12}V\cos(\alpha) + B_{12}V^s\cos(\alpha^s) - \frac{1}{2}B_{22}V^2 \\ & + \frac{1}{2}B_{22}(V^s)^2 + P_L(\alpha-\alpha^s) + Q_L\ln\left(\frac{V}{V^s}\right) \end{aligned}$$

$$+ \quad (G_{12}V^s\cos(\alpha^s) + G_{22}(V^s)^2)\,(\alpha-\alpha^s)$$
$$+ G_{12}V^s\sin(\alpha^s)\,(\frac{V}{V^s}) \qquad (2\text{-}12)$$

As was done earlier, this revised function can be used to calculate an associated energy difference for any feasible load point (P,Q) in a system which includes transmission line losses. For example Figure 2-8 plots the energy contours of the system used for Figure 2-5 but with the addition of conductance terms $G_{12} = -G_{22} = -5.0$. As was the case with the earlier figure, the energy contours are again both parallel to the feasible region boundary and fairly evenly spaced. This suggest that the modified energy approach still provides a good index of proximity to voltage collapse in a two bus system, even when transmission line losses are included. In the next section the approach is extended to an arbitrary sized system.

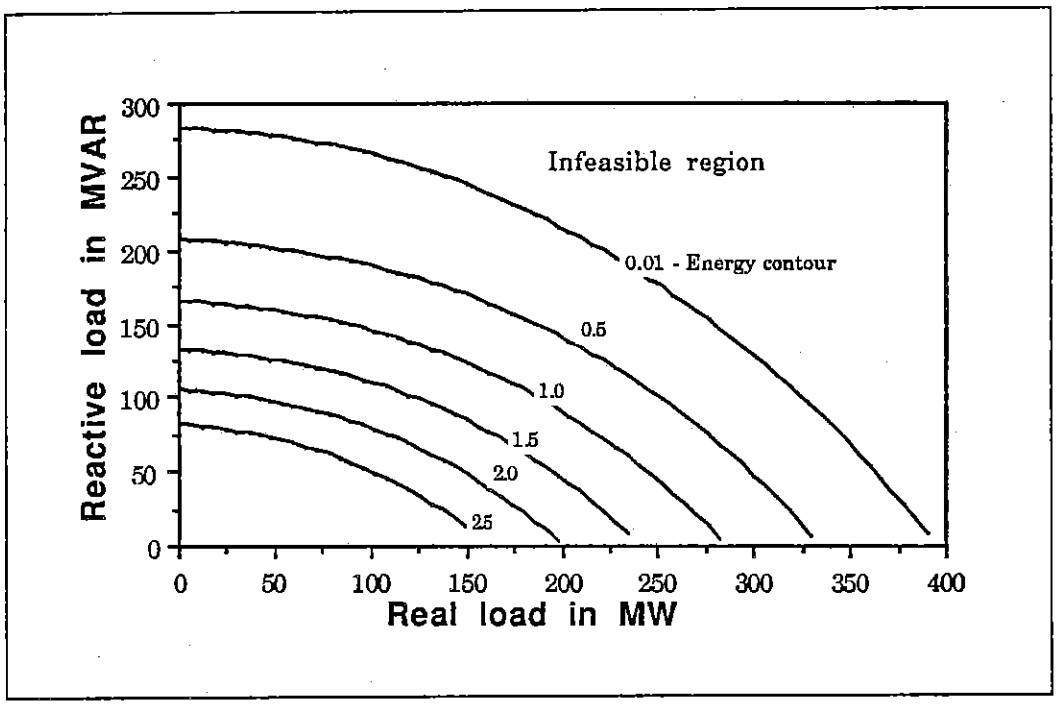

Figure 2-8 : Contours of Energy Function ϑ for Two Bus System with Losses

2.3 Application to Multiple Bus Power Systems

The two bus system model used in earlier sections allows simple graphical display of the concepts being developed but is, of course, much too small to analyze all but the simplest of power systems. Today it is quite common for utilities to include several thousand buses in their power system models in order to accurately model the behavior of their electrical systems. In this section the extension of

the energy function method to multiple bus system is discussed. Before delving into a discussion of the application of energy functions to multiple bus systems, it is important to clarify one point. For the two bus system the calculation of the operable and the low voltage solutions was straightforward; there was at most one low voltage solution. In general this is no longer the case for systems with more than two buses. Throughout this section the assumption is made that both the operable solution and the appropriate low voltage solutions of the power flow equations are available. The current operating point (or high voltage solution) is normally either available on-line from the state estimator, or known in a planning study. The means of calculating the appropriate low voltage solutions is touched upon in this section, but will be examined in much more detail in Chapters 3 and 4.

The system dynamics from (2-5) can be generalized for a system of arbitrary size. Assume that for an n bus system, the buses are partitioned so that the n_L load buses are numbered 1 through n_L, and the n_G generator buses are number n_L+1 through n. Bus n is chosen as the system slack. The system dynamics can then be written in matrix form as [44]:

$$\dot{\omega}_g = - \mathbf{M}_g^{-1}\mathbf{D}_g\omega_g - \mathbf{M}_g^{-1}\mathbf{T}_2^{T}\mathbf{f}(\alpha,\mathbf{V}) \qquad (2\text{-}13a)$$

$$\dot{\alpha} = \mathbf{T}_2\omega_g - \mathbf{T}_1\mathbf{D}_l^{-1}\mathbf{T}_1^T f(\alpha,V) \quad (2\text{-}13b)$$

$$\varepsilon\dot{V} = -\mathbf{V}^{-1}g(\alpha,V) \quad (2\text{-}13c)$$

where

$$\omega_g = [\omega_{n_L+1},\ldots,\omega_n]^T$$

$$\alpha = [\alpha_1,\ldots\alpha_n]^T$$

$$\mathbf{V} = [V_1,\ldots,V_n]^T$$

$$\mathbf{M}_g = \text{diag}\{M_{gn_L+1},\ldots,M_{gn}\} \quad (M_{gi} > 0)$$

$$\mathbf{D}_l = \text{diag}\{D_1,..,D_{n_L}\} \quad (D_i > 0)$$

$$\mathbf{D}_g = \text{diag}(D_{n_L+1},\ldots,D_n\} \quad (D_i > 0)$$

$$\mathbf{T}_1 = \begin{bmatrix} \mathbf{I}_{n_L} \\ \ldots \\ \mathbf{0} \end{bmatrix} \in R^{(n-1)\ x\ n_L}$$

$$\mathbf{T}_2 = \begin{bmatrix} \mathbf{0} & \\ \ldots & -\mathbf{e} \\ \mathbf{I}_{n_G-1} & \end{bmatrix} \in R^{(n-1)\ x\ n_G}$$

$$\mathbf{e} = [1,\ldots,1]^T$$

ε = Constant positive diagonal matrix of parameters for singularly perturbed system model.

The power flow equations at each bus, f_i and g_i, can be written as

$$f_i(\alpha,V) = P_i - \sum_{j=1}^{n} B_{ij}|V_i||V_j|\sin(\alpha_i-\alpha_j)$$

$$- \sum_{j=1}^{n} G_{ij} |V_i| |V_j| \cos(\alpha_i - \alpha_j) \qquad (2\text{-}14a)$$

$$g_i(\alpha, V) = Q_i(V_i) + \sum_{j=1}^{n} B_{ij} |V_i| |V_j| \cos(\alpha_i - \alpha_j)$$

$$- \sum_{j=1}^{n} G_{ij} |V_i| |V_j| \sin(\alpha_i - \alpha_j) \qquad (2\text{-}14b)$$

where

B_{ij}, G_{ij} - Susceptance and conductance between buses i and j

V_i - Voltage magnitude at bus i

α_i - Voltage angle at bus i

P_i - Real power injection into the network at bus i (thus generation is positive, load is negative)

$Q_i(V_i)$ - Reactive power injection into the network at bus i, specified as a (once) differentiable function of bus voltage.

In a similar manner to what was done for the two bus case, a scalar energy function ϑ can be developed using (2-7). In [45], it is shown that for a lossless system (i.e $\mathbf{G} = \mathbf{0}$) ϑ is formally a Lyapunov function. However for ϑ to define a true Lyapunov function, the construction does place restrictions on allowable load models.

Reactive power demand may, for example, be an arbitrary polynomial or exponential function of bus voltage magnitude; path independence of the generalized integral from (2-7) requires that active power demand not depend on bus voltage magnitudes. However, experience in energy functions for transient stability studies [46] has shown that a path dependent integration may be used to represent voltage dependent real loads, with the resulting energy function still approximating many properties of a Lyapunov function. As an alternative, a local correction that adds a constant term similar to that employed for losses may be employed.

Additionally, the development of ϑ places restrictions on the allowable models of system dynamics. In particular the generator excitation control loop is not modeled in detail; the assumption being that the voltage control loop is stable. The model employed here assumes a type of fast exciter representation with reactive power output of a generator allowed to vary in order to hold its bus voltage constant. Exciter saturation is included by restricting the allowable reactive power output. If a limit is reached, the exciter is considered saturated, and the generator's reactive output is held constant at that limit. This is a standard approach to treating generator voltage control in power flow calculations. However, as discussed in [47], if the flux decay dynamics and excitation control loop introduce instabilities, then the system may experience voltage instabilities associated with

complex eigenvalues crossing the imaginary axis when the energy function is nonzero. The use of the energy function method to predict vulnerability to voltage instabilities is here restricted to those cases where voltage instability is caused by the loss of the steady state equilibrium point (i.e. singularity of the power flow Jacobian).

For the energy function method to accurately handle realistic system models, which include losses, it is important that the effects of the conductance matrix **G** be included. A difficulty which could arise if ϑ did not include the effects of **G** would be that of $(\alpha^s, \mathbf{V}^s)$ no longer defining a local minimum of the ϑ. As was done for the two bus case, this difficulty is resolved at the stable operating point $(\alpha^s, \mathbf{V}^s)$ by redefining **f** and **g** used in the integral definition of ϑ to be

$$f_i(\alpha,V) = P_i(V_i) - \sum_{j=1}^{n} B_{ij} |V_i| |V_j| \sin(\alpha_i-\alpha_j) - \sum_{j=1}^{n} G_{ij} |V_i^s| |V_j^s| \cos(\alpha_i^s-\alpha_j^s) \qquad (2\text{-}15a)$$

$$g_i(\alpha,V) = Q_i(V_i) + \sum_{j=1}^{n} B_{ij} |V_i| |V_j| \cos(\alpha_i-\alpha_j) - \sum_{j=1}^{n} G_{ij} |V_i^s| |V_j^s| \sin(\alpha_i^s-\alpha_j^s) \qquad (2\text{-}15b)$$

Since at (α^s,V^s) equations (2-15) are identical to (2-14), the gradient of the energy function at the stable equilibrium is now identically zero. The revised form of the energy function can then be expressed in closed form as [31]:

$$\vartheta(\mathbf{x}^u) = -\frac{1}{2}\sum_{i=1}^{n}\sum_{j=1}^{n}B_{ij}|V_i^u||V_j^u|\cos(\alpha_i^u-\alpha_j^u)$$

$$+\frac{1}{2}\sum_{i=1}^{n}\sum_{j=1}^{n}B_{ij}|V_i^s||V_j^s|\cos(\alpha_i^s-\alpha_j^s)$$

$$-\begin{bmatrix} V_i^u \\ \sum_{i=1}^{n}\int \frac{Q_i(x)}{x}dx \\ V_i^s \end{bmatrix} - \mathbf{P}^T(\alpha^u-\alpha^s)$$

$$-\sum_{i=1}^{n}\left[\sum_{j=1}^{n}G_{ij}|V_i^s||V_j^s|\cos(\alpha_i^s-\alpha_j^s)(\alpha_i^u-\alpha_i^s)\right]$$

$$-\sum_{i=1}^{n}\left[V_i^s\right]^{-1}\sum_{j=1}^{n}G_{ij}|V_i^s||V_j^s|\sin(\alpha_i^s-\alpha_j^s)\ (V_i^u-V_i^s) \qquad (2\text{-}16)$$

In deriving (2-16), the integration in (2-7) was assumed to be between the stable equilibrium point (α^s,V^s) and an unstable equilibrium point (α^u,V^u); it thus represents only the potential component of the system

energy. However to assess system voltage security, only the values of the energy function at the equilibrium points (where $\omega = \mathbf{0}$ by definition) need to be computed. We are thus only concerned with the potential energy function, which is a function of the voltage magnitudes and angles, but not of ω. Additionally, for notational simplicity the dependence of $\vartheta(\mathbf{x}^u)$ upon the stable operating point $\mathbf{x}^s$ will not be explicitly identified.

The evaluation of the summation terms in (2-16) is straightforward. Since the equations are sparse (i.e. many of the B_{ij} and G_{ij} terms are identically zero), the computational cost for calculating these sums is small (much less than that of a single power flow solution iteration). For the non-generator buses, the integral term can be quite easily evaluated, provided the reactive load is modeled in the common form of either a polynomial or exponential function of bus voltage. For example, if the reactive load at bus i is modeled as a constant component plus component linearly dependent upon the bus i voltage magnitude

$$Q_i = k_1 + k_2 V_i$$

then the integral evaluates to

$$k_1 \ln \left(\frac{V_i^u}{V_i^s} \right) + k_2 (V_i^u - V_i^s) \qquad (2\text{-}17)$$

At the generator buses in the system the voltage magnitude is generally specified, rather than the reactive power output. The reactive injection at the generator bus then is assumed to vary in order to hold its bus voltage within a small tolerance of a specified voltage (the voltage setpoint). Exciter saturation is modeled by representing the reactive output of the generator as a function of terminal voltage, with saturation to specified upper and lower limits. With this model, the mathematical framework for treating voltage regulating generators is identical to that for voltage dependent reactive loads. A typical reactive power output versus terminal voltage characteristic is shown in Figure 2-9.

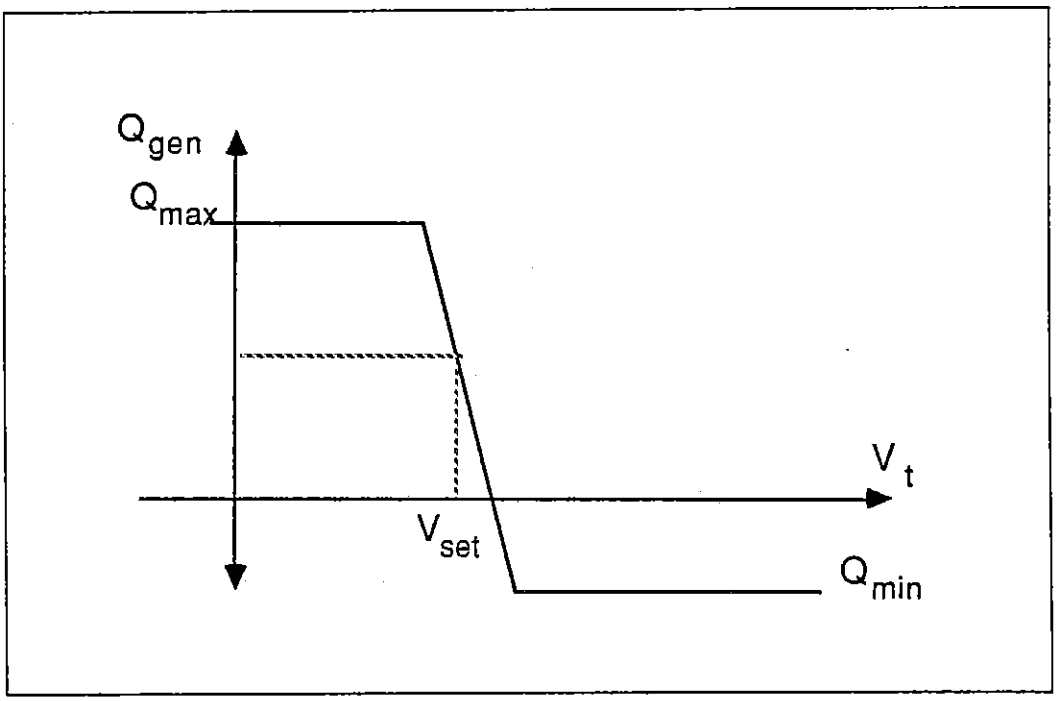

Figure 2-9 : Generator Reactive Output versus Terminal Voltage

If the reactive output of a given generator has not yet reached a limit at both the high or low voltage solution, then the deviation from this voltage setpoint is assumed to be very small. Thus the resulting integral term is negligible because the limits of integration are nearly identical. It is, however, quite common for a number of generators to be pushed to their limits in the low voltage solution, while the generators are still regulating in the high voltage solution. In that case the integral term is well approximated by

$$Q_{lim(max)} * \ln\left[\frac{V_i^u}{V_i^s}\right] \qquad (2\text{-}18)$$

The rationale for this approximation is that along the integration path from the high solution V_i^s to the low solution V_i^u, the reactive output of the generator would rapidly saturate once the voltage had moved outside the small tolerance about its setpoint (Figure 2-9), and thus may be considered as a constant. This is to be expected since the generator bus is saturated along most of the path of integration and thus would behave as a constant reactive power source.

The application of energy methods to multiple bus system is more formidable than for the case of a two bus system because of the possible presence of multiple low voltage solutions. As the first step in complexity beyond the two bus system, consider the system shown in Figure 2-10. The system consists of a strong generator bus (an infinite or slack bus), with two separate load buses connected to the generator through realistic (i.e. with losses) transmission lines. This system could be a rough representation of a large generating area supplying power to two separate urban centers. Mathematically the system is equivalent to two independent two bus systems; it is clear that there are at most four power flow solutions (both load buses at the high solution, one high and the other low, or both low) for this system.

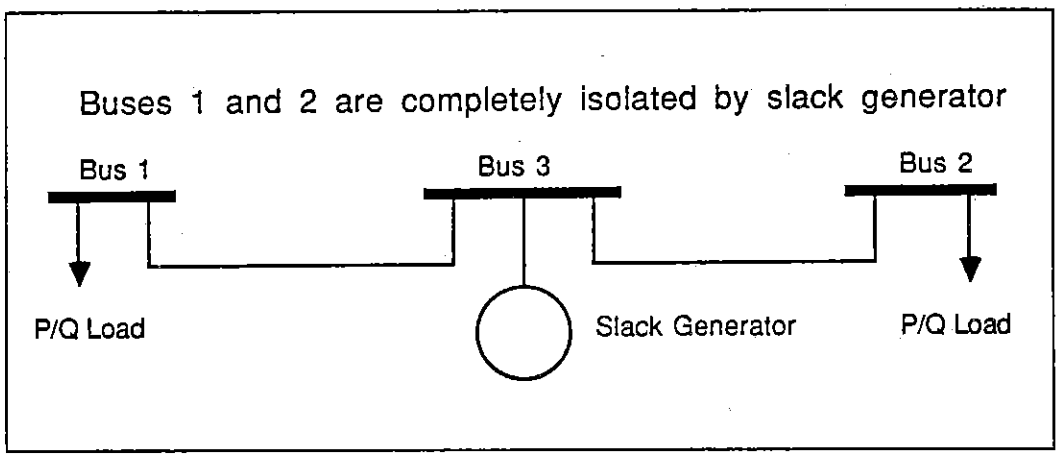

Figure 2-10 : One-line Diagram for Double Radial System

Using (2-16), an energy measure could then be calculated for each of these low voltage solutions. The presence of multiple energy measures requires that an explanation be provided as to their individual significance. For the uncoupled three bus system, the independence of the two load buses allows for a straight forward interpretation of the energy measures. An energy measure found using the solution with one bus high and the other low can be used as a proximity indicator for voltage collapse at the bus with the depressed voltage magnitude. Since the two loads are truly independent, the risk of voltage collapse at each bus is also independent. Thus to provide a complete assessment of the system voltage stability, the two independent security measures, provided by evaluating the energy function at the individual low voltage solutions,

are needed. The energy measure calculated using the solution with both buses low is simply the sum of the other two indicators; it is interpreted to represent the risk of voltage collapse occurring simultaneously in both areas. Since energy measures are available using the other low voltage solutions for each separate area, this value is not needed. Therefore only the first two low voltage solutions are of interest. The key point is that a single measure could not be used to adequately assess the system's voltage stability.

The next logical extension of this system is to couple the two loads by adding a third transmission line between them (Figure 2-11). Additionally, a generator is added at bus 1, but is assumed to be initially off-line. The question then is to determine the voltage security of the system when it is characterized by a given load distribution (P_1,Q_1,P_2,Q_2). In the remainder of this section the applicability of the energy method to providing such a measure is demonstrated.

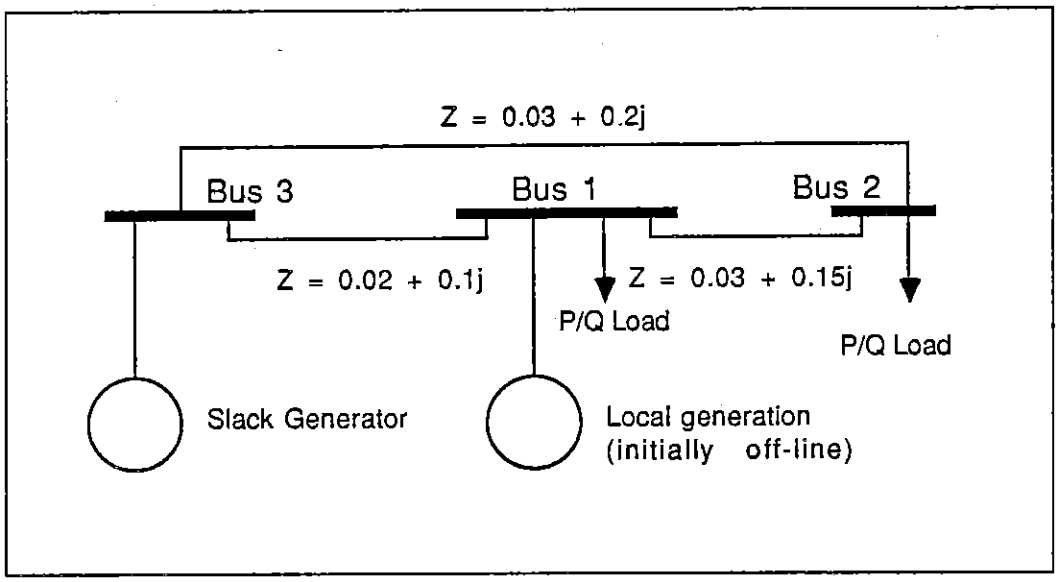

Figure 2-11 : One-line Diagram for Coupled Three Bus System

To determine the voltage vulnerability of this system using the energy approach, it is first necessary to calculate the appropriate low voltage solutions. Theoretically for an n bus power system there are believed to be at most 2^{n-1} solutions of the power flow equations [48], [33]. However for a large system there are normally substantially fewer solutions, and only a small subset of these will need to actually be determined. The technique used here is to only consider those equilibrium points which are of type-one. A type-one equilibrium point is one in which a single eigenvalue of the linearized system about that equilibrium point has a positive real part. The motivation for this approach comes from [49] where it is shown that for system models of the type examined here (2-13) will generically lose steady

state stability by a saddle node bifurcation between the SEP and a type-one UEP. Note that as was mentioned earlier, the models do not include detailed representation of the generator voltage control loop; fast exciter representation is assumed.

Classifying low voltage solutions as type-one raise the issue of identifying the stability properties of a power flow solution with respect to the linearized dynamic model. A number of authors have examined the issue of relating small disturbance stability of the linearized power system dynamics to the eigenvalues of the power flow Jacobian (see [47] and references therein). In [44] it is shown that the Jacobian of (2-13) and the Jacobian of the power flow equations (2-14) have the same number of eigenvalues with positive real part. Therefore the low voltage solutions can be classified as type-one by examining at the eigenvalues of the power flow Jacobian.

Returning to the three bus system, with the assumption of constant load power factor (making Q_1 and Q_2 dependent variables), Figure 2-12 plots the energy contours of the feasible region in the (P_1,P_2) space. As was the case in Figure 2-6, the energy contours are nearly parallel to the feasible region boundary and fairly evenly spaced. This again suggests that the energy measures provide a method of ranking the operating points (frozen equilibrium points) of the system.

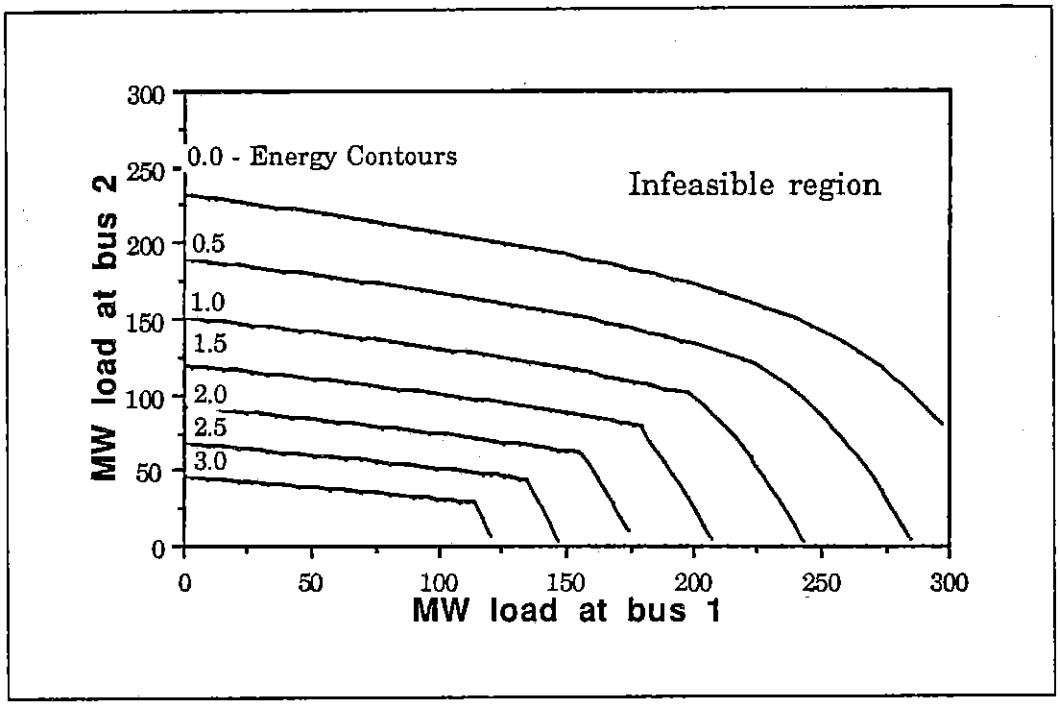

Figure 2-12 : Energy Contours for Three Bus System in P_1-P_2 Space

It is important to note that the computation required for the construction of Figure 2-12 was not as simple as for the two bus case. Since in a multi-bus power system there is often more than a single low voltage solution, there are correspondingly often more than a single energy measure. For the coupled three bus system one may identify a single SEP, two type-one UEPs, and a single UEP of type greater than one. This can be illustrated by plotting the voltage magnitudes at buses 1 and 2 for each solution as the system load is varied. For an initial load of 20 MW and 10 MVAR at each load bus, four solutions are possible. Figure 2-13 shows the solutions trajectories in the (V_1,V_2) space as the loads at both buses are

increased proportionally, maintaining a constant power factor. The initial starting voltage points are labeled 1,2,3 and 4. Table 2-1 lists the four eigenvalues of the power flow Jacobian, associated with each initial equilibrium point. As can be seen, solution one is an SEP, while solutions two and three are type-one UEPs, and solution four is a type-two UEP.

Solution #	Eigenvalues			
1	-19.9 + 3.9j	-19.9 - 3.9j	-6.6 + 1.1j	-6.6 - 1.1j
2	5.6	-0.5	-2.1	-4.3
3	-8.6	-6.5	4.0	-0.5
4	4.4	-0.5	-0.6	2.0

Table 2-1 - Solution Eigenvalues

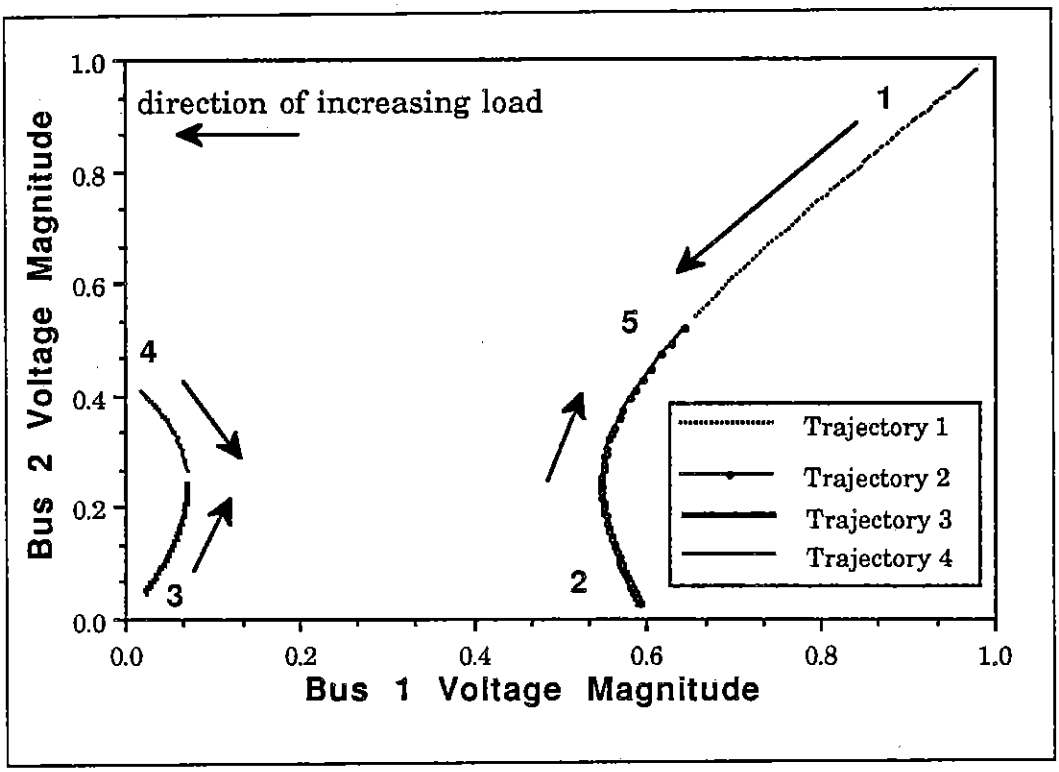

Figure 2-13: Variation in Voltage Magnitudes as Load is Increased

As the load is uniformly increased at buses 1 and 2, trajectory 1 moves downward to the left, indicating that the voltages at both buses are falling. This is reasonable behavior for a power system without voltage regulation. Eventually the voltage collapse point is reached (labeled point 5); at this critical point the Jacobian becomes singular and no further increase in load is possible. The power system loses its stable equilibrium point through a saddle node bifurcation with solution from trajectory 2. Subsequently, the deterministic dynamics of the system would then display a number of negative dV/dt terms,

indicating voltage collapse. Likewise, as the load is increased from its initial value, the solutions associated with the three low voltage solutions also move in the directions shown. However at a load level significantly less than the load associated with the critical point, the solutions associated with trajectories 3 and 4 coalesce. This occurs at a load of $P_1 = P_2 = 67$ MW; at this point the Jacobian of the power flow equations is singular. For further increases in load these two solutions no longer exist. As the load is further increased, trajectory 2 continues upward, eventually meeting with trajectory 1 at point 5.

Thus the number of power flow solutions is dependent upon the loading of the system. In general as the loading on a system increases the number of solutions tends to decrease, with the solutions vanishing (or occasionally appearing) in pairs [33]. As the system approaches the voltage collapse critical point, the number of solutions typically goes to two. These two solutions eventually coalesce at the critical point. For the example system this occurred at a load of $P_1 = P_2 =$ 192 MW.

An alternative way to present the voltage collapse scenario is to plot the energy measures associated with each of the low voltage solutions as a function of the system load. This is shown in Figure 2-14. Since there are initially three low voltage solutions, there are three energy measures. However as the load is increased, the upper two energy

measures vanish when their respective solutions coalesce. For higher loads there is only a single energy measure for the system. The near linearity of the lower energy measure curve in the figure is due to the evenly spaced contours of Figure 2-12 parallel to the feasibility region boundary. To construct Figure 2-12 for those loadings with more than one associated energy difference, the lowest energy difference was chosen (which was always associated with a type-one equilibrium). When there was only a single low voltage solution (such as in the example above for loads greater than 67 MW) then that energy measure was used. Figure 2-15 shows the energy contours in the (P_1,P_2) space associated with the individual type-one solutions.

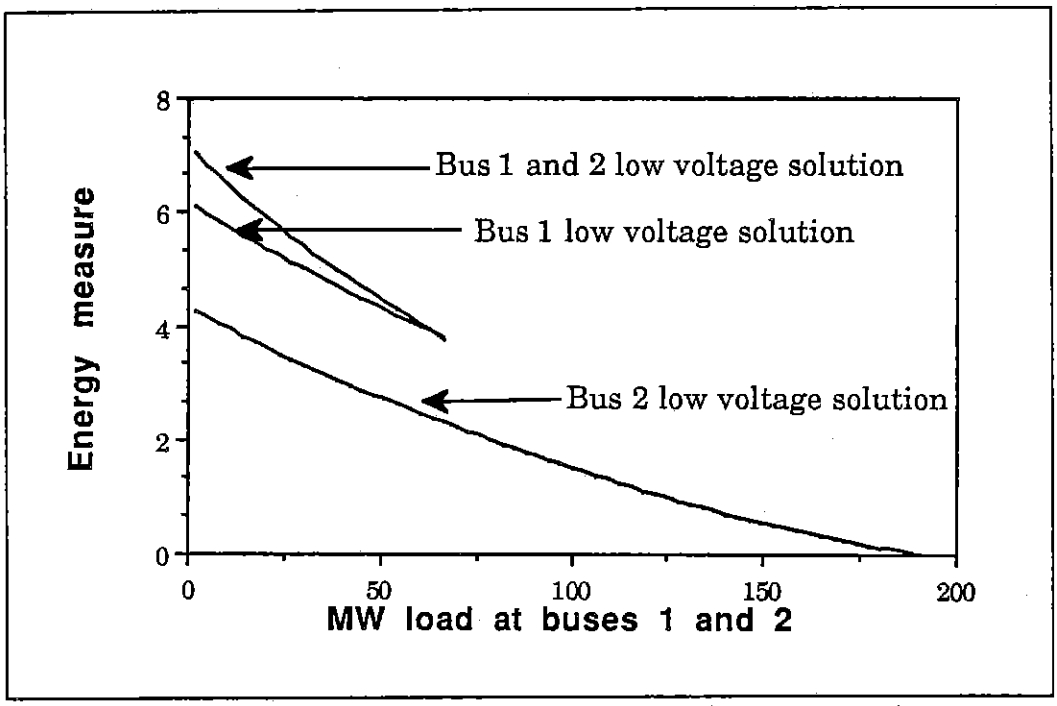

Figure 2-14 : Energy Measures for each Low Voltage Solution versus Load

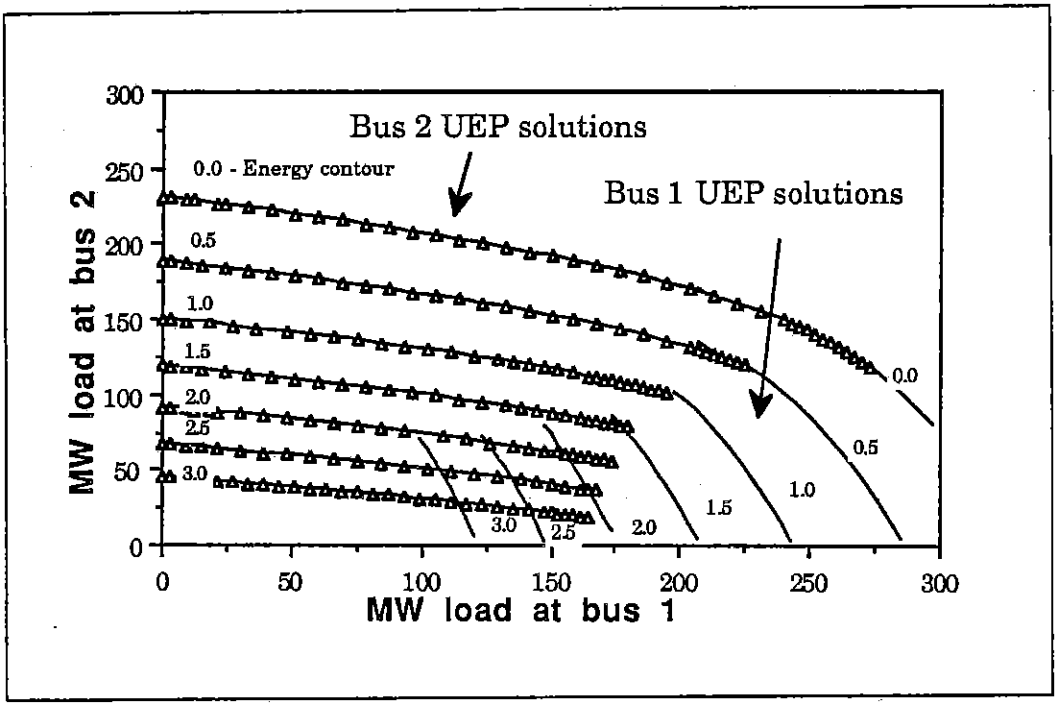

Figure 2-15 : Energy Contours for Each Type-one UEP

For those load levels with more than a single type-one equilibrium, it is necessary to determine which of the possible energy measures are appropriate to use. This selection process can be illuminated by briefly discussing some properties of the low voltage solutions. At the point of bifurcation between the SEP $\mathbf{x}^0$ and a type-one UEP $\mathbf{x}^1$ ($\mathbf{x}^0=\mathbf{x}^1=\mathbf{x}^*$ at the bifurcation point), the SEP loses asymptotic stability with its Jacobian having a zero eigenvalue, $\lambda^1 = 0$. A slight perturbation in the state would then result in voltage collapse according to the deterministic dynamics of the system. In [50] and [49] it is shown that the initial direction of the voltage collapse is

along the right eigenvector $v^0 = v^1 = v^*$ corresponding to the zero eigenvalue of the Jacobian at x^*. The magnitudes of the individual components of v^* provide a relative ranking of the initial changes in the voltage magnitude and phase angle at each individual bus. Generally the magnitude of this initial voltage drop or angle slip is significant only at a subset of the system buses. This indicates that if voltage collapse were to occur via a bifurcation of x^0 and x^1, this subset would lead the rest of the system in collapse. Thus while voltage collapse is characterized by loss of a steady state equilibrium for the entire system, its initial effects are normally apparent only at a subset of the system buses. Since these buses are usually electrically close to each other, the subset is referred to as an area. Notationally this area will be referred to as Area(x^1). Thus we can talk about voltage collapse occurring in only an area of this system, while tacitly remembering that voltage instability is a system wide phenomenon. The extent to which a voltage collapse propagates depends upon the system dynamics, and upon the amount and location of protective equipment on the system.

Now assume that the system has not yet reached the point of bifurcation (x^0 and x^1 still separate). Assuming that the system varies quasi-statically, whether x^0 and x^1 will coalesce depends upon the variation in $u^{slow}(t)$. Since x^1 is a type-one equilibrium, the eigenvector v^1 associated with the positive eigenvalue of its Jacobian

can be calculated. Interestingly, numerical testing of a number of systems indicates that the relative sizes of the components of $\mathbf{v}^1$ are fairly insensitive to the distance between $\mathbf{x}^0$ and $\mathbf{x}^1$ (the energy measure $\vartheta[\mathbf{x}^1]$ is used as a distance function). In particular, the bus associated with the largest component $\mathbf{v}^1$ usually does not vary. Thus even while the two solutions are still quite far apart in state space, the magnitudes of the components of $\mathbf{v}^1$ indicate which buses would be most affected by the voltage collapse if the variation of $\mathbf{u}(t)$ was such that $\mathbf{x}^0$ and $\mathbf{x}^1$ eventually coalesced. Thus by defining $\vartheta(\mathbf{x}^1)$ to be the energy difference between the low voltage solution $\mathbf{x}^1$ and the operable solution $\mathbf{x}^0$, $\vartheta(\mathbf{x}^1)$ can be interpreted as a proximity indicator for voltage collapse in Area($\mathbf{x}^1$). When a system has more than a single type-one low voltage solution, a separate energy measure could be calculated for each Area($\mathbf{x}^i$), with $\vartheta(\mathbf{x}^i)$ interpreted as a proximity indicator to voltage collapse occurring in Area($\mathbf{x}^i$). The determination of multiple voltage security indicators is required in an actual system, where there may be a number of areas independently vulnerable to voltage collapse.

As an example, Table 2-2 shows the variation in the components of the eigenvectors associated with each of the two type-one solutions for the three bus system for various loadings at buses 1 and 2.

Load - MW		Eigenvalues		Positive eigenvalue eigenvector		Energy Measures	
P_1	P_2	x^1	x^2	v^1	v^2	$\vartheta(x^1)$	$\vartheta(x^2)$
20	20	5.60	-8.61	-0.87	0.13	5.36	3.61
		-0.48	-6.46	-0.45	-0.10		
		-2.06	3.99	0.08	-0.88		
		-4.30	-0.48	-0.10	-0.47		
50	50	5.35	-8.32	-0.87	0.11	4.32	2.72
		-3.63	-6.28	-0.48	-0.12		
		-1.44	3.90	0.03	-0.87		
		-1.13	-1.15	-0.12	-0.50		
180	180	-	-10.08	-	-0.16	-	0.10
			-0.58		-0.31		
			1.40		0.72		
			-0.58		0.60		

Note: The first two rows of the four component eigenvectors correspond to the voltage angle (in radians) and magnitude at bus one, while the last two rows correspond to the voltage angle and magnitude at bus two.

Table 2-2 - Low Voltage Solutions Eigenvector

At the first two load levels in Table 2-2 there are two type-one solutions, while for the highest load level there is just a single type-one solution (the solutions can be verified as being type-one by noting that they have a single positive eigenvalue). Note that regardless of load, the largest components of the $\mathbf{x}^1$ solution are associated with the bus 1 quantities, while the largest components of the $\mathbf{x}^2$ solution are associated with the bus 2 quantities. Thus the energy measure $\vartheta(\mathbf{x}^1)$ can be interpreted as providing an indication of the vulnerability to voltage collapse of an area centered around bus 1 (because of the small system size, each area contains just a single bus). Likewise $\vartheta(\mathbf{x}^2)$ is an indicator for vulnerability around bus 2. For low load levels the areas tend to be independent, and therefore have separate energy measures. The lower value of $\vartheta(\mathbf{x}^2)$ indicates that bus 2 is the more vulnerable portion of the system. This is due to the higher impedance of the line from the slack bus to bus 2. As the load is increased, the areas tend to merge, inferred by the loss of a type-one solution. Thus for load values greater than 67 MW, where $\mathbf{x}^1$ no longer exists, $\vartheta(\mathbf{x}^2)$ provides an indication of voltage collapse occurring in the merged area of buses 1 and 2.

For the energy measure to provide an accurate indication of system proximity to voltage instability, it is important to include the effects of the various automatic controls of the system. Power systems normally contain a number of automatic controllers which attempt to maintain

various system variables within predefined limits. Examples of such controls are excitation systems on generators, which regulate the generator terminal voltage; speed governors on generators, which maintain a constant system frequency; automatic generation control (AGC), which regulates the interchange of power between utilities; and load tap changing (LTC) transformers, which regulate the transformer voltage. These controllers also have limits on their control ranges. Once a control has reached its limit, it is no longer able to regulate its control variable. In normal operation most controls are within their regulation range. However, it is not uncommon (even in normal operation) for some controllers to be at their limits. The time constants on these controllers vary, but are typically on the order from under a second (generator excitation systems) to a few minutes (LTCs). Since the time scale of the voltage collapse problem under consideration here is on the order of minutes to hours, it is important to include the effects of these controllers.

The applicable dynamic ranges of these controllers can be intrinsically included in the energy measure by assuming that they regulate both at the stable solution and at the low voltage solutions. Hence limits on controller action must also be enforced at both solutions. The low voltage solution could be quite unrealistic if controller limits are not enforced. This could cause the energy difference to provide an

unreliable measure an proximity to voltage collapse (this is demonstrated in the example of the next paragraph).

The next example demonstrates an important property of the energy function approach: its ability to incorporate saturation of the generator excitation system. Using the three bus system from Figure 2-11, assume that the generator at bus 1 is now on-line but is only supplying reactive power for voltage support, holding its terminal voltage at 1.0 per unit. This system is a slightly more detailed representation of the type of system prone to voltage collapse. A large load local (buses 1 and 2) is being supplied mostly from distant generation (slack at bus 3). However some local voltage support is being provided (generator at bus 1). Voltage collapse will normally not occur until the local voltage support has saturated and is no longer able to maintain its setpoint voltage. Voltage regulation is modeled here by allowing the reactive output of the generator at bus 1 (Q_{G1}) to vary within some limits ($Q_{G1[max,min]}$) in order to hold its bus voltage constant. This is known as PV mode. When the reactive power has reached its maximum or minimum limit, the generator's exciter is assumed to have saturated, and the generator's reactive output is subsequently held constant. This is known as PQ mode.

One would expect that the more maximum reactive power the generator can provide, the greater the load which can be tolerated, and

the subsequently the more secure the system for any particular load. Figure 2-16 shows that this is indeed the case. Using the voltage collapse scenario from the earlier example (bus 1 load = bus 2 load), the lowest curve shows how the energy measure would vary if there was zero output from G1 (in other words the generator is off-line) and is therefore a repeat of the lower curve from Figure 2-14. The next three curves show how the energy function varies as the maximum reactive power output of generator 1 is increased in increments of 100 MVAR. During the sequence of power flow/energy calculations, the voltage at bus 1 was held at 1.0 per unit as load ramped up until Q_{G1} reached its limit. Thereafter the reactive power output was held at its maximum (i.e. the generator had switched from PV to PQ). Table 2-3 shows how the generator reactive output and energy measures vary as the maximum reactive power limit is varied for an example load of $P_1 = P_2 = 150$MW.

Load MW		Bus 1 MVAR Generation .			
bus1	bus2	SEP solution	UEP solution	Max MVAR	Energy measure
150	150	0	0	0	0.55
150	150	100	100	100	0.92
150	150	192	200	200	1.26
150	150	192	300	300	1.54

Table 2-3 - Generator Reactive Limits

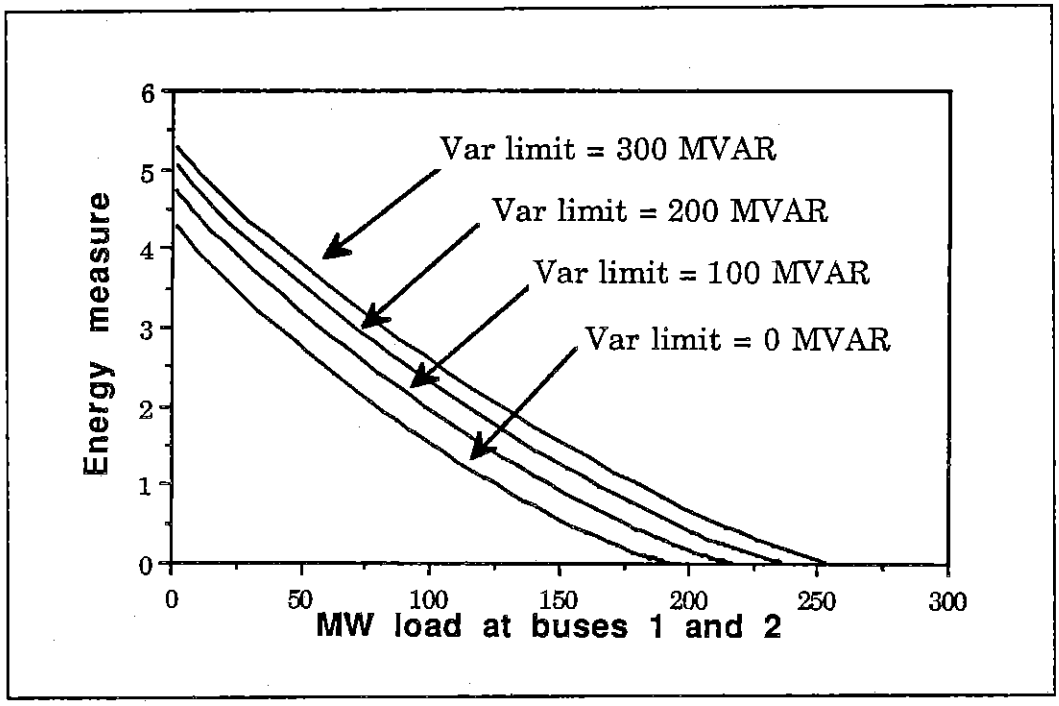

Figure 2-16 : Effect of Generator MVAR Limits on Energy Measure

As would be desired, the energy measure increases as the maximum reactive limit of the unit is increased. Note that the limits on available

var (reactive power) support are taken into account even when the current system operating point does not push the generators to these limits. This property is important since one would like an accurate determination of system voltage security before local generators have saturated (at which point it may be too late to prevent voltage collapse).

Intuitively, the ability of the energy measure to incorporate reactive limits of non-saturated units is because the low voltage solution tends to push the var sources to their limits. The var limits thus reduce the height of the potential energy boundary that the system must cross to experience voltage collapse. If the generator regulation status at the low voltage solution was assumed to always be that of the high voltage solution (PV or PQ), the energy curve could exhibit discontinuities when the generator switches modes (PV to PQ or vice versa). This is shown in Figure 2-17 for the case with G1 var limits of ± 300 MVAR. The reason for the discontinuities is apparent from a plot of low voltage generator reactive output vs system load shown in Figure 2-18. For load levels less than about 200 MW, G1 is assumed to be in the PV mode (i.e. holding its terminal voltage constant at 1.0 P.U) at both solutions because it has not yet reached its limit in the operable solution. While this is reasonable modeling for the operable solution, it is unrealistic for the low voltage solution since it would require a reactive power output of more than twice the limit of 300

MVAR. When G1 hits its limit in the operable solution, the reactive output is then fixed at 300 MVAR, resulting in a discontinuous drop in the var output of G1 at the low voltage solution from about 750 down to 300 MVAR. This in turn results in the discontinuity shown in Figure 2-17. Therefore generator reactive power limits should be enforced independently at both solutions.

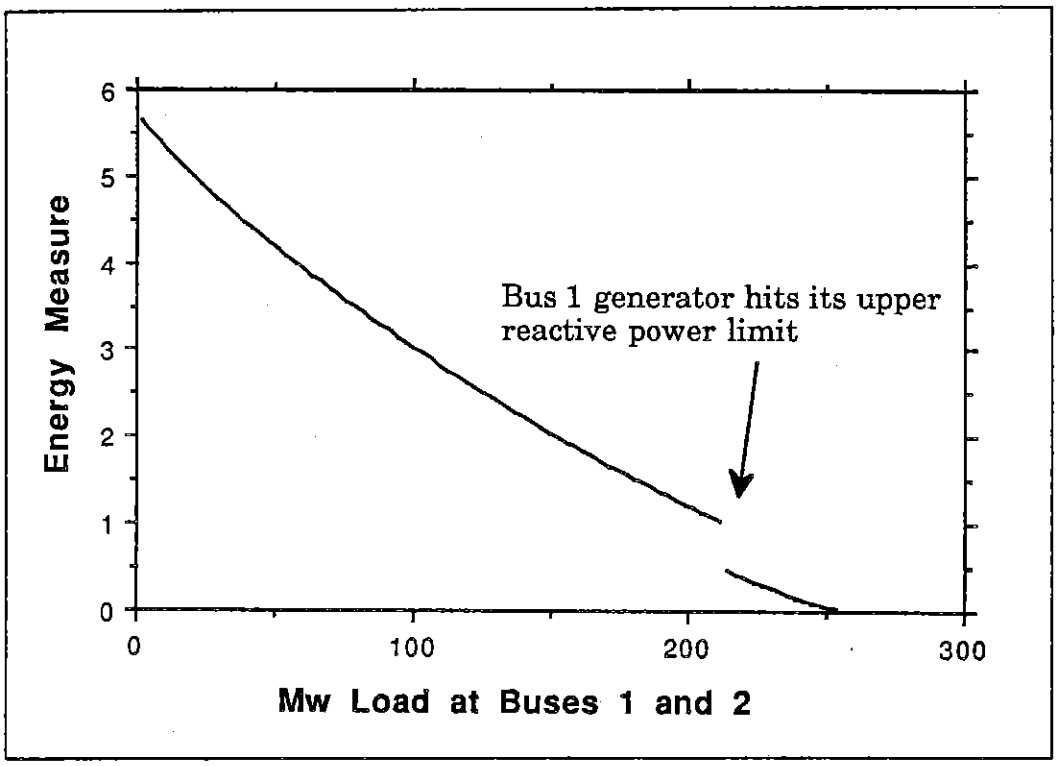

Figure 2-17 : Energy Measure versus Load when Var Limits are not Enforced at Low Voltage Solution

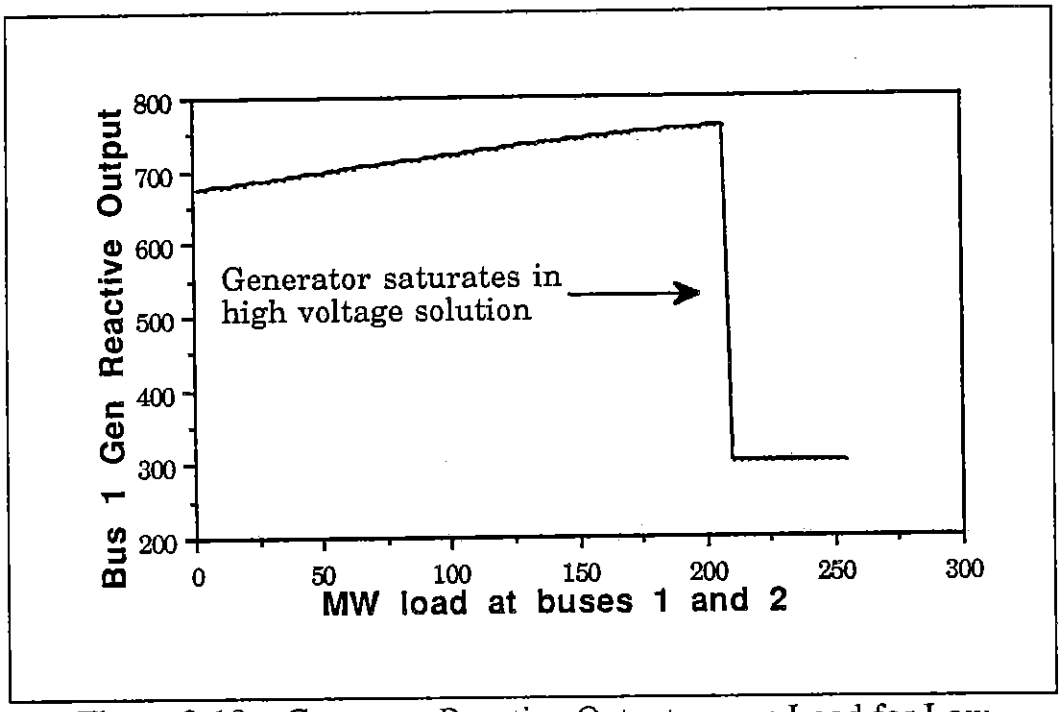

Figure 2-18 : Generator Reactive Output versus Load for Low Voltage Solution

The energy method can also be applied to larger systems. As with the case of the three bus system, energy measures are calculated using the stable operable solution and the appropriate type-one low voltage solution. These energy measures then provide an indication of how close the system is to voltage instability. Methods for locating the appropriate low voltage are discussed in Chapters 3 and 4.

The New England 30 bus system (NE30) [27] was chosen as the first test system since it is the standard system for testing measures of proximity to voltage collapse. The voltage collapse scenario selected

was to increase the reactive power at bus 11 (Q_{11}) until voltage collapse occurred, while keeping all other loads and generator MW outputs fixed. The two curves in Figure 2-19 represent the energy differences between two type-one low voltage solutions and the operable solution, as the reactive load at bus 11 is increased (until voltage collapse occurs). The upper left-hand curve corresponds to the energy measure associated with voltage collapse in the area centered at bus 12. The lower right-hand curve corresponds to the energy measure associated with voltage collapse in the area centered at bus 11. Recall that the center bus in each area can be determined from the largest component of the eigenvector of the positive eigenvalue of the Jacobian. However in Chapter 3 it is shown that this bus is directly known from the low voltage solution technique.

For low load levels, only the bus 12 low voltage solution exists; for load levels of Q_{11} between about 450 and 550 MVARS both solutions exist; while for higher loads, only the bus 11 low voltage solution exists. Because only the reactive load at bus 11 is being increased in this scenario, it is not surprising that voltage collapse should ultimately be characterized by a bifurcation between the low voltage solution associated with bus 11 and the stable solution. Note the energy measures vary in a proportional way to the increase in the load at bus 11, and in particular that there are no discontinuities in the measures. Figure 2-19 may be compared to plots of other voltage

security measures in [51] and [16] for the same voltage collapse scenario.

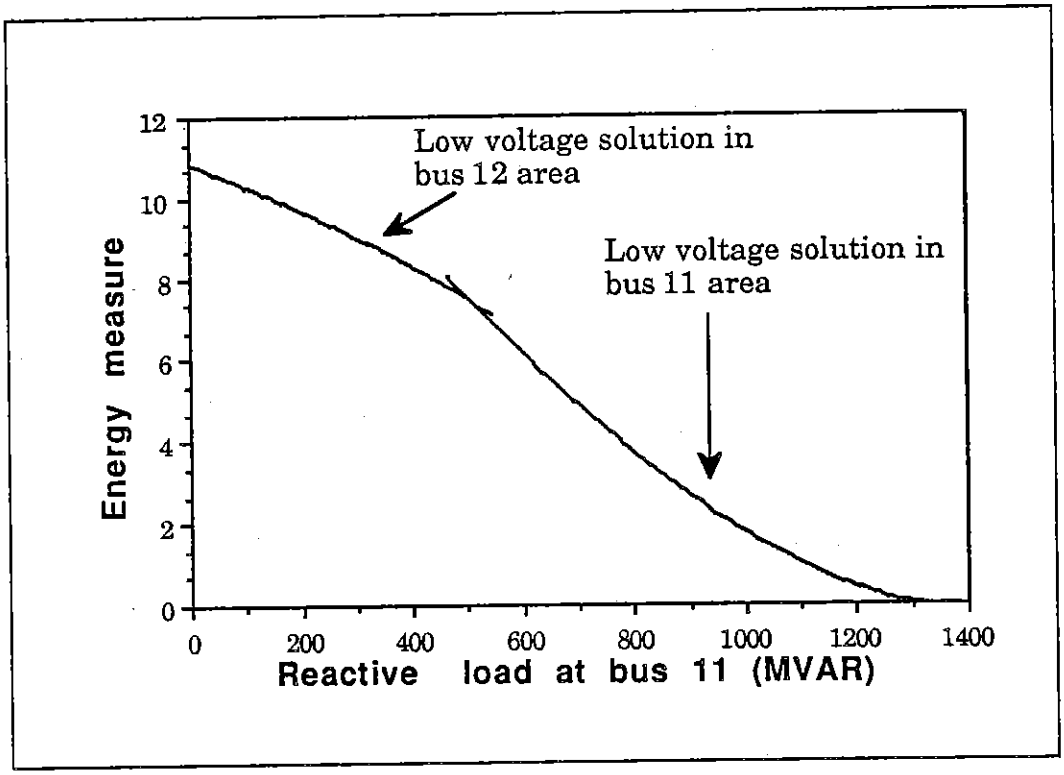

Figure 2-19 : Energy Measure Variation for NE30 System

The method was also tested on the IEEE 118 bus system (the data for this case is provided in Appendix A in the IEEE Common Data Format, which is described in [52]). In this example the loads at all buses were first assumed to be a linear function of a parameter k (k=1 for basecase). As k was increased, the system generation was varied in order to keep the real power delivered by the system slack (bus 69)

constant. This was done to simulate an area maintaining constant interchange with the rest of the interconnected electrical grid (represented here by the slack bus), as the load within the area varies. The generation participation factors used are also provided in Appendix A.

Figure 2-20 shows the variation in the energy measures with respect to k for the six solutions having lowest energy. For low load levels the high energy levels indicate that the system is relatively secure, with the weakest areas in the vicinity of buses 44, 43, and 21. As the load is increased, all the energy measures tend to decrease, with the rate of decrease dependent upon the rate of change of the system parameters. For example while the area in the vicinity of bus 95 is quite secure initially, the high subsequent load increase (due to its large basecase load) causes a rapid drop in its voltage security and hence its energy measure. The underscores the necessity of monitoring more than just the lowest energy solution. For any given system state, the energy measures provide a relative ranking of the voltage security of the areas of the system. When combined with their rate of change, the energy values provide the system operator with a very good indication of how close the system is to voltage collapse, and where collapse would initially occur. For this case the steady state operable solution vanishes at k=3.0 when it coalesces with the bus 44 solution.

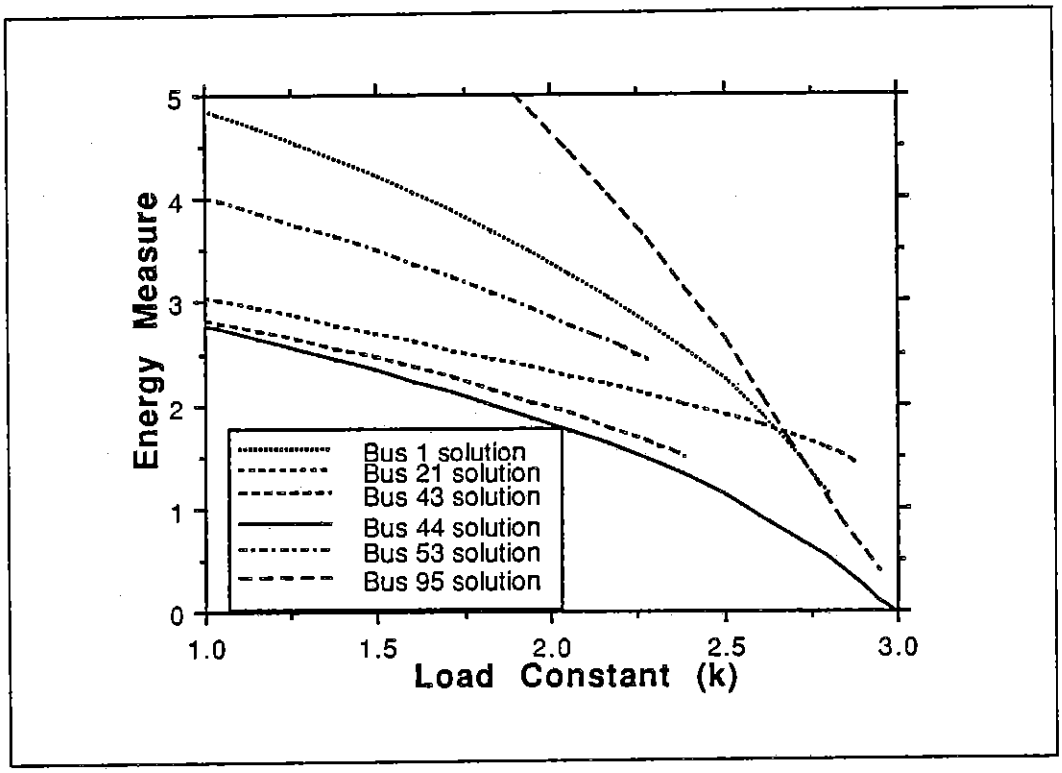

Figure 2-20 : Energy Measure Variation for E118 System

Note that the energy measures variation in Figure 2-20 is smooth, even though as k was increased a number of generators reached their reactive power limits. The generators, along with the value of k when they switched from PV mode to PQ mode, are shown in Table 2-4.

Gen #	k	Gen #	k	Gen #	k	Gen #	k
74	1.00	103	1.00	104	1.00	105	1.00
12	1.04	56	1.16	77	1.16	85	1.20

92	1.24	19	1.28	110	1.28	110	1.32
76	1.36	15	1.44	34	1.44	49	1.44
1	1.48	36	1.48	55	1.60	70	1.60
18	1.64	59	1.64	80	1.64	6	1.80
65	1.88	62	2.04	46	2.24	8	2.52
54	2.60	99	2.64	66	2.72	89	2.76
40	2.80	113	2.84	32	2.92	107	2.92
61	2.96						

Table 2-4 : Values of k when Generators reached Reactive Limits

To demonstrate that the energy measures are providing an indication of the voltage security in a particular area of the system, the voltage collapse scenario was modified so that all of the load increase occurred at bus 21. The results for this case are shown in Figure 2-21. As expected, as the load is increased the energy measure associated with bus 21 decreased in a proportional manner, again with no discontinuities. The other energy measures, however, remain relatively constant, indicating that the voltage security in those areas of the system is essentially unchanged. For this example the steady state operable solution vanishes due to a coalescence with the bus 21 solution. Thus each energy measure provides an indication of the voltage security in a particular area of the system.

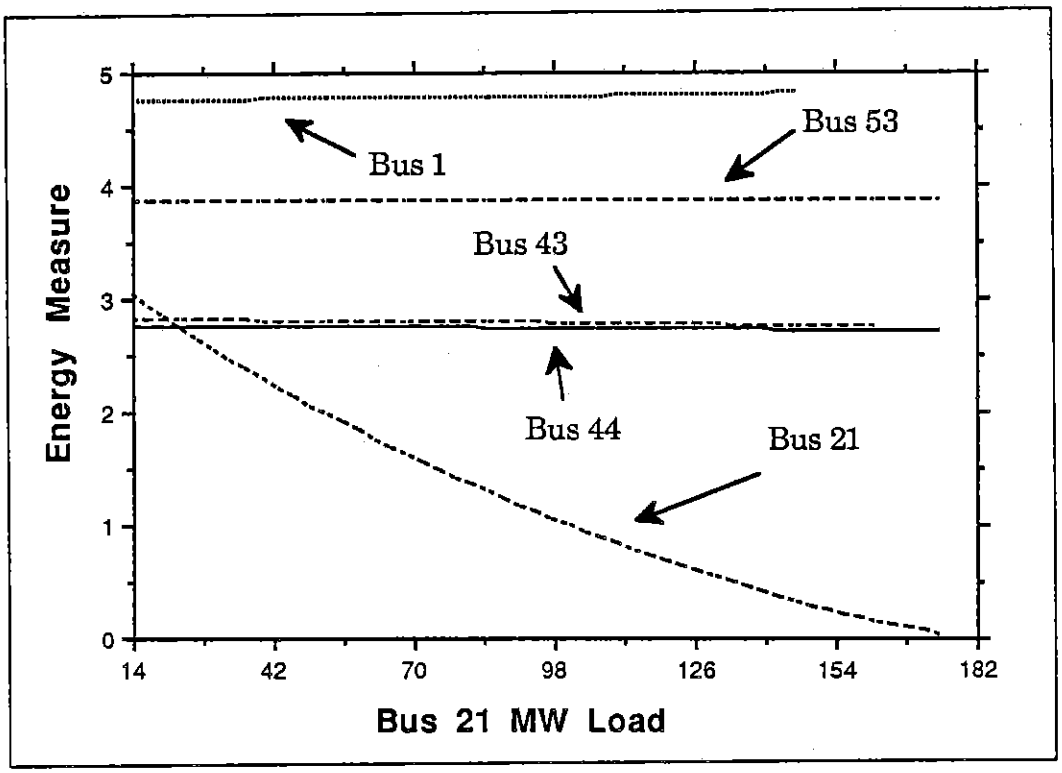

Figure 2-21 : Increase in Load Only at Bus 21

2.4 Energy Function Summary

In this chapter the method of assessing vulnerability of a power system operating point to voltage collapse based upon an energy function approach has been described. The system voltage stability is quantified by determining energy differences, using a closed form energy function, between the operable solution and the type-one low voltage solutions. A separate energy difference can be calculated for each type-one low voltage solution, with each energy difference

providing a measure of the voltage stability in the portion of the system corresponding to the largest components of the eigenvector associated with the positive eigenvalue of the power flow Jacobian. The energy measures vary smoothly with respect to continuous changes in the state of the power system, with the var limits on generators taken into account even before these limits have been reached by the current operating point. Characteristics of the low voltage solutions, along with solution techniques, will be discussed in Chapters 3 and 4.

Chapter 3 - Low Voltage Power Flow Solutions

As was seen in Chapter 2, in order to apply energy function techniques to the voltage collapse problem, it is imperative that the appropriate low voltage solutions (UEPs) be found with reasonable computational effort. In this chapter some of the properties of these solutions, along with solution techniques are discussed. In Chapter 2 the power flow equations (2-14) were written with the complex voltages expressed in polar form. This method was chosen in order to exploit the physical meaning of bus voltage magnitude and angle in the derivation and use of the energy function. However, these equations could also be rewritten with the voltages expressed in rectangular form of $V_i = e_i + jf_i$. The equivalents to (2-14) are then

$$f_i(\mathbf{e},\mathbf{f}) = P_i - \sum_{j=1}^{n} \{e_i (e_j G_{ij} - f_j B_{ij}) + f_i (f_j G_{ij} + f_j B_{ij})\} \quad (3\text{-}1a)$$

$$g_i(\mathbf{e},\mathbf{f}) = Q_i - \sum_{j=1}^{n} \{f_i (e_j G_{ij} - f_j B_{ij}) - e_i (f_j G_{ij} + e_j B_{ij})\} \quad (3\text{-}1b)$$

Experience has shown that the rectangular form of the power flow equations is often the preferred representation for computing the low voltage solutions [53], [54], [55]. Therefore the rectangular representation will be primarily used in this chapter.

3.1 A General Method for Determining Low Voltage Solutions

The determination of the appropriate low voltage solutions is of crucial importance in applying the energy function method to the voltage instability problem. As mentioned in Chapter 2, for an n bus power system there are believed to be at most $2^{(n-1)}$ separate power flow solutions. If it was necessary to find all these solutions, the energy method would be computationally intractable for all but the smallest systems. In this section the properties of, and general solution algorithm for determining the low voltage solutions of multiple bus systems are be examined.

An early algorithm to calculate all of the low voltage solutions of a system was presented in [62], and can be summarized as follows:

0. Obtain the stable operating point power flow solution $\mathbf{V}^s$.
1. Using the quadratic algorithm from Appendix B (which is based on a similar algorithm from [62]), calculate the low voltage "solution" for each load bus assuming that the voltages at all the other buses are fixed. This calculation is not performed at buses which have voltage

regulation (PV buses), including the system slack bus. Denote this voltage as V_i^u.

2. Select either V_i^s or V_i^u as initial voltage guesses for the rectangular Newton-Raphson algorithm. Form all of the $2^{(n-m)} - 1$ possible combinations of initial voltage guesses with at least one bus set to its V_i^u value (where m is the number of PV buses).
3. Compute power flow solutions using the rectangular Newton-Raphson algorithm for each of the $2^{(n-m)} - 1$ initial voltage guess permutations. The optimal multiplier method [56] is used to lessen the possibility of the algorithm diverging or oscillating.

The idea behind the above algorithm is that by varying the initial voltage guess the rectangular Newton-Raphson iteration can be initialized within the region of attraction for different solutions of (3-1). The algorithm presents a systematic method of creating such a set of initial voltage guess vectors. Using this exhaustive search technique, the authors of [62] attempted to demonstrate that the number of actual solutions in most systems was substantially less than the presumed maximum number. For example, in a lightly loaded eleven bus system with two PV buses, out of the 255 possible solutions only 57 were found. Additionally, as the loading on the system increased, the number of solutions tended to decrease until

immediately before the loss of the stable equilibrium solution (i.e. the point of voltage collapse) only a single low voltage solution exists. However in order to find this small number of solutions, the above algorithm requires tests of the $2^{(n-m)} - 1$ initial guesses. This would be computationally prohibitive in systems of realistic size.

As an alternative, a "Simplified" algorithm was also presented in [62] which substantially decreased the number of necessary initial guesses. The Simplified algorithm is essentially the same as the exhaustive method, except that rather than forming all of the $2^{(n-m)} - 1$ initial voltage guess combinations, only the n-m combinations corresponding to the use of V_i^u at a single bus are calculated. The initial voltage vector with V_i^u set at the single bus i will be referred to as the "bus i low voltage guess." Using this method on the sample 11 bus system, power flow iterations had to be performed only for the eight bus i low voltage guesses. Not all of these converge to solutions; the number of solutions which are actually found depends upon the loading of the system. During the course of the research for this thesis, the Simplified technique was often used to determine low voltage solutions. However in this work controller limits were enforced at the low voltage solutions so the bus i low voltage guesses were calculated for all buses in the system (except the system slack), as opposed to locating solutions only at the PQ buses as in [62].

Interestingly, numerical testing on a number of systems suggests that the solutions obtained by the Simplified method correspond to the type-one UEPs mentioned in Chapter 2. Recall that loss of voltage stability, if it were to occur, would take place by a bifurcation between the SEP and a type-one UEP. This suggests that the number of low voltage solutions, and hence energy measures, can be restricted to those solutions obtained by the Simplified method. Additionally, the voltage collapse areas defined in Chapter 2 are centered on the bus with the low initial voltage guess. This allows for an straightforward interpretation of the energy measures: the energy measure associated with the power flow solution found with the bus i low voltage guess provides a measure of the voltage security in the area of bus i. There is no need to explicitly calculate the eigenvector associated with the positive eigenvalue of the power flow Jacobian.

For example, consider the voltage collapse scenario from Chapter 2, where the reactive load at bus 11 of the New England 30 bus system was increased. The energy measures used to construct the lower right-hand curve in Figure 2-19 (labeled as "Low voltage solution in bus 11 area") were found by initializing the power flow with the bus 11 low voltage guess. Hence one would expect the eigenvector associated with the positive eigenvalue of the low voltage Jacobian should have its largest components at bus 11. To confirm this, the eigenvector components are shown in Figure 3-1 for a reactive load at

bus 11 of 1300 MVAR. The largest component was indeed at bus 11 (the eigenvector was normalized so that the largest component was 1.0), with the next largest components at the first neighbors of bus 11 (buses 6, 10, and 12). Figure 3-2 shows the eigenvector components when load is decreased to 800 MVAR. Again the largest component was at bus 11, with other significant components at its first and second neighbors. As the load at bus 11 is decreased, eventually the low voltage solution found by initializing with the bus 11 low voltage guess disappears. However a new solution, found by initializing the power flow with the bus 12 low voltage guess, appears. This solution was used to construct the upper left-hand curve in Figure 2-19 (labeled as "Low Voltage solution in bus 12 area"). Figure 3-3 shows the components for this solution's positive eigenvalue eigenvector when the load at bus 11 is 400 MVAR. As would be expected, the largest component is now at bus 12.

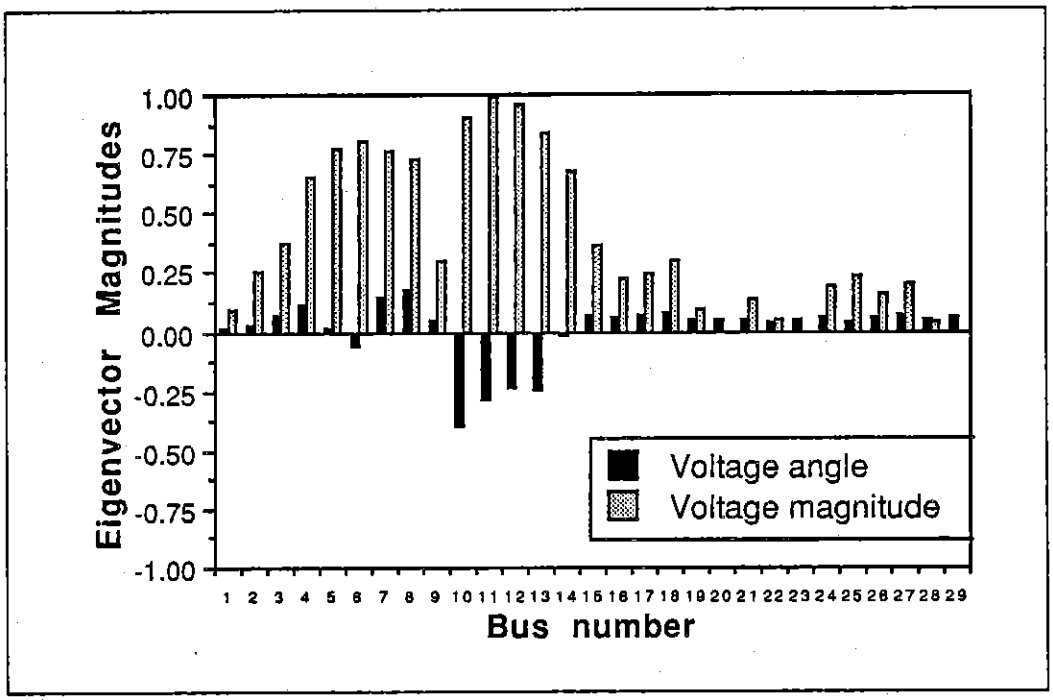

Figure 3-1 : Components of eigenvector associated with positive eigenvalue of UEP solution Jacobian when reactive load at bus 11 = 1300 MVAR

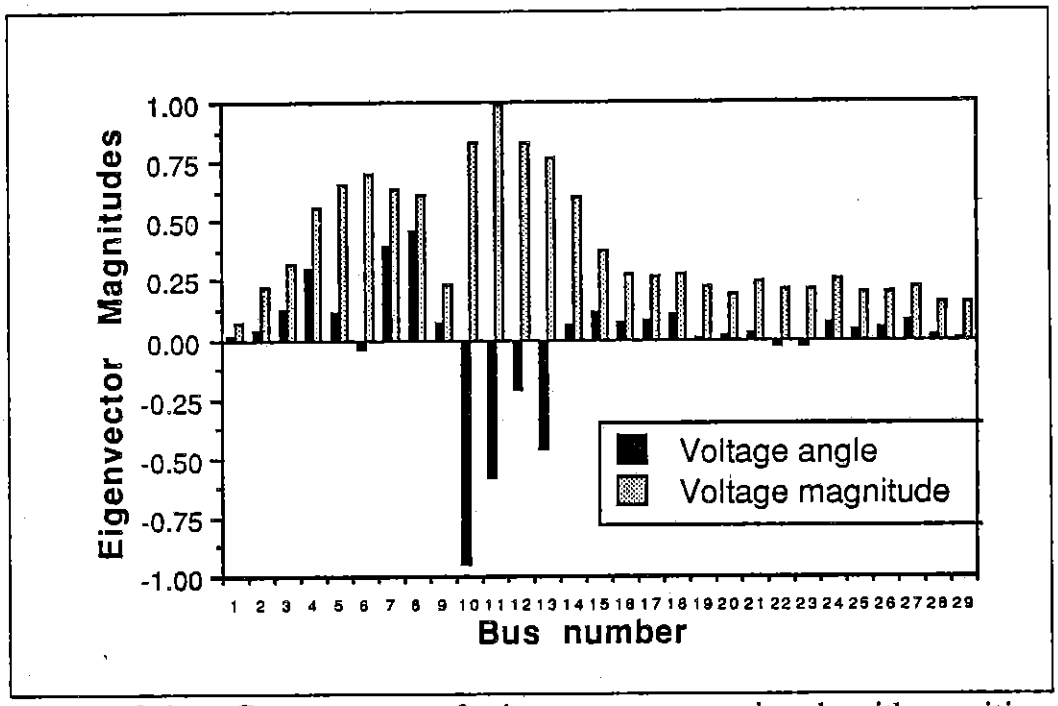

Figure 3-2 : Components of eigenvector associated with positive eigenvalue of UEP solution Jacobian when reactive load at bus 11 = 800 MVAR

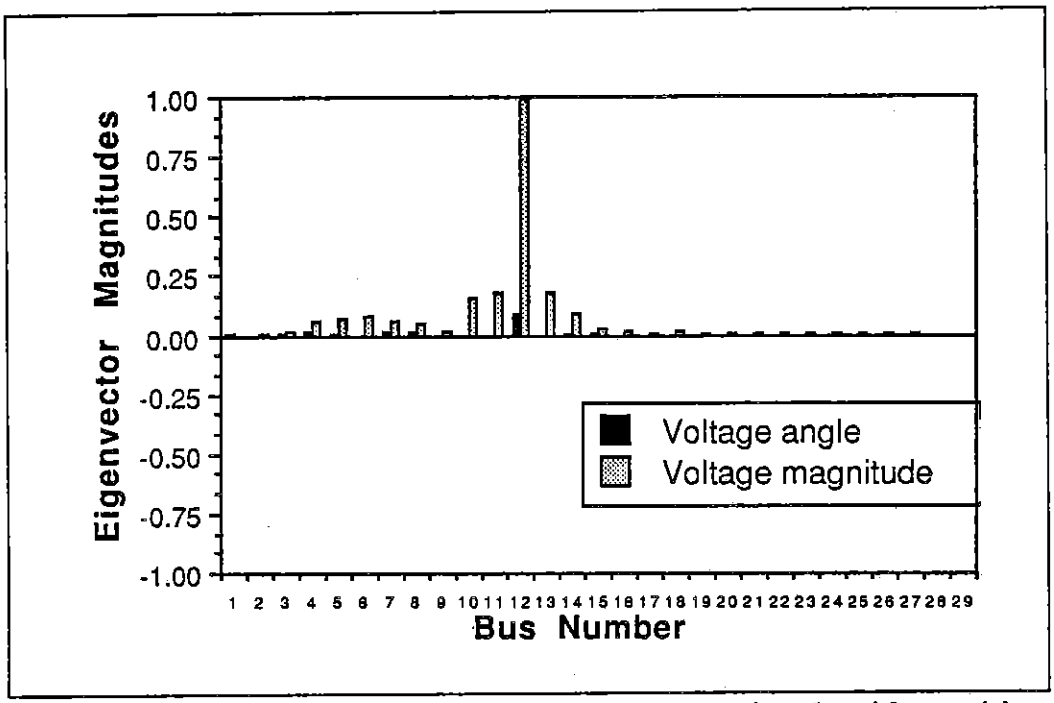

Figure 3-3 : Components of eigenvector associated with positive eigenvalue of UEP solution Jacobian when reactive load at bus 11 = 400 MVAR

Thus the energy measure calculated using the bus i Simplified method solution provides a measure of the voltage security in the vicinity of bus i. If no solution exists for the bus i low voltage guess, then either the bus i area is relatively invulnerable to voltage collapse, or an energy measure exists for a nearby bus.

A shortcoming of the Simplified method is its requirement of n-1 full power flow solutions to calculate energy measures for an entire n bus system. Such high computational requirements would preclude on-line use for large system models. A second shortcoming is that there

is no guarantee that the rectangular Newton-Raphson power flow will converge to the bus i solution, when initialized with the bus i low voltage guess, even when the solution exists. The initial bus i low voltage guess must be in the region of attraction (with respect to the modified step size Newton-Raphson algorithm) of the bus i solution. The size, however, of this region of attraction is increased due to the use of the optimal multiplier [56]. While testing indicates that the vast majority of solutions do converge correctly, such convergence is not guaranteed. The remaining sections of this chapter present two alternative methods of calculating the low voltage solutions.

3.2 Optimal Multiplier Method

A new method of finding a low voltage solution for a system was recently presented in [57]. This technique exploits the convergence characteristics of the Newton-Raphson method when the power flow equations are expressed in rectangular from (3-1). In order to explain this technique, it is necessary to first discuss the optimal multiplier theory originally presented in [56].

The rectangular power flow equations from (3-1) can be expressed as a set of quadratic equations having no first order terms:

$$\begin{bmatrix} \mathbf{s} \end{bmatrix} = \theta(\mathbf{x}) = \begin{bmatrix} \mathbf{A} \end{bmatrix} \begin{bmatrix} x_1x_1 \\ x_1x_2 \\ \cdot \\ \cdot \\ x_ix_j \\ \cdot \\ \cdot \\ x_nx_n \end{bmatrix} \tag{3-2}$$

where **A** is a constant matrix of the susceptances and conductances from (3-1), $\mathbf{s} \in R^{2n}$ is the vector of the bus real and reactive power injections, and $\mathbf{x} \in R^{2n}$ is the vector of bus voltages expressed in rectangular coordinates. For any guess of $\mathbf{x}^k$, using a Taylor series expansion about $\theta(\mathbf{x}^k)$, the value of **s** can be expressed exactly (since **A** is constant) as

$$\mathbf{s} = \theta(\mathbf{x}^k) + J(\mathbf{x}^k)\,\Delta\mathbf{x} + \theta(\Delta\mathbf{x}) \tag{3-3}$$

The standard method of solving using the Newton-Raphson power flow is then to ignore the third term and obtain an approximation of $\Delta\mathbf{x}$ as

$$\Delta\mathbf{x} = \mathbf{J}(\mathbf{x}^k)^{-1}\,[\mathbf{s} - \theta(\mathbf{x}^k)] \tag{3-4}$$

The best increment to approximately solve (3-3) is then given by $\Delta\mathbf{x}$. The new voltage guess is then determined by

$$\mathbf{x}^{k+1} = \mathbf{x}^k - \mu \Delta \mathbf{x} \tag{3-5}$$

where μ is normally unity. However because (3-3) is exact, it is possible to solve directly for the value of μ which minimizes the norm of the mismatches in the direction $\Delta \mathbf{x}$. This analytic expression for μ is derived by first defining a cost function as

$$h = ||\mathbf{a} - \mu\mathbf{a} + \mu^2\mathbf{c}||^2 \tag{3-6}$$

with

$$\mathbf{a} = \mathbf{s} - \theta(\mathbf{x}^k) = -\mathbf{J}(\mathbf{x}^k)\Delta\mathbf{x}$$
$$\mathbf{c} = -\theta(\Delta\mathbf{x})$$

Then solve for

$$\frac{\partial h}{\partial \mu} = g_3\mu^3 + g_2\mu^2 + g_1\mu + g_0 = 0 \tag{3-7}$$

where

$$g_0 = -\mathbf{a} \bullet \mathbf{a}$$
$$g_1 = \mathbf{a} \bullet \mathbf{a} + 2\,\mathbf{a} \bullet \mathbf{c}$$
$$g_2 = -3\,\mathbf{a} \bullet \mathbf{c}$$
$$g_3 = 2\,\mathbf{c} \bullet \mathbf{c}$$

Since (3-7) is a cubic equation, it has three roots. The roots are either three real numbers, or one real and two imaginary numbers. For the latter case, (3-6) only has a single local extreme value in the direction of $\Delta \mathbf{x}$. The value can be seen to be a minimum because unless **a** and **c** are zero (which means the solution has been reached), (3-6) goes to infinity as μ goes to $\pm\infty$. For the case of three real roots, there will be two local minima of (3-6) and a single local maximum in the direction of $\Delta \mathbf{x}$. Define μ as the smallest (or only) real root of (3-6), denoting it as the optimal multiplier; and μ_2 and μ_3 as either the imaginary roots or as the middle and largest real roots. Using the optimal multiplier μ in (3-5) results in the new $\mathbf{x}^{k+1}$ always defining at least a new local minimum in the direction given by $\Delta \mathbf{x}$. This prevents divergence of the power flow solution.

Returning again to [57], this method exploits an interesting convergence property of the rectangular Newton-Raphson power flow method that when a pair of multiple solutions of the power flow equations are located close to each other, the power flow tends to converge in the direction of the line containing the two solutions. If the convergent loci are exactly on this line, it is then possible to calculate the two solutions directly using the optimal multiplier, since each solution is a global minimum of (3-6) (note that even though the solutions are distinct, each is still a global minimum since the value of (3-6) is equal to zero at each solution). The authors provide no

mathematical explanation as to why the method works, but rather provide a number of test results supporting their hypothesis.

However it is possible to prove that once an iterant $\mathbf{x}^k$ is an element of the line passing through two solutions, all subsequent elements of the iteration sequence $\{\mathbf{x}^l\}$, $l \geq k$, will also be elements of this line. Define $\mathbf{x}^s$ and $\mathbf{x}^u$ as two distinct solutions of the power flow equations (3-1), with $\mathbf{x}^s$ being the stable high voltage solution, and $\mathbf{x}^u$ the unstable low voltage solution. The line through $\mathbf{x}^s$ and $\mathbf{x}^u$ is defined as the set

$$\mathbf{L} = \{ \mathbf{x} \mid \mathbf{x} = (1-\lambda)\mathbf{x}^s + \lambda\mathbf{x}^u , \lambda \in R\}$$

Let

$$\mathbf{x}^s = \mathbf{x}^k + \mathbf{B}$$
$$\mathbf{x}^u = \mathbf{x}^k - \alpha\mathbf{B}$$

where $\mathbf{x}^k$ and $\mathbf{B}$ are vectors of the same dimension of $\mathbf{x}$, $\mathbf{x}^k \in \mathbf{L}$, $\mathbf{x}^k \neq \mathbf{x}^s$, $\mathbf{x}^k \neq \mathbf{x}^u$, and $\alpha \in R$.

Then since (3-3) is an exact Taylor expansion and (3-2) is a set of quadratic equations with no first order terms, we can write $\mathbf{s}$ from (3-3) as

$$\mathbf{s} = \theta(\mathbf{x}^k) + \mathbf{J}(\mathbf{x}^k)\mathbf{B} + \theta(\mathbf{B})$$

$$\mathbf{s} = \theta(\mathbf{x}^k) - \alpha \mathbf{J}(\mathbf{x}^k)\mathbf{B} + \alpha^2\theta(\mathbf{B})$$

Assuming that $\mathbf{J}(\mathbf{x}^k)$ is nonsingular, the new direction $\Delta\mathbf{x}$ from the Newton-Raphson power flow is given by (3-4). We must then show that $\Delta\mathbf{x}$ is tangent to $\mathbf{L}$ or equivalently that $\Delta\mathbf{x} = \lambda\mathbf{B}$ where $\lambda \in R$. Since from (3-4)

$$\Delta\mathbf{x} = \mathbf{J}(\mathbf{x}^k)^{-1}\,(\mathbf{s} - \theta(\mathbf{x}^k)) = \mathbf{B} + \mathbf{J}(\mathbf{x}^k)^{-1}\theta(\mathbf{B})$$

we can write

$$\Delta\mathbf{x} = \mathbf{B} + \mathbf{J}(\mathbf{x}^k)^{-1}\theta(\mathbf{B}) \;=\; -\alpha\mathbf{B} + \alpha^2\mathbf{J}(\mathbf{x}^k)^{-1}\theta(\mathbf{B})$$

Solving for $\mathbf{J}(\mathbf{x}^k)^{-1}\theta(\mathbf{B})$ in terms of $\mathbf{B}$ we get

$$\mathbf{J}(\mathbf{x}^k)^{-1}\theta(\mathbf{B}) \;=\; \frac{1+\alpha}{\alpha^2-1}\,\mathbf{B}$$

Provided $\alpha \neq 1$ we can write $\Delta\mathbf{x}$ as a linear function of $\mathbf{B}$

$$\Delta\mathbf{x} \;=\; \mathbf{B} + \frac{1+\alpha}{1-\alpha^2}\,\mathbf{B} \;=\; \frac{2+\alpha-\alpha^2}{1-\alpha^2}\,\mathbf{B}.$$

Because $\Delta\mathbf{x}$ is tangent to L, the new point $\mathbf{x}^{k+1} = \mathbf{x}^k + \Delta\mathbf{x}$ is also an element of $\mathbf{L}$. ♦

As an example of optimal multiplier method, consider the three bus system from Figure 2-11. For a load of 150 MW at both buses 1 and 2, the system has the two solutions shown in Table 3-1.

Bus Number	High Solution		Low Solution	
	e	f	e	f
1	0.7979	-0.1665	0.5203	-0.1778
2	0.7347	-0.2127	0.1909	-0.1887
3	1.0	0.0	1.0	0.0

Table 3-1 : Three Bus System Solutions

To calculate both solutions, the standard Newton-Raphson algorithm is first performed, with the optimal multipliers being calculated each iteration. The first five columns of Table 3-2 shows these values, along with the maximum mismatch, for each iteration. To illustrate that the solution is actually converging along the line through $\mathbf{x}^s$ and $\mathbf{x}^u$, the last column in Table 3-2 shows the angle (in degrees) between the vector from $\mathbf{x}^u$ to $\mathbf{x}^s$ and the vector from $\mathbf{x}^s$ to $\mathbf{x}^k$. Since the angle is converging to zero, $\mathbf{x}^k$ is also converging towards the line through $\mathbf{x}^s$ and $\mathbf{x}^u$.

Iteration	Mismatch	μ	μ_2	μ_3	Angle
0	150.00	1.036	1.347+1.4j	1.347-1.4j	
1	43.78	1.153	4.581	6.741	8.4°
2	5.82	1.027	20.42	36.05	5.7°
3	0.16	1.001	684.7	1321.0	3.3°
4	1.2e-6	1.000	9.22e5	1.23e6	1.7°

Table 3-2 : Newton-Raphson Iterations for Three Bus System

For those iterations in which three real optimal multipliers are obtained, the cost function h from (3-6) has two local minima in the direction $\Delta\mathbf{x}$. These local minima occur at $\mathbf{x}^k - \mu_1\Delta\mathbf{x}$ (normally the high voltage solution) and $\mathbf{x}^k - \mu_3\Delta\mathbf{x}$ (normally the low voltage solution). The value of the cost function $h(\mathbf{x}^1 - \lambda\Delta\mathbf{x})$ (after the first iteration from Table 3-2) is plotted in Figure 3-4 as a function λ. As would be expected, the local minima occur at $\lambda = 1.1$ (μ) and 6.7 (μ_3). Since the angle between the solutions is not yet close to zero, the value of $h(\mathbf{x}^1 - \mu_3\Delta\mathbf{x})$ is rather high. However as the angle between the solutions goes to zero, the value of the $h(\mathbf{x}^k - \mu_3\Delta\mathbf{x})$ also tends towards zero.

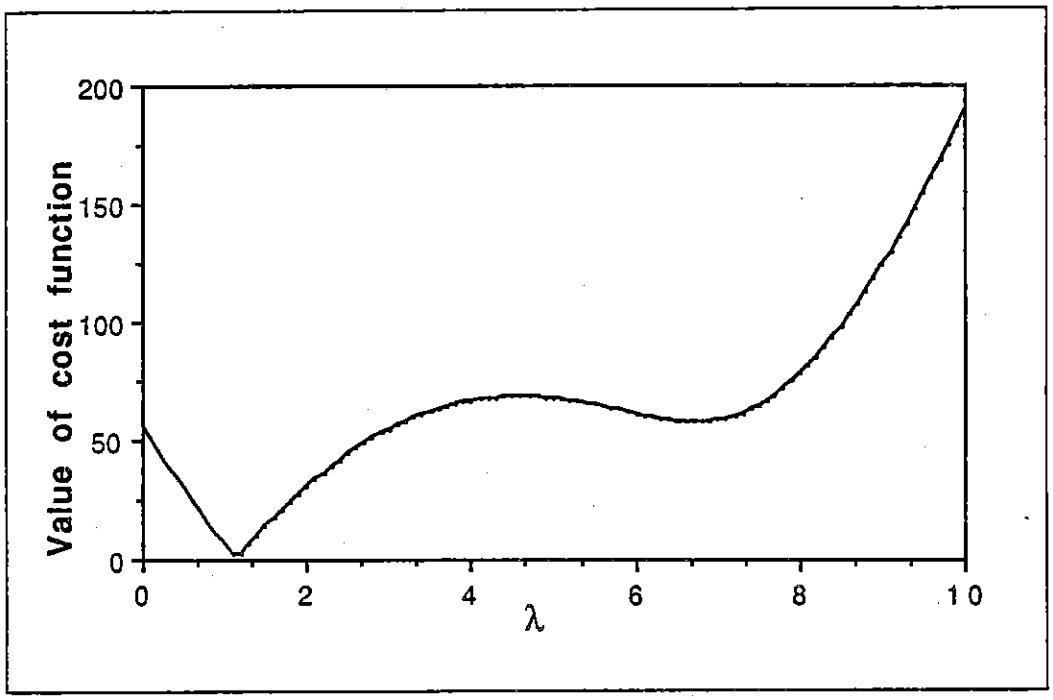

Figure 3-4: Variation of Cost Function in Direction $\Delta \mathbf{x}$

Once the high voltage solution has been solved with sufficient accuracy, a guess of the low voltage solution is then given by

$$\mathbf{x}^{u0} = \mathbf{x} - \mu_3 \Delta \mathbf{x} \tag{3-8}$$

The error associated with this estimate is a function of how close the angle between the solution vectors is to zero. The value of the low voltage solution can then be computed precisely using the standard Newton-Raphson algorithm with $\mathbf{x}^{u0}$ as the initial guess.

Since the cost of calculating the optimal multipliers is negligible compared to the cost of the rest of the Newton-Raphson algorithm, the optimal multiplier method provides a quick method of determining an initial guess of a low voltage solution. The accuracy of the value from (3-8) appears to be a function of the relative closeness of the two solutions. When the load for the three bus systems was 190MW at buses 1 and 2 (close to the critical load of 192 MW, so the high and the low voltage solutions were also close), the value of $h(\mathbf{x}^{u0})$ was just 0.001 MVA. However as the load was decreased (causing the solutions to move apart), the value of $h(\mathbf{x}^{u0})$ increased, reaching 6.6 MVA for a load of 150 MW and 37 MVA when the load was 100 MW.

The optimal multiplier method can be used on arbitrary sized systems. However the method can only, at best, determine one of the low voltage solutions, though this normally is the solution with the lowest associated energy measure. Since in the energy function approach a number of low voltage solutions may need to be determined, the optimal multiplier method would have to be supplemented with other techniques. Additionally, a problem develops when a generator's reactive output is saturated at one solution (the generator is modeled as PQ) while still regulating at the other solution (PV). Because of the type switching of the generator from PV to PQ (or vice versa), the matrix **A** from (3-2) is no longer identical for both solutions.

Therefore the two solutions are no longer both defined as minima of (3-6). Nevertheless, provided the perturbation introduced by generator type switching is not too severe, $\mathbf{x}^{u0}$ can often still provide a fairly good starting guess to locate the low voltage solution. In conclusion, the optimal multiplier method provides a fairly good technique of getting an initial guess of the closest low voltage solution, and could be useful when used in conjunction with other techniques to determine the pertinent low voltage solutions.

3.3 Energy Contour Search Method

To use energy methods to assess proximity to voltage collapse, it is important to determine the set of low voltage solutions with lowest associated energies. Both of the methods presented thus far in the chapter for determining low voltage solutions depend upon the convergence characteristics of the Newton-Raphson power flow. In this section an alternative technique is presented which does not make use of the Newton-Raphson method. In the energy contour search method, the technique to determine the set of low voltage solutions is to expand the constant contours of the energy function ϑ about the equilibrium point $\mathbf{x}^s$ [58]. Since the energy function is positive definite about $\mathbf{x}^s$, the contours for sufficiently small energy values will define closed surfaces. Increasing the energy value will yield a nested

family of contours. The low voltage solutions would then be the points $\mathbf{x}^i$ on each contour which satisfy the constraint $h(\mathbf{x}^i) = 0$, where

$$h(\mathbf{x}) = \frac{1}{2}\theta(\mathbf{x})^T\theta(\mathbf{x}) = \frac{1}{2}||\theta(\mathbf{x})||_2^2$$

and θ corresponds to the real and reactive power flow mismatch equations defined in [3-1]. Thus by expanding the constant energy contours out from $\mathbf{x}^s$, the set of low voltage solutions could be determined, ranked by energy.

An algorithm to locate this set of points is given below. The notation used is that within the iterative solution, the iteration numbers are indicated by square brackets. For example, $\mathbf{x}^i[3]$ would represent the vector $\mathbf{x}^i$ at its third iteration.

0. Start from the stable operating solution $\mathbf{x}^s$, where $\vartheta(\mathbf{x}^s) \equiv 0$. Select an initial target energy contour value $C[0] = \varepsilon$ (a small positive constant), and "initial guesses" of the members of the set of low voltage solutions for the iterative optimization: $\{\mathbf{x}^1[0], \mathbf{x}^2[0], ...,\mathbf{x}^m[0]\}$ (the value of m depends upon how many solutions are desired. Each $\mathbf{x}^k[0]$ satisfies $\vartheta(\mathbf{x}^k[0]) = \varepsilon$. Select δ as the convergence tolerance: $h(\mathbf{x}^k) \approx 0$, when $h(\mathbf{x}^i) < \delta$.

1. Identify set L of indices k for which $h(\mathbf{x}^k[i]) \geq \delta$. Save those $\mathbf{x}^k[i]$ for which $h(\mathbf{x}^k[i]) < \delta$; these are the desired solutions. If L is an empty set, then Quit; otherwise increment $C[i+1] = C[i] + \varepsilon$.

2. For each $k \in L$
   a. Select a search direction $\Delta\mathbf{x}^k[i]$.
   b. Move in direction $\Delta\mathbf{x}^k[i]$ until $\vartheta(\mathbf{x}^k[i] + \gamma\ \Delta\mathbf{x}^k[i]) = C[i+1]$.
   c. Numerically solve the following constrained optimization problem using $\mathbf{x}^k[i]$ as the initial guess: minimize $\mathbf{h}(\mathbf{x}^k[i])$ such that $\vartheta(\mathbf{x}^k[i]) = C[i+1]$
   d. Set $\mathbf{x}^k[i+1]$ equal to the resulting minimizer.

3. Let $i = i + 1$; goto 1.

Because of the nonconvexity of the problem, there could be a large number of local minima of $h(\mathbf{x})$ on the constraint surface. Thus the selection of the initial starting points $\mathbf{x}^i[0]$ in step 0 is of particular importance. In [58] it is proved that provided C[0] is small enough, the initial local minima and maxima on the constraint manifold $\vartheta[\mathbf{x}] = C[0]$ are given by the 2n points obtained by moving from $\mathbf{x}^s$ in the directions of the ±eigenvectors of the power flow Jacobian at $\mathbf{x}^s$, $\mathbf{J}(\mathbf{x}^s)$. A summary of the proof is as follows.

For an optimization problem with a single equality constraint, a necessary condition for a local minimum is that the gradient of the objective must be orthogonal to the tangent space of the constraint manifold.

Proposition

Consider $\hat{\mathbf{x}} \in \{\mathbf{x} \mid \vartheta(\mathbf{x}) = C\}$. If $\hat{\mathbf{x}}$ is an extreme point of $||\nabla\vartheta(\mathbf{x})||_2^2$ on this manifold, then $\nabla\vartheta(\mathbf{x})$ is an eigenvector of $J(\hat{\mathbf{x}}) = \nabla^2\vartheta(\mathbf{x})$.

Proof

The gradient of the objective function is given by $2J(\hat{\mathbf{x}})\,\nabla\vartheta(\hat{\mathbf{x}})$. The outward normal of the constraint manifold is simply $\nabla\vartheta(\hat{\mathbf{x}})$. If $\hat{\mathbf{x}}$ is a local minimum or maximum, then at this point the gradient of the objective function must be collinear with the outward normal of the constraint manifold. It then follows that there exists a real scalar λ such that

$$J(\hat{\mathbf{x}})\,\nabla\vartheta(\hat{\mathbf{x}}) = \lambda\,\nabla\vartheta(\hat{\mathbf{x}})$$

which implies by definition that $\nabla\vartheta(\hat{\mathbf{x}})$ is an eigenvector of $J(\hat{\mathbf{x}})$.

To use this result to identify candidate local minima, C[0] must be chosen "sufficiently small" so that on the set $\{\mathbf{x} \mid \vartheta(\mathbf{x}) = C[0]\}$,

$\nabla\vartheta(\mathbf{x}^s+\Delta\mathbf{x})$ can be well approximated by its linearization $\mathbf{J}(\mathbf{x}^s)\Delta\mathbf{x}$ (since $\nabla\vartheta(\mathbf{x}^s+\Delta\mathbf{x}) \approx \nabla\vartheta(\mathbf{x}^s) + \mathbf{J}(\mathbf{x}^s)\Delta\mathbf{x}$, and $\nabla\vartheta(\mathbf{x}^s) = \mathbf{0}$). Under these conditions, consider a point $\hat{\mathbf{x}}$ obtained at one of the two intersections between the constant energy manifold and the ±directions given by an eigenvector $\mathbf{v}$ of $\mathbf{J}(\mathbf{x}^s)$ (note: $\mathbf{v}$ is translated to be based at $\mathbf{x}^s$). Let $\Delta\mathbf{x} = \hat{\mathbf{x}} - \mathbf{x}^s$, and λ be the eigenvalue corresponding to $\mathbf{v}$. Then, since $\nabla\vartheta(\hat{\mathbf{x}}) \approx \mathbf{J}(\mathbf{x}^s)\Delta\mathbf{x} = \lambda\Delta\mathbf{x}$, $\nabla\vartheta(\hat{\mathbf{x}})$ will be collinear with an eigenvector of $\mathbf{J}(\mathbf{x}^s)$ (up to the accuracy of the linear approximation). This implies that the 2n points, obtained by intersecting the constant energy manifold in directions of the ±eigenvectors of $\mathbf{J}(\mathbf{x}^s)$ starting from $\mathbf{x}^s$, should approximate the local minima and maxima of the cost function h on the manifold. Thus they can serve as the initial guesses $\{\mathbf{x}^1[0], \mathbf{x}^2[0],...\mathbf{x}^{2n}[0]\}$. Only the local minima would be of interest. ♦

To illustrate the energy contour search method, consider the case shown in Figure 2-2, with a load of P = 200 MW and Q = 100 MVAR. For this load level the system has an operable solution $\mathbf{x}^s$ of (V^s,α^s) = (0.855, -13.52°), and a low voltage solution $\mathbf{x}^u$ of (0.261, -49.91°) with an energy measure of 0.861. The contours of the energy function are shown in Figure 2-4. The Hessian of $\vartheta(\mathbf{x}^s)$ is equal to

$$\nabla^2\vartheta(\mathbf{x}) = \begin{bmatrix} -8.314 & 2.338 \\ 2.338 & -8.632 \end{bmatrix}$$

with eigenvalues of $\lambda_1 = -10.8$ and $\lambda_2 = -6.13$; and eigenvectors of

$$\mathbf{v}_1 = \begin{bmatrix} -0.683 \\ 0.731 \end{bmatrix} \qquad \mathbf{v}_2 = \begin{bmatrix} 0.731 \\ 0.683 \end{bmatrix}$$

where the first component of the vector corresponds to the bus 1 voltage angle (in radians), while the second component corresponds to the bus 1 voltage magnitude. Thus the initial search directions for the algorithm are $\pm\mathbf{v}_1$ and $\pm\mathbf{v}_2$. To demonstrate that the eigenvectors actually do point in the direction of the local minima and maxima on the constant energy manifold, a value of C[0] is selected sufficiently small, C[0] = 0.01. Figure 3-5 plots the values of $||\nabla\vartheta(\mathbf{x})||_2^2$ at the point of intersection between a vector $\mathbf{d}(\theta)$ translated to be based at $\mathbf{x}^s$ and the constant energy surface C[0] = 0.01 enclosing $\mathbf{x}^s$, as a function of θ. The search direction θ is the angle between $\mathbf{d}(\theta)$ and $\mathbf{v}_1$. Thus $\mathbf{d}(0°) = \mathbf{v}_1$, $\mathbf{d}(90°) = \mathbf{v}_2$, $\mathbf{d}(180°) = -\mathbf{v}_1$, and $\mathbf{d}(270°) = -\mathbf{v}_2$. Note from the figure that the local minima and maxima do indeed occur in the directions of plus/minus the eigenvectors of $\nabla^2\vartheta(\mathbf{x}^s)$, with the minima occurring in directions $\pm\mathbf{v}_2$, and the maxima occurring in directions $\pm\mathbf{v}_1$.

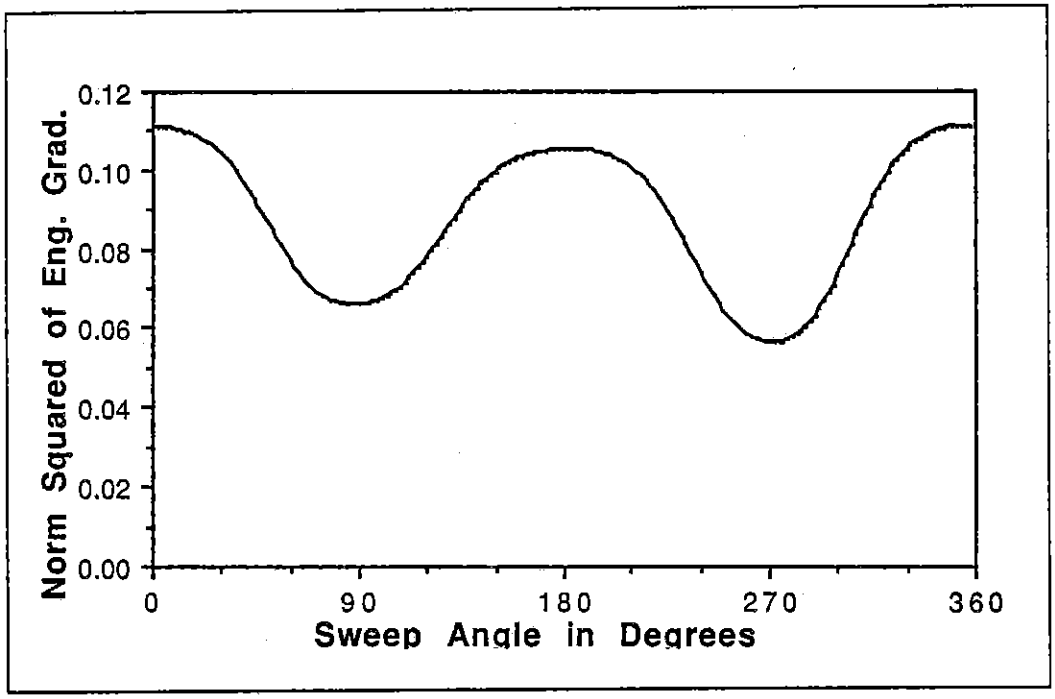

Figure 3-5 : Two Bus System Cost Function on Energy = 0.01 Surface

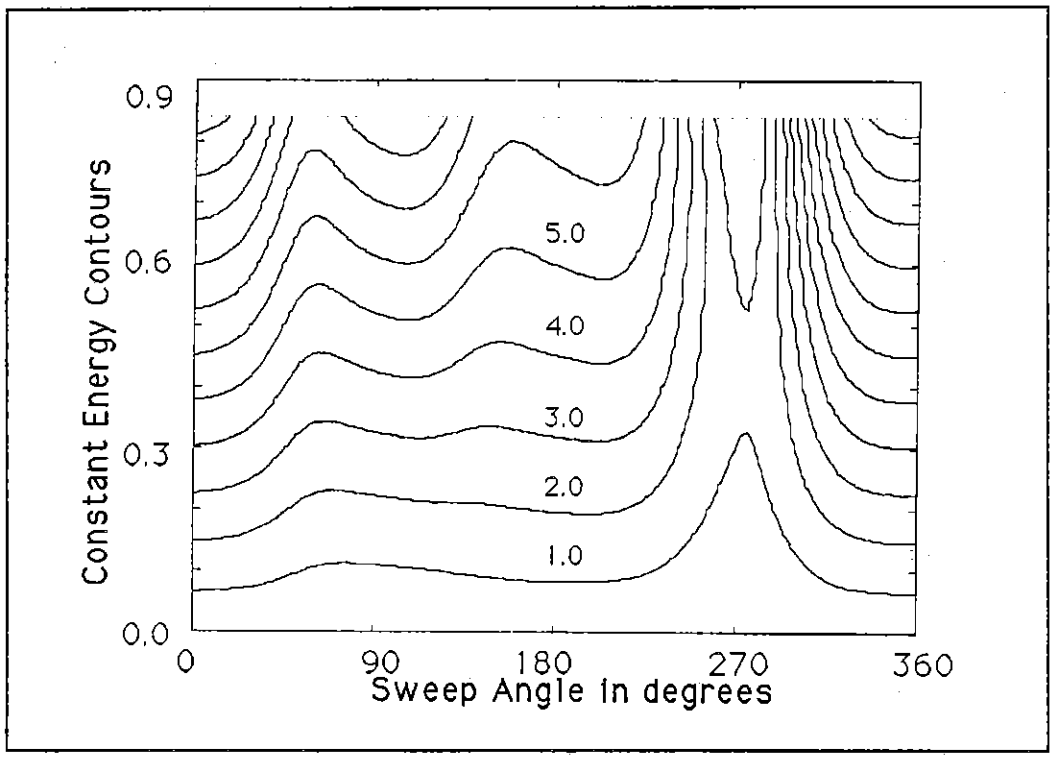

Figure 3-6 : Two Bus System Constant Energy Manifold Cost Function Contours

Figure 3-6 shows a contour plot of the cost function as a function of the search direction angle θ on the x-axis, and the value of the energy contour (enclosing x^s) on the y-axis. Notice that the global minimum on the constant energy manifolds is always in the approximate direction of $-v_2$ (270°) out to the equilibrium point occurring at $\vartheta(x^u) = 0.86$. With an initial guess in the direction of $-v_2$, the energy contour search algorithm would follow this "valley" out to x^u, correctly locating the unstable equilibrium point. The other local minimum at C[0] = 0.01, in the direction v_2 (90°), also continues to be

a local minimum as the constant energy contour value is increased. With an initial guess in the direction of v_2, the algorithm would also follow this "valley", but this unfortunately would not result in finding the equilibrium point. An additional local minimum "valley" develops at about $\vartheta(\mathbf{x}) = 0.30$. This local minimum would not be found using the energy contour search algorithm since it is not an initial local minimum in the direction of an eigenvector of $\nabla^2\vartheta(\mathbf{x}^s)$. Initial guesses in directions of the local maxima at C[0] would not be followed because the constrained minimization in step 2c would move their solution to one of the local minima, which presumably would have already been found using one of the other starting directions. Table 3-3 shows the cost function value and the load bus voltage at the local minima associated with initial guesses in the directions of $\pm v_2$ on various constant energy contours. The trajectory following the initial guess in the direction of $-v_2$ moves toward the low voltage solution at $\vartheta(\mathbf{x}) = 0.86$. This can be seen by noting that the cost reaches a maximum at about $\vartheta(\mathbf{x}) = 0.5$, and then decreases towards zero. It is not necessary to exactly determine the point where the cost goes to zero; once $h(\mathbf{x}^k[i]) < \delta$, the low voltage solution could be determined quite accurately using standard power flow techniques initialized at $\mathbf{x}^k[i]$.

	Initial $x^i[0]$ in direction of v_2.			Initial $x^i[0]$ in direction of $-v_2$.		
Energy Contour	Cost	Volt Mag.	Volt Angle	Cost	Volt Mag.	Volt Angle
0.10	0.77	1.00	-9.2°	0.56	0.70	-19.4°
0.20	1.60	1.07	-7.9°	0.98	0.63	-22.4°
0.30	2.45	1.11	-7.0°	1.31	0.58	-25.0°
0.40	3.33	1.15	-6.3°	1.54	0.53	-27.5°
0.50	4.22	1.19	-5.8°	1.64	0.48	-30.1°
0.60	5.12	1.22	-5.4°	1.60	0.43	-32.9°
0.70	6.03	1.25	-5.0°	1.34	0.39	-36.2°
0.80	6.95	1.28	-4.7°	0.74	0.33	-41.1°
0.90	7.86	1.30	-4.4°			
1.00	8.80	1.33	-4.1°			

Table 3-3 : Energy Contour Search Algorithm for 2 Bus System

In step 2a of the algorithm, a new direction to move $\Delta x^k[i]$ has to be chosen to move out to the next contour. Ideally this direction should result in $\vartheta(x^k[i] + \gamma\, \Delta x^k[i]) = C[i+1]$, with the new value close to the local minimum on the new contour, and within the same "valley" as the previous $x^k[i]$. The method which appeared to work best was to move in the direction given by $x^k[i] - x^k[i-1]$. The allowable increase in the constant energy contour, ε, depends upon how well the search

direction $\Delta x^k[i]$ approximates the direction of the local minimum valley.

Once $\Delta x^k[i]$ has been chosen, the value of γ can be determined quite rapidly by using an iterative procedure in which $\vartheta(x^k[i] + \gamma \Delta x^k[i])$ is approximated using a second order Taylor expansion:

$$\vartheta(x^k[i] + \gamma \Delta x^k[i]) \approx \vartheta(x^k) + \frac{\partial \vartheta(x^k)}{\partial x} \gamma \Delta x^k + \frac{1}{2} \gamma^2 (\Delta x^k)^T \frac{\partial^2 \vartheta(x^k)}{\partial x^2} (\Delta x^k) \qquad (3\text{-}9)$$

Because the Hessian of $\vartheta(x^k)$ is sparse, and since all other quantities are known, γ can be calculated using the quadratic equation. Normally only a few iterations are needed so that $\vartheta(x^k[i] + \gamma \Delta x^k[i])$ is sufficiently close to C[i+1]. If (3-9) has no real solution, then the value of C[i+1] must be decreased; either the energy function has a saddle point in the direction $\Delta x^k[i]$ from $x^k[i]$, or the energy function about $\vartheta(x^k[i])$ can not be well approximated by a second order Taylor expansion.

The actual constrained minimization from step 2c could be performed using the iterative generalized reduced gradient method [59]. At each loop k[m] within this minimization the following three steps are performed. First, the vector $x^{k[m]}[i] \in R^{2n}$ is partitioned into the

dependent and independent variables y and **z** respectively. Since there is only a single constraint in the minimization, y is a scalar. Let the values of y and **z** be given by the components of $\mathbf{x}^{k[m]}[i]$ with

$$y^{k[m]} = [x_r]$$
$$\mathbf{z}^{k[m]} = [x_1, x_2, \ldots, x_{r-1}, x_{r+1}, \ldots, x_{2n}]$$

Second, the minimization of the cost function is accomplished by moving in the reduced gradient direction given by

$$\Delta \mathbf{z} = -\left[\frac{\partial h}{\partial \mathbf{z}} - \frac{\partial h}{\partial y}\left[\frac{\partial \vartheta}{\partial y}\right]^{-1}\frac{\partial \vartheta}{\partial \mathbf{z}}\right] \qquad (3\text{-}10)$$

where

$$\frac{\partial h}{\partial \mathbf{z}} = \theta^T(\mathbf{x}^{k[m]}[i])\, \mathbf{J}_z(\mathbf{x}^{k[m]}[i])$$

$\mathbf{J}_z(\mathbf{x}^{k[m]}[i]) = \frac{\partial \theta}{\partial \mathbf{z}}$ = the power flow Jacobian, with column representing partial derivatives with respect to y removed.

Then $\mathbf{z}^{k[m+1]} = \mathbf{z}^{k[m]} + \mu\Delta\mathbf{z}$, where μ is a scalar "step-size" parameter. Ordinarily the value of μ which minimizes $h(\mathbf{x}^{k[m]}[i])$ would have to be determined using a line search method such as the Fibonacci or golden section techniques. However because of the structure of $h(y^{k[m]}, \mathbf{z}^{k[m]}+\mu\Delta\mathbf{z})$, it is possible to determine μ analytically with the

optimal multiplier method from the previous section using (3-6). However because the direction of movement, $\Delta \mathbf{z}$, is no longer defined by (3-4), (3-6) has to be rewritten as

$$h = ||\mathbf{a} + \mu\mathbf{b} + \mu^2\mathbf{c}||^2 \qquad (3\text{-}11)$$

with

$$\mathbf{a} = \mathbf{s} - \theta(\mathbf{x}^k)$$
$$\mathbf{b} = \mathbf{J}_z(\mathbf{x})\Delta\mathbf{z}$$
$$\mathbf{c} = -\theta(\Delta\mathbf{x})$$

The coefficients of (3-7) are then redefined as

$$g_0 = \mathbf{a} \bullet \mathbf{b}$$
$$g_1 = \mathbf{b} \bullet \mathbf{b} + 2\,\mathbf{a} \bullet \mathbf{c}$$
$$g_2 = 3\,\mathbf{b} \bullet \mathbf{c}$$
$$g_3 = 2\,\mathbf{c} \bullet \mathbf{c}$$

As before, the roots of the cubic equation are used to determine the minimum(s) of (3-11) in the direction $\Delta \mathbf{z}$.

The third step in the constrained minimization is to solve the equation $\vartheta(y^{k[m+1]},z^{k[m+1]}) = C[i+1]$, treating $y^{k[m+1]}$ as an unknown, and $z^{k[m+1]}$ as fixed. This step is necessary due to the nonlinearity of the constraint surface. The movement in the previous step in the direction

of the reduced gradient is tangential to the constraint surface; a corrective step is needed to move back onto this surface. This can be accomplished quite quickly using an iterative procedure in which $\vartheta(\mathbf{y}^{k[m+1]},\mathbf{z}^{k[m+1]})$ is approximated using a second order Taylor expansion

$$\vartheta(\mathbf{y}^{k[m+1]},\mathbf{z}^{k[m+1]}) \approx \vartheta(\mathbf{y}^{k[m]},\mathbf{z}^{k[m+1]}) + \frac{\partial\vartheta(\mathbf{y}^{k[m]},\mathbf{z}^{k[m+1]})}{\partial \mathbf{y}}\Delta \mathbf{y} + \frac{1}{2}\frac{\partial^2\vartheta(\mathbf{y}^{k[m]},\mathbf{z}^{k[m+1]})}{\partial \mathbf{y}^2}(\Delta \mathbf{y})^2 \qquad (3\text{-}12)$$

The value of $\Delta \mathbf{y}$ can then be determined by the quadratic equation; if [3-12] has no real solution, then $\mathbf{x}^{k[m]}[i]$ must be repartitioned with a different variable chosen for y. If a solution exists, $\Delta \mathbf{y}$ approximates how much to change $\mathbf{y}^{k[m]}$ in order to move back to the constant energy manifold. Since the Taylor expansion is not exact, a few iterations may be needed before $\vartheta(\mathbf{y}^{k[m+1]},\mathbf{z}^{k[m+1]})$ is sufficiently close to C[i+1]. However experience has shown that seldom more than one or two iterations are needed. The calculation of $\partial\vartheta/\partial \mathbf{y}$ is straightforward since $\nabla\vartheta(\mathbf{x})$ is just the power flow mismatch equations neglecting the conductance terms, with the reactive mismatch equation for each bus scaled by the inverse of the voltage magnitude at the bus. The calculation of $\partial^2\vartheta/\partial \mathbf{y}^2$ is similar to the

calculation of a diagonal element of the power flow Jacobian and is computationally dependent only upon the first neighbors of y.

The stopping criteria for the constrained minimization is when the change in the cost function $h(x^k[i])$ from previous value is sufficiently small. Otherwise m = m+1, and the three steps detailed above are repeated.

The energy contour search method provides an alternative to the earlier methods, which are dependent upon the convergence characteristics of the Newton-Raphson power flow. The advantage of this method is that if the minimum of the cost function can be found for each contour, the method would provide a straightforward way of determining the most pertinent low voltage solutions, namely those with the lowest energy differences.

However the implementation of the energy contour method does present at least one major obstacle. The key to the algorithm is the ability to determine the local minima on each constant energy contour. This is rather straightforward provided the local minima are continuous with respect to variation in the energy contour levels from the operable solution $\mathbf{x}^s$ out to each of the desired low voltage solutions. The algorithm would simply follow the "valley" out to the solution. This, however, is not the case. As was seen in Figure 3-6 it

is possible for a new local minimum to appear on a contour. While for this case the new local minima did not lead to a low voltage solution, this is not the case in general.

For example consider the Stagg and El-Abiad five bus system from [60] with the loads scaled by 0.8. This case then has a bus 5 low voltage solution (with an associated energy measure of 2.8), and a bus 4 solution (with an energy measure of 4.2). The bus 5 solution can be determined using the energy contour search method with an initial guess in the direction of the eigenvector associated with the smallest magnitude eigenvalue. A continuous local minimum "valley" exists out to this solution. Unfortunately no such valley exists out to the bus 4 solution. This was verified by starting at the bus 4 solution (known a priori from the Simplified method), and trying to move backward along constantly decreasing energy contours to $\mathbf{x}^s$. A local minimum valley existed from $\vartheta(\mathbf{x}) = 4.2$ down to $\vartheta(\mathbf{x}) = 3.0$, but then vanished. Testing on larger systems also indicated that while the low voltage solution with the lowest energy measure could often be found with an initial guess in the direction of the eigenvector associated with the smallest magnitude eigenvalue, no such local minimum valleys appeared to exist out to other nearby low voltage solutions.

The promise of the energy contour search method was its independence of the convergence characteristics of the Newton-

is possible for a new local minimum to appear on a contour. While for this case the new local minima did not lead to a low voltage solution, this is not the case in general.

For example consider the Stagg and El-Abiad five bus system from [60] with the loads scaled by 0.8. This case then has a bus 5 low voltage solution (with an associated energy measure of 2.8), and a bus 4 solution (with an energy measure of 4.2). The bus 5 solution can be determined using the energy contour search method with an initial guess in the direction of the eigenvector associated with the smallest magnitude eigenvalue. A continuous local minimum "valley" exists out to this solution. Unfortunately no such valley exists out to the bus 4 solution. This was verified by starting at the bus 4 solution (known a priori from the Simplified method), and trying to move backward along constantly decreasing energy contours to $\mathbf{x}^s$. A local minimum valley existed from $\vartheta(\mathbf{x}) = 4.2$ down to $\vartheta(\mathbf{x}) = 3.0$, but then vanished. Testing on larger systems also indicated that while the low voltage solution with the lowest energy measure could often be found with an initial guess in the direction of the eigenvector associated with the smallest magnitude eigenvalue, no such local minimum valleys appeared to exist out to other nearby low voltage solutions.

The promise of the energy contour search method was its independence of the convergence characteristics of the Newton-

Raphson power flow. However its inability to reliably determine the local minima of the cost function on the energy contours greatly decreases the usefulness of the method. In the next chapter an efficient and reliable method of calculating the low voltage solutions with the lowest associated energy measures is presented.

Chapter 4 - Efficient Calculation of Low Energy Solutions

In order for energy methods to be used effectively, it is imperative that an efficient method be developed for determining low voltage power flow solutions, particularly those with low associated energy measures. As was mentioned earlier, for an n bus power system, there are believed to be up to $2^n - 1$ separate low voltage power flow solutions. However as was seen in earlier chapters, energy measures only need to be calculated for those solutions which are type-one. For a small system these solutions can be determined quite rapidly using the Simplified Method from Chapter 3. However the large size and high degree of interconnections present in many modern utility systems often require a models consisting of several thousand buses. The use of the Simplified Method on such a large system would be computationally prohibitive for on-line or even most study applications. Therefore it is essential that a computationally efficient algorithm be developed for locating the appropriate low voltage solutions. Such an algorithm is developed in this chapter.

In the Simplified Method the solution for each bus i is calculated by initializing the rectangular Newton-Raphson power flow with a low initial guess at bus i. If a solution exists, then the energy measure associated with this solution can be calculated. In Chapter 3 these

energy measures were shown to provide an indication of the voltage security in the area of bus i. Experience indicates that if no solution exists for a low initial guess at bus i, then either the bus i area is relatively invulnerable to voltage collapse, or an energy measure exists for a nearby bus. The solutions with the lowest energy measures indicate the most vulnerable areas of the system. Conversely, the solutions with higher energy measures indicate the more secure portions of the system. Due to the assumed slow variation in the power system operating point, and since the energy measures have been shown to vary smoothly with respect to changes in system parameters, the voltage security of the system can be assessed by only calculating the solutions with low associated energy measures. This is normally only a small subset of the total system buses. Thus a drawback of the Simplified Method is that in order to determine this small subset of low energy solutions, it is necessary to perform n-1 power flow solutions.

4.1 Determination of Low Energy Solutions by Solving Equivalent Systems

An insight into the development of an efficient method of determining the subset of low energy solutions is suggested by two characteristics of these solutions. First, recall that by definition the energy measure

is an integration from the operable solution to a low voltage solution. Hence the lowest energy measures tend to be associated with the low voltage solutions which are "close" (in state space) to the operable solution. This is not surprising since if voltage collapse were to occur, it would be preceded by these two solutions coalescing. Second, the deviation in the bus i solution voltages from the operable voltages tends to be localized about bus i. Often for a large portion of the system there is not a significant difference in the voltages between the two solutions. Since the energy measure is an integration between the two solutions, the portion of the energy measure associated with the areas of the system where the two solutions are nearly identical is quite small (i.e. the result of the integration of the power mismatches in that portion of the system is quite small). This implies that the bus i energy can be approximated by a partial system solution. The degree of this localization is dependent upon the system parameters, particularly upon the location of sources of reactive power, since the low voltage solutions are characterized by higher reactive flows.

A second insight into the improvement of the Simplified Method comes from the interpretation of the energy measure associated with the bus i solution as an indicator of the voltage security in the area of bus i. For a utility to accurately represent the portion of the electrical system for which it has operational control, its system model must often include both a detailed representation of the their own system

(known as the internal system) and a large portion of neighboring electrical systems (known as the external system). The need for modeling the external system arises because of the high degree of interconnections in the transmission system; events in one utility's system can often have a major impact on neighboring systems. Due to restrictions on the overall size of the model, a large portion of the external system is often represented by some sort of equivalent system (i.e. the individual transmission lines and aggregate substation loads are no longer represented explicitly). Since the utility has no operational control over the external system, and because it is only represented in equivalent form, voltage security measures for many of the buses need not be calculated. The search for low voltage solutions can be restricted to buses in the internal system and perhaps a few neighboring buses in the external system. The set of buses to be examined can be further reduced by recognizing that the lowest energy measures tend to be associated with the portions of the system with large loads, which are often connected to the lower voltage level buses. Higher voltage buses and generator buses are normally relatively secure. The search for low voltage solutions can thus concentrate on a set on candidate buses which are the lower voltage, higher load buses of the internal portion of the system.

Therefore an alternative approach for rapidly determining the low energy solutions is to first identify a small equivalent system

associated with each of these candidate buses. An estimate of the energy can then be determined by solving this smaller equivalent system. Full low voltage solutions are then only calculated for the buses with the lowest energy measures for the equivalent systems. The equivalent system is created by explicitly retaining bus i, along with a set of neighboring buses, and the path set associated with these buses [68]. By using adaptive reduction techniques [61], the computational effort to create each equivalent system is minimal. The energy measure can then be determined using the low voltage solution of the bus i equivalent system and the operable solution of the equivalent system (the bus voltages for the operable solution of the equivalent system are identical to the voltages of the full system operable solution). The accuracy of the energy estimate is dependent upon the number of buses retained and the method used to calculate the equivalent portion of the system. In particular it is important that nearby buses with reactive reserve (such as PV buses) be explicitly retained. The engineering tradeoff therefore is between increased accuracy and increased size of the equivalent (and hence increased computation). If a bus i low voltage solution exists for the equivalent system, an equivalent energy measure is calculated. Full low voltage solutions are calculated only for those buses whose equivalent system energy is sufficiently low. If the equivalent system contains no bus i solution, then it is assumed that the full system also does not possess a

bus i solution. This technique, referred to here as the EQV method, is summarized as follows:

0. Obtain the operable solution $\mathbf{V}^s$.

1. Reorder and factor the bus admittance matrix (Ybus) matrix.

2. For each candidate bus in the system (Screening Stage)
   a. Determine the set of buses to be explicitly retained in the equivalent (including bus i), and their path set.
   b. Using adaptive reduction techniques, build an equivalent system.
   c. As in the Simplified Method, calculate the low initial guess at bus i, V_i^u, using the closed form expression contained in Appendix B [62], with the assumption that the voltages at all other buses are fixed.
   d. Form the power flow initial voltage guess for the equivalent system with V_j^s for $j \neq i$ and V_j^u for $j = i$.
   e. Solve the equivalent system using the rectangular Newton-Raphson method.
   f. If a solution exists calculate its energy measure. Store the solution if the energy measure is below a predetermined threshold.

3. For each bus with a sufficiently small energy measure (Solution Stage)
   a. Form the power flow initial voltage guess using equivalent system solutions for buses within the equivalent and V_j^s for j not in the equivalent.
   b. Solve the full system using the rectangular Newton-Raphson method.
   c. If a solution exists calculate its energy measure. This energy measure then provides a measure of voltage security in the area of bus i.

The practicality of the above method rests on its ability to rapidly and accurately determine the set of low voltage solutions with low associated energy measures. This, in turn, depends upon the equivalencing approach used. Ideally, the equivalent should have a bus i solution if and only if the full network has a bus i solution. Realistically, one would prefer errors where the equivalent system has a solution when the full system does not (a false alarm), rather than the equivalent not displaying a solution when a solution exists for the full system (a missed solution). A second desirable property of the equivalent is that if a solution exists, the resulting energy should provide a good estimate of the energy for the full solution. A precise estimate of the energy, while desirable, is not strictly necessary since the equivalent energies are only used to determine the set of low

energy buses. A third useful property is that ability to rapidly create and solve the equivalent systems. The equivalent system should be sufficiently small and maintain the sparsity of the original network.

A number of different equivalencing techniques are described and tested in [63], and [64]. For standard equivalent usage (such as in a contingency analysis application) the accuracy of a technique is usually assessed by comparing the voltages and power flows of the equivalenced system to those of the non-equivalenced system over a number of severe disturbances (such as the loss of a heavily loaded transmission line or a large generator). Whether an equivalent should be used depends on the size and extent of the expected disturbance(s). For sufficiently small disturbances the linearization methods from [63] would work well. However the problem under consideration here requires finding an alternative solution to the power flow equations, and thus fundamentally reflects the nonlinear nature of the power flow. Therefore a reduction of the bus admittance matrix (also known a Ward equivalent [65]) was used rather than a linearization method.

To derive the Ward equivalent, let the set of system buses be partitioned into two groups: Set E - the buses to be eliminated, and Set R - the buses to be retained in the equivalent system. The bus admittance equations can then be written as:

$$\begin{bmatrix} \mathbf{Y}_{EE} & \mathbf{Y}_{ER} \\ \mathbf{Y}_{RE} & \mathbf{Y}_{RR} \end{bmatrix} \begin{bmatrix} \mathbf{V}_E \\ \mathbf{V}_R \end{bmatrix} = \begin{bmatrix} \mathbf{I}_E \\ \mathbf{I}_R \end{bmatrix} \tag{4-1}$$

with **V** and **I** being the vectors of phasor voltages and current injections at each bus.

Eliminating set E, the equation can be rewritten as:

$$\hat{\mathbf{Y}}_{RR} \mathbf{V}_R = \hat{\mathbf{I}}_R \tag{4-2}$$

where

$$\hat{\mathbf{Y}}_{RR} = \mathbf{Y}_{RR} - \mathbf{Y}_{RE} \mathbf{Y}_{EE}^{-1} \mathbf{Y}_{ER} \tag{4-3}$$

and

$$\hat{\mathbf{I}}_R = \mathbf{I}_R - \mathbf{Y}_{RE} \mathbf{Y}_{EE}^{-1} \mathbf{I}_E$$

Note that the reduction of the above equations only affects those buses in the retained set R with original connections to the buses in set E. These buses are known as the boundary buses. The portion of **Y** associated with the non-boundary buses is unaffected by the reduction.

There are a number of variations to the Ward equivalencing method. Using the notation from [64], in the Ward Admittance method (WY

method) all the bus injections in set E are first converted to equivalent shunt admittances (i.e. $\mathbf{I}_E = 0$). This method results in very large shunts admittances at the boundary buses. For the traditional use of an equivalent, these large shunts can be problematic since they make the shunt power injections unnaturally sensitive to changes in the boundary bus voltage magnitude. However for application here these shunts can be beneficial since they result in a less "stiff" system which tends to aid in convergence to the low voltage solution. In the Ward Injection method the external system loads are not converted to shunt admittances. Once $\hat{\mathbf{Y}}_{RR}$ has been calculated, the constant power injections at the boundary buses can be calculated without explicitly determining $\hat{\mathbf{I}}_R$ since all the bus voltages are known. This technique is known as the WI-1 method. In a variation of the Ward Injection method, known as the WI-2 method, only the series elements in the external system are represented. This is done because the low series impedances of the external system result in an unrealistic aggregation of all the shunts in the external network at the boundary buses. Numerical tests reported later in this chapter indicate that the energies associated with the WI-1 and WI-2 type equivalents approximate the full solution energy more closely than the energies associated with the WY type equivalents. However the WI-1 and WI-2 methods suffer from more missed solutions than does the WY method. Therefore the WY method is judged to be preferable for this application.

In order to construct each equivalent, it is first necessary to determine the set of buses to be retained. The existence of an equivalent system solution, along with accuracy of the associated energy approximation, depends upon the number, type and location of the buses retained. However as the number of retained buses increases, the time necessary to solve the equivalent system also increases. In general, the accuracy of the bus i system solution is increased by the retention of additional buses nearby to bus i, and in particular by the retention of nearby buses with reactive reserve (PV type buses). The high sensitivity of the equivalent accuracy to the retention of nearby PV buses is due to the high reactive losses in the transmission system. These high losses (due to the high values of line reactance relative to resistance) make it difficult to transmit reactive power. The difficulty in transmitting reactive power over long distances is actually the main cause of voltage collapse, since reactive power is usually available elsewhere in the system. Since the low voltage solution at bus i is characterized by high reactive flows in the vicinity of bus i, it is important that the sources of this reactive power (i.e the nearby PV buses) be retained. In the studies performed here, the algorithm used to determine the set of retained buses explicitly retained all buses up to the second neighbor of bus i, and all PV buses up to its fourth neighbor. More sophisticated algorithms could, of course, be developed.

Once the set of retained buses has been determined, the equivalent system network could be calculated using equation (4-3) directly. This is viewed as computationally intractable because of the need to calculate $\mathbf{Y}_{EE}^{-1}$ (an $O(n^3)$ operation). A more efficient method of calculating $\hat{\mathbf{Y}}_{RR}$ is to perform a partial factorization of $\mathbf{Y}$ [66]. However because the EQV Method requires calculation of a large number of equivalents (one for each candidate bus), the adaptive reduction technique [61] is more suitable computationally. In the adaptive reduction technique, the $\mathbf{Y}$ matrix is assumed to have first been factored into LU form:

$$\begin{bmatrix} \mathbf{Y}_{EE} & \mathbf{Y}_{ER} \\ \mathbf{Y}_{RE} & \mathbf{Y}_{RR} \end{bmatrix} = \begin{bmatrix} \mathbf{L}_{EE} & \mathbf{0} \\ \mathbf{L}_{RE} & \mathbf{L}_{RR} \end{bmatrix} \begin{bmatrix} \mathbf{U}_{EE} & \mathbf{U}_{ER} \\ \mathbf{0} & \mathbf{U}_{RR} \end{bmatrix} \tag{4-4}$$

In [67] it is shown that

$$\begin{aligned} \mathbf{Y}_{RE}\,\mathbf{Y}_{EE}^{-1}\,\mathbf{Y}_{ER} &= (\mathbf{L}_{RE}\mathbf{U}_{EE})(\mathbf{L}_{EE}\mathbf{U}_{EE})^{-1}(\mathbf{L}_{EE}\mathbf{U}_{EB}) \\ &= \mathbf{L}_{BE}\mathbf{U}_{EE}\mathbf{U}_{EE}^{-1}\mathbf{U}_{EE}^{-1}\mathbf{L}_{EE}\mathbf{U}_{EB} \\ &= \mathbf{L}_{BE}\mathbf{U}_{EB} \end{aligned} \tag{4-5}$$

Thus once $\mathbf{Y}$ has been factored, $\hat{\mathbf{Y}}_{RR}$ from (4-3) can be calculated as

$$\hat{\mathbf{Y}}_{RR} = \mathbf{Y}_{RR} - \mathbf{L}_{BE}\mathbf{U}_{EB} \tag{4-6}$$

The multiplication of $\mathbf{L}_{BE}$ and $\mathbf{U}_{EB}$ can be performed quite quickly since both matrices are usually sparse. The net result is the ability to calculate $\hat{\mathbf{Y}}_{RR}$ many times faster than performing a partial matrix factorization. Intuitively adaptive reduction proves efficient because most of the work necessary to calculate $\hat{\mathbf{Y}}_{RR}$ has already been done during the factorization of **Y**. Since the EQV Method requires the calculation of a large number of equivalent systems, it is much more efficient to factor **Y** once, and use (4-6) to calculate each equivalent system. The use of adaptive reduction does not require that **Y** be ordered so that set R (the set of retained buses) is physically last. However it is necessary that it be possible to make set R conceptually last. That is, during the factorization of **Y**, the calculation of the elements of $\mathbf{L}_{BE}$ and $\mathbf{U}_{EB}$ must be independent of the calculation of the elements of $\mathbf{Y}_{RR}$. This can be accomplished by augmenting set R to include its path set. The path set for any bus can be determined according to the following algorithm [68]:

1. Let i be the first bus in path.
2. Get the number of next element in column i of **L** (or row i of **U**). Replace i with this number and add it to the path.
3. If k = last bus in **L** (or **U**) then exit; else Goto 2.

The path set of R is the union of the path sets for the individual buses in R. The augmentation of R by its path set eliminates the need to

reorder the buses. The elements in any path set are, of course, dependent upon the original ordering used during the matrix factorization.

In standard power system applications the buses are usually ordered to minimize the number of fill-ins which will occur during the factorization. The most popular ordering technique is Tinney Scheme 2 [69]. However in the EQV Method the use of a different ordering technique is often preferable. This is because since the **Y** matrix only needs to be factored once at the beginning of the algorithm, the majority of the computation is spent in solving the equivalent systems. However since the number of elements in each equivalent system includes the original set R augmented by its path set, the total size of the equivalent system can be reduced by minimizing the size of the path sets. With a large number of equivalent systems to be solved in the EQV Method, it is not beneficial to order **Y** to explicitly reduce the length of the path sets for any small set of buses. Rather the matrix should be ordered to reduce the average minimum length of the path sets for all buses. In [70] the Minimum Degree Minimum Length (MDML) algorithm is proposed to minimize the average length of the path sets. The lengths of the factorization paths are decreased by explicitly ordering the nodes to increase the width of the factorization path graph. A comparison of the solution times for Tinney Scheme 2 versus the MDML algorithm is provided later in the chapter.

The computational improvement of the EQV method versus calculating a full system low voltage solution for each candidate bus (i.e. those buses where voltage security measures are desired) is dependent upon the size of the system. This is because the number of explicitly retained buses in an equivalent system is only dependent upon the local topology about the bus of interest. This set would normally include about 10 to 20 buses. Thus for small systems (under approximately 50 buses) there is little benefit in using the EQV Method since the size of set R (the set of explicitly retained buses and their path set) is a sizeable portion of the total system size. But since the number of buses explicitly retained is independent of total system size, the percentage of total buses retained decreases as the size of the system increases. The equivalent is not, however, totally independent of the size of the original system. The equivalent must include the path set of the explicitly retained buses. The path set is dependent upon the ordering of the original system, and in general, increases with the number of buses in the original system.

4.2 EQV Method Experimental Results

The EQV method was tested on the standard IEEE 118 bus case. Recall that the goal here is to provide a qualitative assessment of the

voltage security of a slowly varying power system. The voltage security is assessed by freezing the system at a given time and then calculating the appropriate energy measures. The security of different operating points can be compared by comparing their respective energy measures. The objective of this section is to demonstrate that the EQV Method provides an accurate and computationally efficient method of determining the set of lowest energy measures.

As was the case for the Chapter 2 example, the loads at all buses in the IEEE 118 bus case were again assumed to be a linear function of a parameter k (k=1 for basecase). System generation was varied in order to keep the real power delivered by the slack bus (bus 69) constant. As k increases the system becomes more heavily loaded until the point of voltage collapse is reached at k=3.0.

As the system load is increased, the number of low voltage solutions tends to decrease. This variation in the number of low voltage solutions identified with respect to k is shown by the upper curve in Figure 4-1 (here all solutions were calculated using the Simplified Method). However recall that only those solutions with low energy measures (indicating areas of the system vulnerable to voltage collapse) need to be calculated. The lower curve in the figure shows the variation in the number of solutions with energy measures less than 3.0 as the system load is increased. For low load levels, when

the system is quite secure, there are only a few solutions with energy values less than 3.0 (the lowest energy value for k=1 is 2.75). As the system loading increases, the number of low energy solutions also tends to increase, indicating that the system is becoming more vulnerable to voltage instability in a number of areas. Still, the number of low energy solutions remains quite moderate. Immediately before voltage collapse there is only a single low voltage solution. Voltage collapse occurs when this solution coalesces with the operable solution. Figure 4-1 shows that regardless of system loading, only a small number of low voltage solutions need to be calculated to assess system voltage security. The applicability of the EQV Method to the problem can be demonstrated by showing that it accurately determines this subset of low energy solutions with reasonable computational cost.

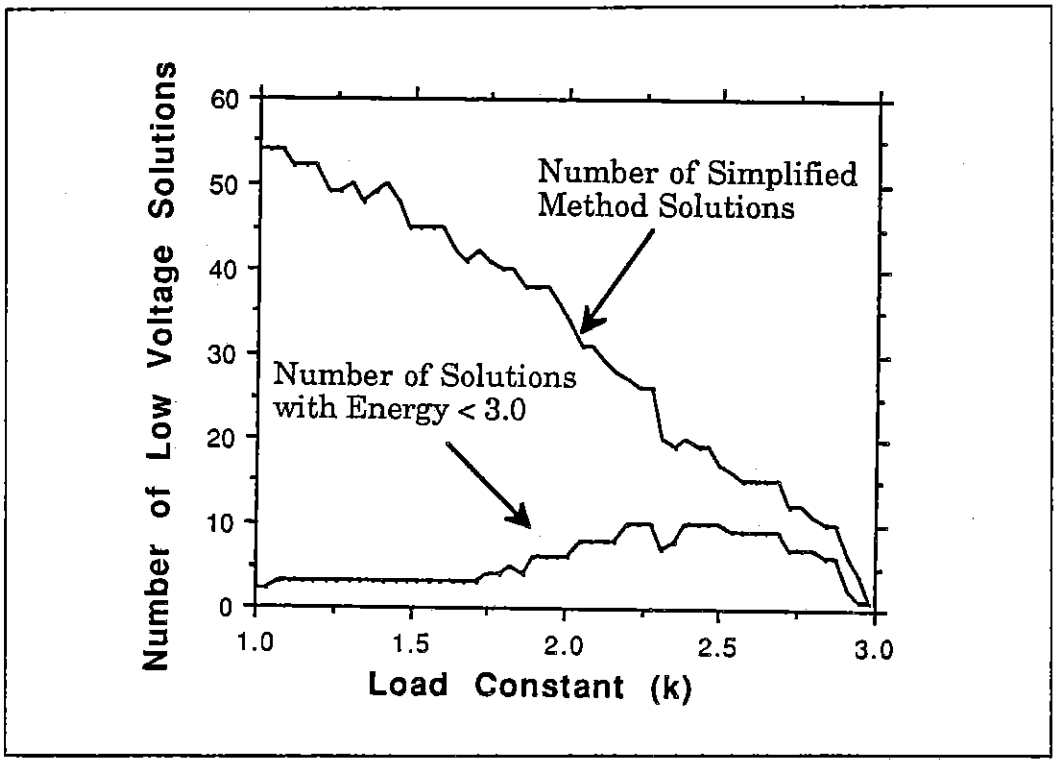

Figure 4-1 : Variation in number of Low Voltage Solutions

In this section the energy estimates obtained using the three equivalencing methods are compared to the Simplified method energies. The accuracy of the EQV Method is demonstrated by comparing these values. At k=1, 49 low voltage solutions were found using the Simplified method, while 52 solutions were found using the Ward Admittance method (WY), 49 solutions using the WI-1 method, and 49 solutions using the WI-2 method. All three methods correctly located the 20 low voltage solutions with the lowest energy measures. Of the 52 solutions found using the WY method, four were false

alarms, while one actual low voltage solution was missed (the energy measure associated with this missed solution was quite high). The WI-1 and WI-2 methods had no false alarms and no missed solutions. Table 4-1 shows a comparison between the full solution energies and those of the equivalent systems for the fifteen lowest values. Note the rankings of the equivalent energies for all three methods correlate quite closely to the ranking of the full solution energies.

Bus #	# of buses in Equiv.	Full Solution Energy	WY Equiv. Energy	WI-1 Equiv. Energy	WI-2 Equiv. Energy
44	35	2.75	2.74	2.77	2.76
43	38	2.81	2.79	2.81	2.81
21	31	3.03	2.99	3.03	3.04
10	25	3.22	3,11	3.25	3.25
22	33	3.52	3.48	3.52	3.53
20	36	3.76	3.69	3.77	3.78
53	28	3.85	3.84	3.87	3.87
52	29	4.01	3.98	4.03	4.03
76	37	4.01	4.00	4.01	4.01
1	28	4.75	4.48	4.86	4.88
101	30	4.88	4.84	4.85	4.89
33	42	5.11	5.01	5.19	5.18
84	24	5.27	5.14	5.27	5.31
74	43	5.38	5.37	5.42	5.42
57	29	5.53	5.47	5.58	5.58

Table 4-1 : Comparison of Full Solution to Equivalent System Energies for k=1

For the equivalent systems at k=1, the average percentage difference between the equivalent energies and the full solution energies was 1.6% for the WY method, 0.5% for the WI-1 method, and 0.5% for the WI-2 method. The average size of the equivalent systems was

34.5 buses. The WY method missed the solution at bus 14 (which had a full solution energy of 6.86), and had false alarms at buses 4, 27, 64, and 113 (with equivalent system energies of 11.1, 28.7, 20.8, and 17.6 respectively). The missing of the bus 14 solution is not significant because of its high energy. In this system, with a load corresponding to k=1, the conclusion is that all three methods of equivalencing do a very good job.

As the load on the system is increased, the number of missed solutions and false alarms also tended to increase. For example at k=2, where there are 31 Simplified Method solutions, there was one missed solution and eight false alarms for method WY, nine missed solutions and two false alarms for method WI-1, and three missed solutions and two false alarms for method WI-2. Table 4-2 compares the energy of the equivalent systems to the full solution energies for the fifteen lowest values at k=2.

Bus #	# of buses in Equiv.	Full Solution Energy	WY Equiv. Energy	WI-1 Equiv. Energy	WI-2 Equiv. Energy
44	32	1.80	1.77	1.77	1.79
43	33	1.96	1.92	1.96	1.97
21	28	2.31	2.23	2.24	2.26
53	27	2.62	2.58	2.64	2.65
10	22	2.64	2.71	2.55	2.56
76	36	2.78	2.76	2.77	2.77
52	28	2.84	2.77	2.88	2.88
1	26	3.28	2.91	2.99	3.06
101	28	3.55	3.43	No Solution	3.54
107	25	3.59	3.36	No Solution	3.58
86	20	3.61	3.54	No Solution	3.59
33	41	3.85	3.73	3.86	3.82
84	21	3.94	3.69	No Solution	3.85
98	46	4.30	4.22	4.28	4.29
74	40	4.38	4.36	4.31	4.32

Table 4-2 : Comparison of Full Solution to Equivalent System Energies for k-2

At k=2 the average percentage difference between the equivalent energies and the full solution energies was 3.3% for the WY method, 1.4% for the WI-1 method, and 1.4% for the WI-2 method. For the WY method the missed solution was at bus 82 (which had a full

solution energy of 5.76), while the only false alarm with relatively low energy was at bus 13 (equivalent system energy of 3.50). As can be seen from the table, the WI-1 method missed a number of the lowest fifteen solutions, although it still managed to locate the lowest eight. The WI-2 method missed the solutions at buses 82, 83 and 93 (which had full solution energies of 5.76, 3.61, and 5.57 respectively).

As k was increased beyond 2.0, both the WI-1 and WI-2 method increasingly missed significant low voltage solutions. For example at k=2.48 the WI-1 method missed the lowest energy solution (at bus 44 with energy = 1.15), while at k=2.36 the WI-2 method missed the third lowest energy solution (at bus 43 with energy = 1.54). The WY method correctly located the top fifteen solutions for all values of $k \leq 2.40$ and the top five solutions for $k \leq 2.48$.

However even the WY had some difficulty locating all solutions as the system moved towards the point of voltage collapse. One reason for the increase in missed solution is that as the system becomes more heavily loaded, local voltage sources reach their limits. The necessary voltage support must then be supplied from increasingly distant sources (PV buses). If these PV buses are not explicitly included in the equivalent system then a missed solution may result. An example of this occurs with the equivalent solution at bus 1. For $k<2.52$ both the equivalent system and the full system have a bus 1 low voltage

solution. But at k=2.52 the solution is missed. If, however, the equivalent is augmented to include the PV generator at bus 42, the equivalent solves with an energy of 1.87 (versus 1.64 for the full solution energy). Nevertheless, since it is possible for the EQV Method to miss significant solutions, it should be used in conjunction with a method with more robust convergence characteristics. Such a method, which will be referred to as the Fixed Boundary Bus Voltage (FBBV) Method, is introduced in the next section.

The advantage of using the EQV method is its increased computational efficiency over the Simplified Method. This is demonstrated in Table 4-3. Values shown are for k=1, and times given are in seconds. For reference, the necessary to calculate the operable power flow solution from a flat start was 3.6 seconds on the machine used.

	Simplified Method	Equivalent System Method
Order/Factor Ybus	N.A.	1.0
Construct 117 equivalents for screening	N.A.	15.4
Solution of 117 equivalent systems and calculation of screening energy	N.A.	138.1
Full Solutions (117 for Simplified Method, top 10 for ES Method)	570.8	53.0
Total	570.8	207.5

Table 4-3 : Comparison of Computation Times between Solution Methods

In the Simplified Method the determination of the set of low energy solutions at each time step required 117 power flow solutions of the full 118 bus system (the 117 arises because low voltage solutions were attempted at each bus except the slack). With the EQV method the Ybus matrix first had to be re-ordered and factored. Then the 117 equivalent systems were constructed using adaptive reduction. As can be seen from Table 4-3, the time to perform these first two steps was relatively small. For cases where a number of studies are being performed using the same Ybus (such as in an on-line environment), most of the work of the first two steps need only be performed during the first study run. The majority of the time was spend solving the 117 equivalent systems, being equal to about 24% of the time

necessary to solve the full systems. This decrease was due to the smaller size of the equivalent systems (average of 34.5 versus 118 buses for the full system). For larger systems the decrease should be even greater since the sizes of the equivalent systems do not increase in proportion to the increase in full system size. The last step in the EQV method was performing full low voltage solutions for those cases with low enough equivalent system energy. Because of the relative accuracy of the equivalent system energies, full low voltage solutions would, at most, need to be performed at a small number of buses. In Table 4-3, full solutions were performed for the ten buses with the lowest screening energy measures.

As was mentioned earlier, the reason the Ybus matrix is reordered to decrease the size of the path set which must be included in the equivalent system. While the Tinney Scheme 2 ordering algorithm normally results in the least number of fills during matrix factorization, it does not result in an ordering which minimizes the average length of the path sets. In [70] a comparison is made for the IEEE 118 bus system between the Tinney Scheme 2 algorithm and the MDML (Minimum Degree Minimum Length) algorithm. For the Tinney method the mean path for the buses of the matrix was 11.6 buses, with a standard deviation of 4.7, and a maximum path of 23. However for the MDML method the mean path was just 8.2, with a standard deviation of 2.2, and a maximum path of 12 buses.

The practical result of using the MDML ordering algorithm is that the equivalent systems are smaller, with a subsequent decrease in solution times. For example if the Tinney Scheme 2 algorithm is used instead of the MDML algorithm, the average size of the equivalent systems increases from 34.5 buses to 37.3 buses, and the solution time increases from 138.1 seconds to 149.8 seconds.

4.3 Fixed Boundary Bus Voltage Screening Method

The EQV method has the advantage that the equivalent system energies closely match the full solution energies. However a disadvantage is that it can occasionally miss low energy solutions. Also because of the need to include the path set of the explicitly retained buses, the size of the equivalent systems is not completely independent of the original system size. To overcome these drawbacks, this section introduces an alternative technique, referred to here as the Fixed Boundary Bus Voltage (FBBV) method.

The idea behind the FBBV method is to approximate the energy of the bus i solution by solving a smaller system consisting of bus i along with some of its neighboring buses. Voltages at all other buses are assumed fixed. Similar techniques have previously been used in

contingency analysis to quickly determine which contingencies are likely to result in violations [71], [72].

Bus i and its neighboring buses will again be referred to as the internal system, while the remaining buses in the system will be referred to as the external system. The buses in the external system which have connections to the internal system will be referred to as the boundary buses. During the solution of the internal system, the voltage magnitudes and angles at all other buses in the system (i.e. the external system) are assumed fixed at their operable solution values. Since the voltage magnitudes are fixed in the external system, the solution of the internal system only requires solving a system consisting of the internal along with the fixed voltage boundary buses. Thus the boundary buses function as "slack" buses during the solution, with fixed V/α and variable power injection P/Q. The simplest FBBV system consists of a solitary internal bus i. This is just the system used to get the initial low voltage guess for the Simplified method; the closed-form expression for the low voltage solution is given in Appendix B.

Since the power injections from the boundary buses are free to vary, the FBBV system is less constrained than the original system. This suggests that the FBBV system should have a bus i low voltage solution if the original system possesses a bus i low voltage solution.

Practically this should result in extremely few missed solutions, at the possible cost of a large number of false alarms (for example an internal system consisting of a single bus i always has a solution). Since the method assumes fixed external bus voltages, obviously how well the bus i solution of its FBBV system approximates the bus i solution of the full system depends upon which buses are included in the FBBV system. If the FBBV system solution exists, it is either a false alarm, or its energy tends to over approximate the energy of the full system bus i solution. Intuitively this energy over approximation arises because allowing the P/Q output of the boundary buses to vary results in a "stronger" system than the original system (i.e any additional power needed by the internal system can be supplied at the boundary buses, rather than from more remote sources).

The advantages of the FBBV method are the lack of missed solutions, and the property that internal system size is independent of the original system size. The latter property holds because there is no need for the internal system's path set. The localized nature of voltage problems, due to the high reactive losses in the transmission system, often results in a fairly accurate energy estimate from the solution of a rather small system. Of course the severe approximation of ignoring the external portion of the system produces estimates that are usually not as accurate as those found using network reduction. However in

an initial search for low voltage solutions, high accuracy is not as important as avoiding missed solutions.

The FBBV method was tested on the IEEE 118 bus system, using the same voltage collapse scenario from the previous section of parameterizing all the loads as a function of k, and then gradually increasing k. For test purposes the equivalent systems consisted of bus i and neighboring buses extended out to a specified level. Five sizes of equivalent systems were tested. The level 0 system consisted of just bus i, the level 1 system consisted of bus i and its first neighbors, the level 2 system of bus i and its first and second neighbors, etc. The average size of the equivalent systems was 1 bus for the level 0 systems, 4.0 buses for level 1, 10.6 buses for level 2, 21.1 buses for level 3, and 34.5 buses for level 4. These equivalent systems were chosen to demonstrate that quite good results were possible, even when a simplistic method of determining the equivalent system buses was employed. More sophisticated algorithms of determining which buses to include in the bus i FBBV system could be used. An example would be to explicitly include more distant reactive power sources.

The variation in the number of low voltage solutions with respect to k for each size of FBBV system is shown in Figure 4-2. As expected, a low voltage solution exists for every level 0 system. But as the size of

the FBBV systems is increased, the number of low voltage solutions decreases. Notice that by just solving a level 2 system (with an average size of only 10.6 buses) almost half of the candidate low voltage solutions can be eliminated. Also note that there were virtually no missed solutions. Table 4-4 shows a comparison between the energies of the FBBV systems versus those of the full solution for the 15 buses with the lowest values at k=1.

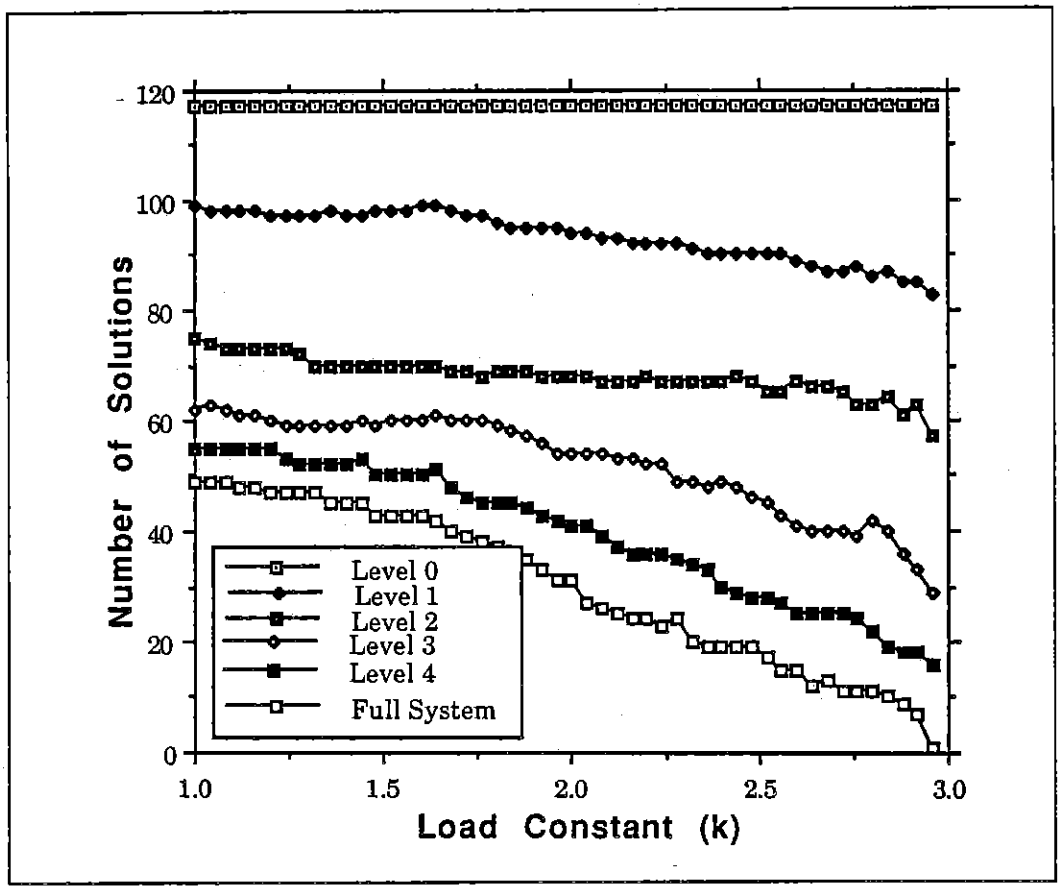

Figure 4-2 : Variation in number of FBBV Low Voltage Solutions

Bus #	Level 0 Energy	Level 1 Energy	Level 2 Energy	Level 3 Energy	Level 4 Energy	Full Solution Energy
44	6.06	3.66	3.01	2.87	2.74	2.75
43	4.51	3.54	3.18	2.82	3.05	2.81
21	9.11	3.98	3.70	3.05	3.01	3.03
10	14.5	6.13	4.21	3.73	3.81	3.22
22	7.04	4.71	4.18	3.93	3.52	3.52
20	9.34	5.96	3.83	4.08	3.76	3.76
53	5.82	5.04	4.21	3.95	3.87	3.85
52	9.11	5.29	4.65	4.06	3.92	4.01
76	9.28	5.61	5.04	4.08	4.11	4.01
1	13.2	7.27	5.50	5.21	5.12	4.75
101	7.15	5.40	5.07	4.75	4.75	4.88
33	6.91	6.32	6.23	5.09	5.19	5.11
84	8.37	5.97	4.94	4.95	5.03	5.27
74	12.4	7.56	6.74	5.52	5.46	5.38
57	8.07	6.87	5.59	5.61	5.50	5.53

Table 4-4 : Comparison of FBBV System Energies to Full System Energies

The average percentage difference in energy values between the FBBV solutions and the full system solutions at k=1 was 36.1% for the level 1 systems, 14.8% for the level 2 systems, 4.7% for the level 3 systems, and 3.4% for the level 4 systems. While these values are

not as low as the average differences for the equivalent systems from Table 4-1, the correlation is still close enough for effective screening of solutions. Recall that the goal of screening is to rapidly locate candidate low energy buses. Buses could be eliminated at each level in the screening if they had no solution at the previous level. Additionally, the bus search order could be prioritized based upon their energies at each level. Buses with sufficiently low energies could be retained, while those with sufficiently large energies eliminated. Once the number of candidate buses has been sufficiently reduced, the EQV method could be used to obtain accurate energy estimates. Full low voltage solutions would then only be performed for the few, if any, buses with extremely low EQV energy measures, or if there was suspicion of a missed solution (i.e. very low FBBV without an equivalent system solution).

The central reason for using a screening method is to decrease the computational time to determine the low energy solutions. Table 4-5 shows the times to perform the screenings for each of the various levels for k=1.0. Only solutions with energies less than a cutoff value were passed on to the next level. Again, for reference, the flat start operable power flow solution time was 3.6 seconds.

	Level 0	Level 1	Level 2	Level 3	Level 4
Cutoff energy	∞	8.0	6.0	5.0	4.0
Number of Solutions	117	99	26	17	13
Solution time in secs.	4.4	17.5	8.6	10.1	15.4

Table 4-5: FBBV Solution Statistics for k=1

The FBBV method reduced the number of candidate buses from 117 to 13 in the time necessary to perform about 14 full power flow solutions. The EQV method equivalents could then be built and solved for these 13 in the time necessary to perform a few more power flow solutions of the full system. The accuracy of these equivalent solution energies (shown in Table 4-1) would mean that it would probably be unnecessary to solve any full low voltage solutions. Thus the voltage security of the system can be determined in the time necessary to perform about 15 to 20 power flow solutions of the full system.

Two methods have been introduced in this chapter for rapidly determining the set of low voltage solutions with low associated energy measures. Both methods reduce the solution time by solving equivalent systems, rather than the full power system, for each candidate bus. In the EQV method the equivalent systems are calculated using the Ward Admittance technique with adaptive

reduction. It was shown that the equivalent system energies closely match the full system energies. However the sizes of the EQV equivalents are not completely independent of original system size, and can occasionally result in missed low energy solutions. The Fixed Boundary Bus Voltage (FBBV) screening method overcame these shortcomings by just solving a subsystem of the original system. The solution technique consisted of fixing the bus voltages are the subsystem boundary buses. The FBBV method has the advantages of very few missed solutions and fast solution times, independent of the original system size. The energy approximations, however, are not as accurate those from the EQV method. Therefore the preferred technique is to use the FBBV method to rapidly eliminate those buses with either no solution or a high energy solution. The EQV method can then be used to provide rapid estimates of the energy of the remaining solutions. The computational suitability of this approach for on-line use is demonstrated in Chapter 5.

Chapter 5 - Enhancement of Voltage Security

The thesis has, thus far, discussed the application of an energy based method for assessing the vulnerability of electrical power systems to voltage collapse. In this chapter it is shown that energy function techniques not only provide a viable method for assessing, but also for enhancing the voltage security of a large power system.

5.1 Application of Energy Based Controller Sensitivities

Once a power system is found to be vulnerable to voltage instability and ultimately to voltage collapse, a method must be provided for enhancing the security of the system. This voltage security enhancement can be accomplished by changing the setting of the various controllers available on a power system. These controllers normally include the real power (MW) output and voltage magnitude setpoint of generators, the tap positions on load tap changing (LTC) transformers, tap positions for phase shifter transformers, variation in the amount of shunt capacitors connected to the system, and (as a last resort) removal of customer loads. However, in order to operate their systems effectively utilities must also take into account economic considerations, and other security constraints such as transmission line and transformer flow limits. Therefore any technique of enhancing

voltage security should be capable of integrating into existing techniques for enhancing the overall security and economics of system operation.

Linear programming (LP) optimization methods have proven effective in solving the problem of minimizing system operating costs, subject to the constraint that no security limits are violated [73], [6]. In these methods constraints enter the problem by first calculating the linear sensitivity of the constraint to the system controllers. These sensitivities then form a row in the LP tableau. In a similar manner, the availability of a closed form differentiable expression for the energy function also allows for the derivation of controller sensitivities through a first order Taylor expansion. These sensitivities could then be integrated into an LP optimization method such as the one presented in [6]. Similar analytic sensitivities have been previously derived for the transient stability energy function. In [74] numerous simulations of actual power systems have shown that such first order sensitivities can often be successfully used to improve system transient stability. In this section the calculation and use of the sensitivities of the energy measure to various controllers are discussed.

The sensitivity of the energy measure given in (2-16) to the controllers is first derived. To facilitate this derivation, let the variables used in (2-16) be partitioned as follows:

- $\mathbf{x}^s,\mathbf{x}^u$ - State variables (voltages and phase angles at all buses except for the slack) at the stable and unstable equilibrium points;
- $\mathbf{u}$ - Control variables (generator real power output and set point voltages, transformer tap positions, etc.);
- $\mathbf{p}$ - Uncontrolled parameters (e.g. line conductance and susceptance terms).

The parameter dependence of the energy function can then be expressed as:

$$\vartheta(\mathbf{u},\mathbf{p},\mathbf{x}^s(\mathbf{u},\mathbf{p}),\mathbf{x}^u(\mathbf{u},\mathbf{p})) \tag{5-1}$$

For the derivation to follow, it is important to stress that the control parameters enter the energy function both explicitly and implicitly; the implicit dependence comes through the motion of the equilibria under the effect of controller changes. With this observation in mind, the first order sensitivity of the energy function with respect to changes in a control variables u_i is calculated by applying the chain rule

$$\frac{d\vartheta}{du_i} = \frac{\partial\vartheta}{\partial u_i} + [\frac{\partial\vartheta}{\partial x^s}]^T \frac{\partial x^s}{\partial u_i} + [\frac{\partial\vartheta}{\partial x^u}]^T \frac{\partial x^u}{\partial u_i} \qquad (5\text{-}2)$$

If the system model is such that the energy function ϑ formally defines a Lyapunov function for the system equations (i.e. if the system equations neglect losses), one would expect that ϑ would have a zero first derivative with respect to the state variables at all equilibrium. Under these conditions, the second and third terms of (5-2) would be identically zero. This is not the case for realistic models which include transmission line real power losses; the second and third terms must be included. Note also that even though the gradient of $\vartheta(\mathbf{x})$ was made identically zero at $\mathbf{x}^s$ by the addition of the conductance terms in (2-15), $\partial\vartheta/\partial\mathbf{x}^s$ is not zero. This is because the added terms that locally correct for conductance,

$$- \sum_{j=1}^{n} G_{ij} |V_i^s| |V_j^s| \cos(\alpha_i^s - \alpha_j^s)$$

in (2-15a) and

$$- \sum_{j=1}^{n} G_{ij} |V_i^s| |V_j^s| \sin(\alpha_i^s - \alpha_j^s)$$

in (2-15b), are themselves a function of $\mathbf{x}^s$.

Sensitivities can be derived for any of the following types of controls: generator MW/MVAR/voltage setpoints, load MW/MVARs, transformer tap positions, MW transactions, phase shifter taps, and shunt capacitance variation. Computationally the cost to calculate each controller sensitivity is quite modest (on the order of a forward and backward substitution of the power flow equations), with most of the effort expended on the calculation of $\partial\vartheta/\partial\mathbf{x}^s$ and $\partial\vartheta/\partial\mathbf{x}^u$. For illustrative purposes, the sensitivity of the energy function to changes in generator real power output (MW) is examined in the following example.

With $\mathbf{x} = [\alpha\ |V|]^T$, the sensitivity of the energy with respect to the real power output of the generator at bus j is given by

$$\frac{d\vartheta}{dP_{Gj}} = (\alpha_j^u - \alpha_j^s) + [\frac{\partial\vartheta}{\partial\mathbf{x}^s}]^T \frac{\partial\mathbf{x}^s}{\partial P_{Gj}} + [\frac{\partial\vartheta}{\partial\mathbf{x}^u}]^T \frac{\partial\mathbf{x}^u}{\partial P_{Gj}} \qquad (5\text{-}3)$$

The first term in (5-3) is due to the explicit dependence of the energy measure upon the power injection at bus j. However since it is just the difference in the voltage phase angle at bus j between the low voltage solution $\mathbf{x}^u$ and the operable solutions $\mathbf{x}^s$, it is known directly. The latter two terms are due to the implicit dependence of ϑ upon P_{Gj}; that is, changing the real power injection at bus j changes the solutions $\mathbf{x}^u$ and $\mathbf{x}^s$ and hence changes the energy measure ϑ. The vectors

$\partial\vartheta/\partial x^s$ and $\partial\vartheta/\partial x^u$ are sparse, with nonzero components only at locations corresponding to bus j and its first neighbor buses. The vectors $\partial x^s/\partial P_{Gj}$ and $\partial x^u/\partial P_{Gj}$ can be calculated quite efficiently using sparse vector methods [68]. Therefore once $\mathbf{x}^s$ and $\mathbf{x}^u$ are known, the computational cost of evaluating (5-3) is quite minimal.

As an example of the application of generator MW controller sensitivities, consider the IEEE 118 bus case from Chapter 4, with loads again modeled as a linear function of a parameter k. The aim of this example is to demonstrate that the use of controller sensitivities provides a good mechanism for increasing system voltage security. Assume for illustration that the system is operating at k=2.6, and that the voltage security criteria for system operation is that no low voltage solutions have energy measures less than 1.0 (this voltage security criteria could be determined through off-line studies and would depend upon the expected variation in the energy measure). At this load level, only the energy measure associated the bus 44 solution is less than 1.0, with ϑ=0.9239. Further assume that the only control actions available are changing the generator MW outputs.

The first step to increase the system's voltage security is to use (5-3) to calculate the sensitivity of this energy measure to a per unit (on 100 MVA base) change in the generator MW outputs. The generators with the largest magnitude sensitivities are listed in Table 5-1.

Generator Bus Number	Current MW Output	Sensitivity of energy to increase in generator MW output
10	450.0	-0.0419
46	116.1	0.2013
49	333.5	0.0794
54	209.9	0.1085
55	194.3	0.1034
56	0.0	0.1084
59	478.8	0.0490
113	26.4	-0.0373

Table 5-1 : Sensitivity of Bus 44 Energy Measure to Generator MW Variation

In an application environment, the selection of which controller(s) to move would require the consideration of a number of different criteria (such as the relative economics of the generator, and the effect of variation in the generator's output on other system variables such as transmission line flows) in addition to the sensitivity of the energy measure. However to simplify the example assume that these factors are ignored; the objective is to increase the energy measure with the minimum amount of change to the generators' outputs. In this case, only generator 46, which has the highest sensitivity, is initially selected. The amount to vary generator 46's output to increase the

energy measure from 0.9239 to 1.0 can be approximated using its sensitivity value of 0.2019:

$$\Delta P_{G46} = \frac{(1.0 - 0.9239)}{0.2019} * 100MW = 37.7\ MW$$

The accuracy of the estimation of ΔP_{G46} depends upon how well the linear sensitivity approximates the actual variation in the energy measure with respect to the generator 46 output. A comparison between this linear approximation and the actual energy variation is shown in Figure 5-1.

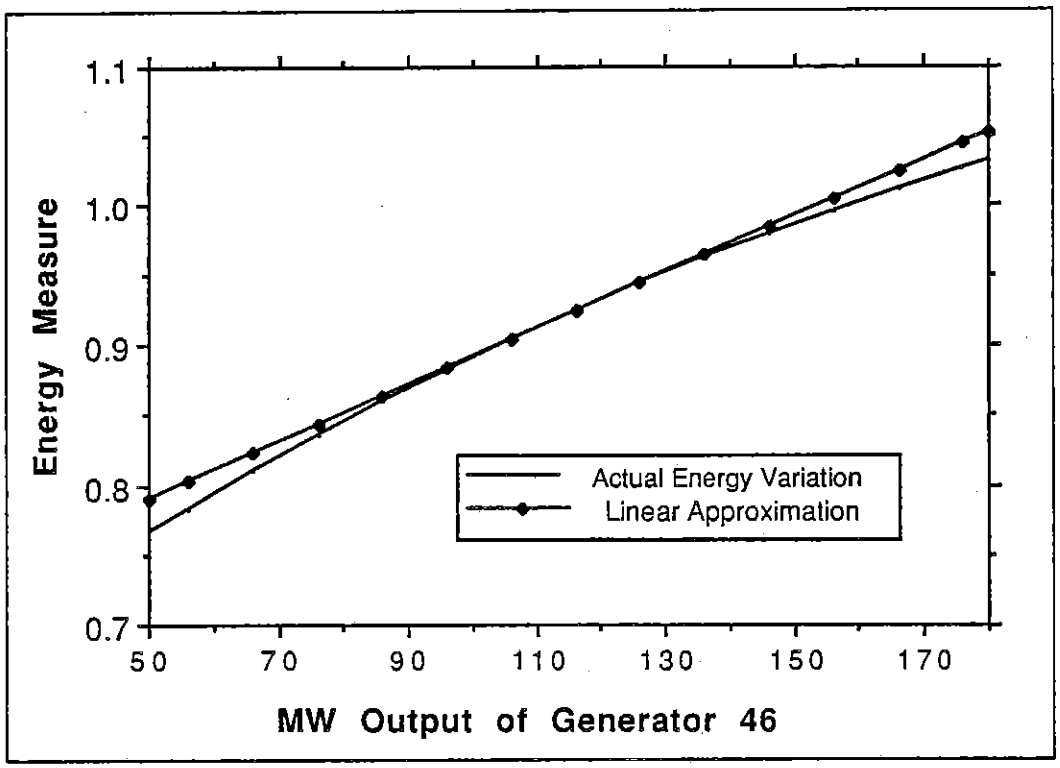

Fig 5-1 : Energy Variation with respect to Generator 46 MW Output

As can be seen, the linear approximation is fairly good. The actual new energy value when the output of generator 46 is increased by ΔP_{G46} to 153.8 MW is 0.99. A second iteration of the above steps at the new value of P_{G46} results in $\vartheta(\mathbf{x}) = 1.00$ when $P_{G46} = 160$ MW. To show that voltage security has actually been improved, Figure 5-2 compares the variation in the bus 44 energy measure with the generator 46 changes to the unmodified system for increasing k. With the redispatch of generator 46, the value of k when at the system loses its steady state operating point has increased by approximately 0.05.

The parallel path of the two plots indicates that change in the energy measure at k = 2.6 provides a good indicator of the increase in system security.

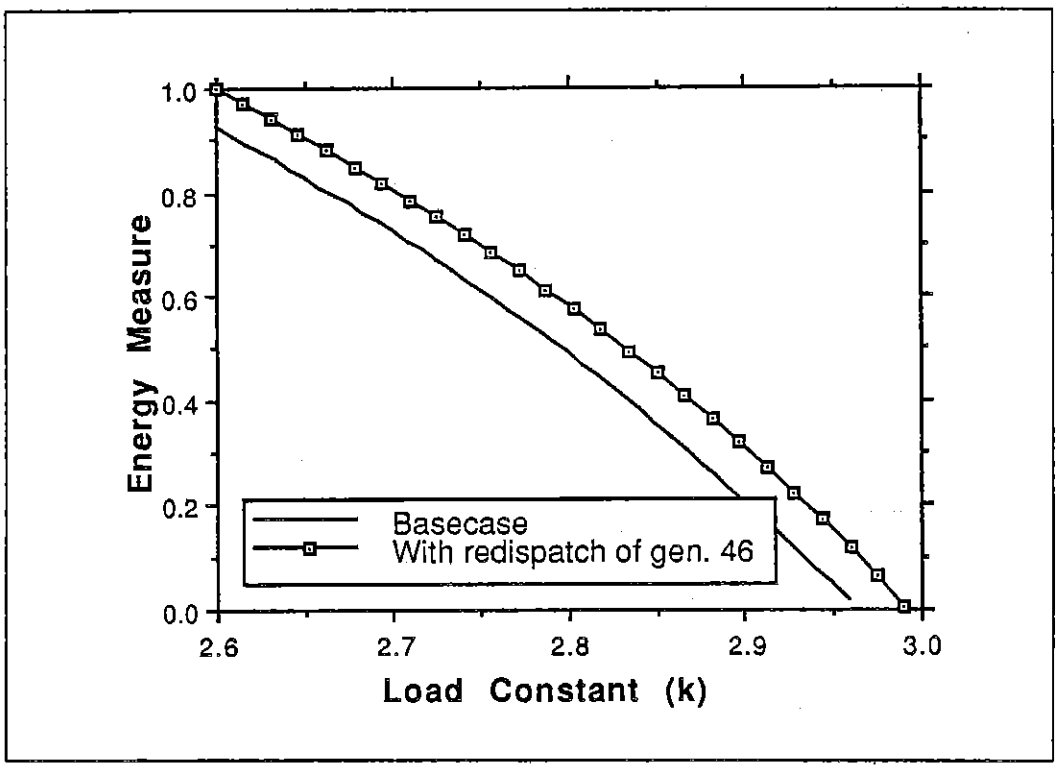

Figure 5-2 : Energy Measure Improvements with Redispatch

In (5-4), equation (5-3) has been modified to include a term to account for the variation in a generator's reactive power limits with respect to changes in real power output.

$$\frac{d\vartheta}{dP_{Gj}} = (\alpha_j^u - \alpha_j^s) + [\frac{\partial\vartheta}{\partial x^s}]^T \frac{\partial x^s}{\partial P_{GJ}} + [\frac{\partial\vartheta}{\partial x^u}]^T \frac{\partial x^u}{\partial P_{GJ}} +$$

$$\left[\frac{\partial\vartheta}{\partial x^u} \frac{\partial x^u}{\partial Q(P_{Gj})_{limit}} + \frac{\partial\vartheta}{\partial x^u} \frac{\partial x^u}{\partial Q(P_{Gj})_{limit}}\right] \frac{\partial Q(P_{Gj})_{limit}}{\partial P_{Gj}} \quad (5\text{-}4)$$

Recall from Chapter 2 that a fast generator exciter model is employed - the generator reactive power output is assumed to vary, within a range between an upper and a lower limit, in order to hold its bus voltage constant. Generator exciter saturation is imposed when its reactive output reaches one of these limits; the generator is switched from being modeled as PV to PQ. These reactive power limits are, however, normally a function of the real power output of the generator. Figure 5-3 shows a typical relationship between the real power output of a unit and its reactive limits. Since systems vulnerable to voltage instability are often characterized by a number of units operating at their reactive power limits, it is important to include the effects of redispatch of real power on the unit's reactive capability when calculating the real power sensitivity. Scenarios where system voltage security is enhanced by backing down the real power output of a saturated unit in order to increase its reactive capability can thus be properly modeled. The value of $\partial Q(P_{Gj})_{limit} / \partial P_{Gj}$ from (5-4) is then the slope of the upper curve in Figure 5-3 if the generator is operating at its maximum reactive power limit, the

slope of the lower curve if the generator is operating at its minimum reactive power limit, or zero if the generator is not saturated.

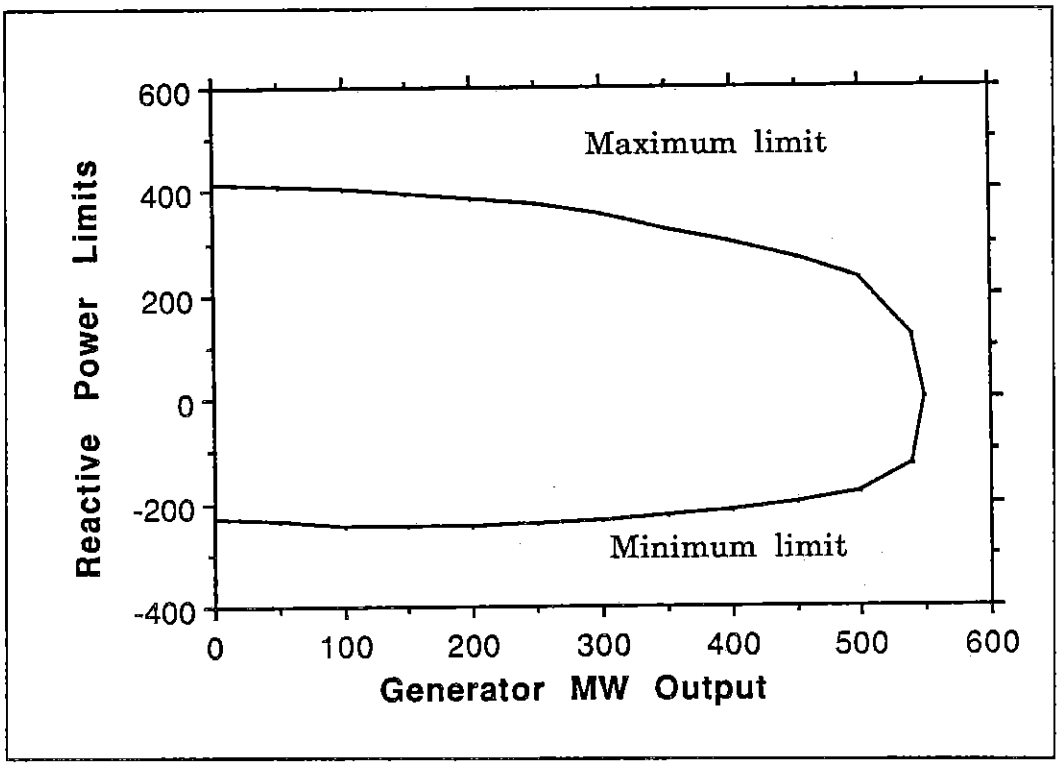

Figure 5-3 : Typical Generator Reactive Capability Curve

Sensitivities for other types of power system controllers could be derived in a similar manner. Voltage security could then be integrated into existing LP optimization methods by requiring that the energy measure for an area of the system always be above a specified threshold. This threshold could be determined using off-line studies. Anytime the energy measure fell below that threshold the energy

constraint would become active. Controller sensitivities could then be calculated; these sensitivities would then form a row in the LP tableau. A system with a number of areas vulnerable to voltage instability (i.e one with a number of separate energy measures below their thresholds) could have a separate row in the LP tableau of the controller sensitivities for each energy measure. Thus energy techniques could prove useful not only for monitoring, but also for enhancing system voltage security.

5.2 On-line Use of Energy Method

In order to demonstrate that the energy method could be used in an on-line environment, a realistically sized system of 415 buses and 609 lines was tested. The test system was divided up into 203 internal buses and 212 external buses, with the assumption that voltage security was only monitored for the internal buses. The test objective then was to monitor the voltage security as the system state evolved over the course of 24 hours. Figure 5-4 shows an assumed typical daily variation in the internal system load. The internal generation was also varied, using participation factors, to maintain constant interchange with the external portion of the system.

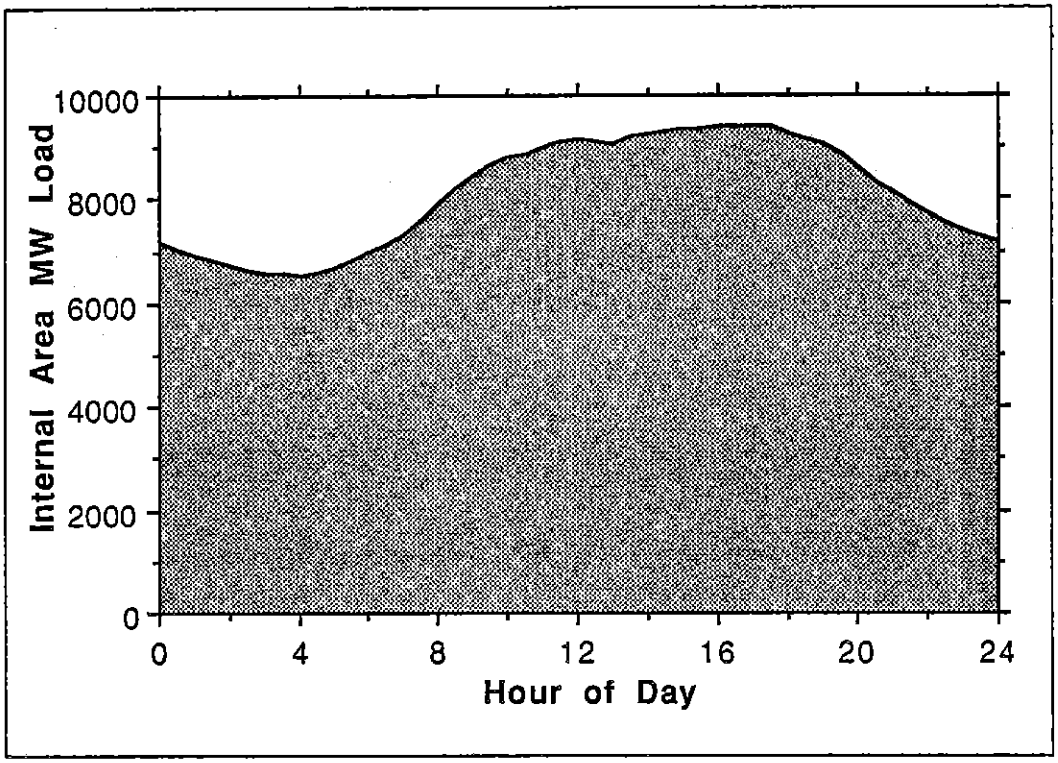

Figure 5-4 : Daily Variation in 415 Bus Internal Load

System voltage security can be assessed by tracking the variation in the energy measures as the system state changes with time. A decreasing energy measure would indicate increased vulnerability to voltage instability in a portion of the system. Since the system loses its stable operating point anytime an energy measure is zero, a number of criteria could be used to notify the operator when voltage collapse is impending. One simple notification criterion could be when an energy measure falls below a given tolerance. The value of this tolerance could be determined in off-line studies, and would depend

upon the network being studied and the amount of parameter variation (e.g. load or generation injections) expected. Another criterion could be to monitor both the energy measures and their rate of change. Then anytime an energy measure is decreasing at a rate such that it would reach zero in less than a specified time tolerance, corrective action could be taken. By setting this tolerance to a large enough time, the operator should have time to take correct action.

The rate at which the voltage security measures are reevaluated depends upon the expected time scale of the variation in the power system parameters. Since in the voltage collapse problem the system is assumed to move from a state of relative security to one of vulnerability over a time period of tens of minutes to hours, a rate of once every five minutes was chosen for evaluation of the voltage security. This is congruous with the periodicity of many utility state estimators.

For on-line use of energy methods, the low energy solutions must be determined as efficiently as possible. For this study, a low energy solution is defined as one with an energy measure less than 2.0. Using the results from Chapter 4, the following algorithm was employed:

0. Operable system state assumed to be available from state estimator.

1. Use Fixed Boundary Bus Voltage (FBBV) screening method to rapidly determine candidate set of low energy solutions. All systems with energy measures less than 2.0 are assumed to be members of set and precede directly to step 3; those systems with energy measures between 2.0 and 4.0 proceed to step 2 for further screening. All others buses are assumed to be secure.

2. For those systems with sufficiently low energies, more accurate estimates are obtained by building and solving the EQV systems. Again, systems with energies less than 2.0 precede to step 3. Those systems with energies between 2.0 and 3.0 are monitored, but no full solution is calculated.

3. For all systems with energies less than 2.0, full system solution energies are calculated. These values are then monitored.

Starting at midnight, when the load was 7190 MW, Table 5-2 shows the solution times necessary to determine the initial system voltage

security. For reference, the time necessary to calculate the operable power flow solution on the machine used was 12.3 seconds.

Algorithm Step #	Description	Solution Time in Seconds
1	Level 1 FBBV Screening : Of 203 buses tested, 41 had solutions with energy less than 10.0.	25.1
1	Level 2 FBBV Screening : Of 41 buses from level 1, 37 had solutions with energy less than 8.0.	6.9
1	Level 3 FBBV Screening : Of 37 buses from level 2, 26 had solutions with energy less than 6.0.	11.9
1	Level 4 FBBV Screening : Of 26 buses from level 3, solutions for buses 83 and 144 had energies less than 2.0 (and proceeded directly to step 2), while 12 had solution energies between 2.0 and 4.0.	13.4
2	Build and solve 12 equivalent systems (for buses with FBBV level 4 screening energy between 2.0 and 4.0.	50.7
3	Calculate full low voltage solutions and energies for buses 83 and 144.	36.0
	Total time:	144.0

Table 5-2 : 415 Bus System Solution Times

During step 1 all of the 203 internal buses were checked for low voltage solutions using the four level FBBV screening method from Chapter 4. At the end of step 1, the number of candidate buses had been reduced from 203 to 14. Of these 14, 2 had screening energies less than 2.0, and proceeded directly to step 3; the remaining 12 were further analyzed using the EQV method. Of these 12, 7 had EQV solution energies between 2.0 and 3.0. These solutions were stored for future monitoring, but because of their relatively high energy no full solution was calculated - the accuracy of the EQV solution was assumed to be sufficient. Full low voltage solutions were calculated for the two buses with energies less than 2.0. The total time to assess the system voltage stability was 144.0 seconds, or about the time necessary to do about 12 full system power flow solutions.

An advantage of using the method on-line is that the slow variation in the system state makes it unnecessary to repeat the above algorithm at each time interval. This is because the set of low energy solution buses tends to remain relatively constant from one interval to the next. The most likely members of the set of low energy solutions at the next time period are the members from the current period. Therefore the entire set of buses could then be searched for new low energy solutions at a much slower frequency, perhaps once every half hour, or by checking one sixth of the buses at each time period. This would reduce the computational cost of monitoring voltage security at each

time period to being equivalent to just a few full power flow solutions. As an example, Table 5-3 compares the low energy solution values between midnight and 1:00 a.m. During this time period only the solution at bus 175 changes from having an energy less than or equal to 3.0 to greater than 3.0. Of course if there were a major perturbation to the system state (such as an unexpected outage of a large generator), all buses could be searched.

Bus #	Midnight Energy	1:00 a.m. Energy
144	1.21	1.29
83	1.55	1.64
195	2.46	2.53
196	2.60	2.64
5	2.73	2.78
8	2.80	2.86
176	2.93	2.98
175	3.00	3.05

Table 5-3 : Low Energy Solutions at Midnight and 1:00 a.m.

Figure 5-5 shows the daily variation in the energy measures. During the times of low load at night the energy measures are relatively high, indicating secure system operation. As the load increases, the energy measures either drop, indicating increased risk of voltage instability in

an area; or vanish, indicating that two vulnerable areas have merged. By monitoring the change in these energy measures, the voltage security of the system is assessed. If an energy measure fell below a given threshold, voltage security could be increased by using the technique from the previous section (provided that there are available controllers to move).

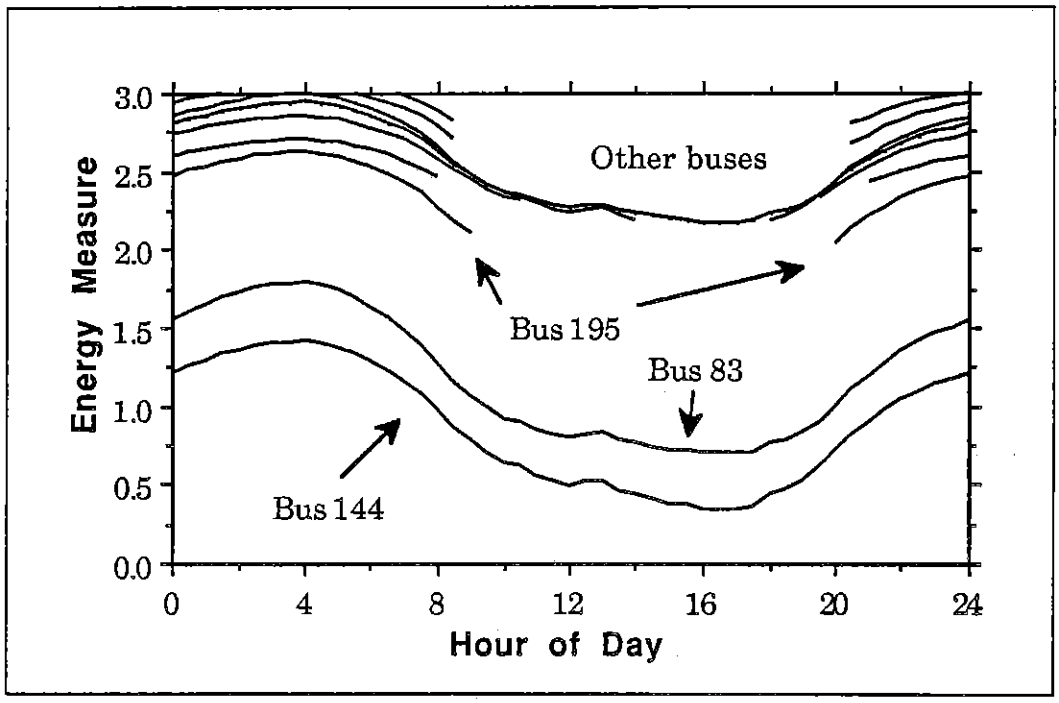

Figure 5-5 : Daily Variation in 415 Bus Energy Measures

The goal of this thesis has been to develop a technique, suitable for on-line implementation, of assessing, and when necessary, improving system voltage security. In this section the actual use of the energy

function techniques on a realistically sized system has been demonstrated. It has been shown that the voltage security of such a system can be effectively monitored and when necessary enhanced with computational requirements on the order of a few power flow solutions, thus allowing for use of the method in an on-line environment.

Chapter 6 - Summary

In this thesis a method of assessment and enhancement of the voltage security of electrical power systems using energy techniques has been presented. Such a method is needed because efficient power system operation is becoming increasingly constrained due to the threat of voltage instability or collapse. The lack of an effective means of assessing voltage security can result in either wide-scale blackouts, or overly conservative and more costly operation.

The energy method presented here is based upon the use of Lyapunov's direct method, which provides a means for assessing the stability of systems of nonlinear differential equations. While the conditions required for existence of a true Lyapunov function are only strictly satisfied in an idealized (lossless) power system model, it is still possible to develop a closed form energy function which approximates a true Lyapunov function, even when power system models which include losses are employed.

Using this energy function, the voltage stability of an area of the power system can be quantified by evaluating the energy difference between the system's operable power flow solution, and one of the alternative solutions of the power flow equations, referred to here as the low voltage solutions. Separate energy differences can be

calculated for each type-one low voltage solution, with each energy difference providing a measure of the voltage security in the portion of the system corresponding to the largest magnitude components of the eigenvector associated with the positive eigenvalue of the power flow Jacobian. As the system moves towards the point of voltage collapse, the energy measures have been shown to vary smoothly with respect to changes in the state of the power system, even when the reactive power limits on generators are included. Voltage collapse is preceded by the coalescence of the operable solution and a type-one low voltage solution; at this point the energy difference is zero.

The type-one low voltage solutions can usually be determined using a rectangular Newton-Raphson method, with an initial low voltage guess at a single bus. Analysis of the components of the eigenvector associated with the positive eigenvalue indicates that the energy measure associated with this bus provides an indication of the voltage stability in the area of the bus with the low initial voltage guess. Thus the voltage security in the vicinity of bus i can be determined by initializing the power flow with a low initial voltage guess at bus i, without having to calculate the eigenvector. Determination of this solution is, however, dependent upon the convergence characteristics of the Newton-Raphson power flow. An alternative method of determining the low voltage solutions expands the constant contours of the energy function about the operable power flow solution in order

to determine the local minima of the norm of the power flow mismatches. However a shortcoming of this technique is its apparent inability to reliably determine the local minima of this function.

Use of the energy method in an on-line environment requires the rapid determination of the low voltage solutions with the lowest associated energy measures. Two methods of solving this problem have been presented, with both methods reducing the solution time by solving equivalent systems, rather than the full power system. In the EQV method the equivalent systems about each bus are calculated using the Ward Admittance technique with adaptive reduction. However while the equivalent system energies closely match the full system energies, the sizes of the EQV equivalents are not completely independent of original system size, which limits the computational benefits of the method. Additionally it can occasionally miss existing low energy solutions. The Fixed Boundary Bus Voltage (FBBV) screening method overcame these shortcomings by just solving a subsystem of the original system, without the need to create an equivalent. The solution technique consisted of solving the subsystem, with the voltages of the boundary buses fixed at the operable solution values. This results in a solution of a smaller and less constrained network. Thus the FBBV method has the advantages of very few missed solutions and fast solution times, independent of the original system size. The energy approximations, however, are not as accurate those

from the EQV method. The preferred technique is to use the FBBV method to rapidly eliminate those buses with either no solution or a high energy solution. The EQV method can then be used to provide rapid estimates of the energy of the remaining solutions.

Lastly, once the set of low energy solutions have been determined, the sensitivities of the energy measures to the various system controllers can be calculated in a computationally tractable manner. Voltage security could then be integrated into existing methods of security enhancement by requiring that the energy measures always be above a predetermined threshold. It the energy measures fell below the threshold, controllers could be improved in such a manner as to improve system voltage security without causing any other types of security violations. In conclusion, this thesis has presented a computationally feasible method, suitable for on-line use, using energy methods for monitoring and improving the voltage security of an electrical power system.

Chapter 7 - References

[1] V. A. Venikov et al., Izv. Akad. Nauk, SSSR (Energetika i Automatika), No. 4, pp. 19, 1962.

[2] C. Barbier and J-P Barret, "Analysis of Phenomena of Voltage Collapse on a Transmission System," *Revue Generale de l'electricite*, Vol. 89, pp. 672-680, Oct. 1980.

[3] A. Kurita and T. Sakurai, "The Power System Failure on July 23, 1987 in Tokyo," *Proc. 27th IEEE Conf. on Decision and Control*, Austin, TX, Dec. 1988.

[4] North American Electric Reliability Council, 1987 System Disturbances, pp. 18, July 1988.

[5] C. W. Taylor, "Voltage Stability Analysis with Emphasis on Load Characteristics and Undervoltage Load Shedding," Panel paper, IEEE PES Summer Meeting, Long Beach, CA, July 1989.

[6] T. J. Bertram, K. D. Demaree, and L. C. Danglemaier, "An Integrated Package for Real-time Security Enhancement," *IEEE Trans. on Power Systems*, Vol. PWRS-5, pp. 592-600, May 1990.

[7] M. Chau et. al., "Understanding Voltage Collapse in Bulk Transmission Systems," *Proceedings: Bulk Power System Voltage Phenomena - Voltage Stability and Security*, EPRI Report EL-6183, Jan. 1989.

[8] B. M. Weedy and B. R. Cox, "Voltage Stability of Radial Power Links," *Proc. IEE*, Vol. 115, pp. 528-536, April 1968.

[9] G. A. Cucchi, "Voltage Stability and Security, the Operator's View: Seeing More Now but Enjoying it Less," *Proceedings: Bulk*

Power System Voltage Phenomena - Voltage Stability and Security, EPRI Report EL-6183, Jan. 1989.

[10] C. W. Brice et. al., "Physically Based Stochastic Models of Power System Loads," U.S. Dept. of Energy Report DOE/ET/29129, Sep. 1982.

[11] IEEE Comittee Report, "Proposed Terms and Definitions for Power System Stability," IEEE Trans. Power App. and Sys., Vol. PAS-101, pp. 1894-1898, June 1982.

[12] I. Jaris and F. D. Galiana, "Analysis and Characterization of Security Regions in Power Systems, Part I," U.S. Dept. of Energy Report DOE/ET/29108-T1-Pt. 1, Mar. 1980.

[13] M. H. Banakar and F. D. Galiana, "Analysis and Characterization of Security Regions in Power Systems, Part II," U.S. Dept. of Energy Report DOE/ET/29108-T1-Pt. 2, Mar. 1980.

[14] F. F. Wu, Y. K. Tsai, and Y. X. Yu, "Probabilistic Steady-State and Dynamic Security Assessment," *IEEE Trans. on Power Systems*, Vol. PWRS-3, pp. 1-9, Feb. 1988.

[15] F. Mercede et al., "A Framework to Predict Voltage Collapse in Power Systems," *IEEE Trans. on Power Systems*, Vol. PWRS-3, pp. 1807-1813, Nov. 1988.

[16] *Voltage Stability of Power Systems: Concepts, Analytical Tools, and Industry Experience,* IEEE, Piscataway, NJ 1990.

[17] D. I. Sun et al., "Optimal Power by Newton Approach," *IEEE Trans. on Power App. and Sys.*, Vol. PAS-103, pp. 2864-2880, Oct. 1984.

[18] F. L. Alvarado and T. H. Jung, "Direct Detection of Voltage Collapse Conditions," *Proceedings: Bulk Power System Voltage Phenomena - Voltage Stability and Security*, EPRI Report EL-6183, Jan. 1989.

[19] F. L. Alvarado et al., "Engineering Foundations for the Determination of Security Costs," IEEE PES Winter Meeting, WM 183-4, New York, NY, Feb. 1991.

[20] I. Dobson, "Observations on the Geometry of Saddle Node Bifurcations and Voltage Collapse in Electric Power Systems," University of Wisconsin Report ECE-90-5, Aug. 1990. To appear in *IEEE Trans. Circuits and Systems*.

[21] I. Dobson, L. Lu, and Y. Hu, "A Direct Method for Computing a Closest Saddle Node Bifurcation in the Load Power Parameter Space of an Electric Power System," To be presented at the International Symposium on Circuits and Systems, Singapore, June 1991.

[22] Y. Sekine, A. Yokoyama and Y. Kumano, "A Method of Detecting a Critical State of Voltage Collapse," *Proceedings: Bulk Power System Voltage Phenomena - Voltage Stability and Security*, EPRI Report EL-6183, Jan. 1989.

[23] C. Lemaitre et al., "An Indicator of the Risk of Voltage Profile Instability for Real-time Applications," *IEEE Trans. on Power Systems*, Vol. PWRS-5, pp. 154-161, Feb. 1990.

[24] P-A. Lof et al., "Fast Calculation of a Voltage Stability Index," IEEE PES Winter Meeting, WM 203-0, New York, NY, Feb. 1991.

[25] A. Tiranuchit and R. J. Thomas, "A Posturing Strategy Against Voltage Instabilities in Electrical Power Systems," *IEEE Trans. on Power Systems*, Vol. PWRS-3, pp. 87-93, Feb. 1988.

[26] A. Tiranuchit et al., "Towards a Computationally Feasible On-line Voltage Instability Index," *IEEE Trans. on Power Systems*, Vol. PWRS-3, pp. 669-675, May 1988.

[27] P. Kessel and H. Glavitsch, "Estimating the Voltage Stability of a Power System," *IEEE Trans. on Power Systems*, Vol. PWRS-1, pp. 346-354, July 1986.

[28] R. A. Schlueter et al., "Voltage Stability and Security Assessment," EPRI Report EL-5967, Project 1999-8, Aug. 1988.

[29] R. A. Schlueter et al., "Methods for Determining Proximity to Voltage Collapse," *IEEE Trans. on Power Systems*, Vol. PWRS-6, pp. 285-292, Feb. 1991.

[30] C. L. DeMarco and T. J. Overbye, "An Energy Based Security Measure for Assessing Vulnerability to Voltage Collapse," IEEE Trans. on Power Syst., Vol. PWRS-5, pp. 419-427, May 1990.

[31] T. J. Overbye and C. L. DeMarco, "Voltage Security Enhancement using Energy Based Sensitivities," IEEE PES Summer Meeting, SM 478-8, Minneapolis, MN, July 1990.

[32] T. J. Overbye and C. L. DeMarco, "Improved Techniques for Power System Voltage Stability Assessment using Energy Methods," IEEE PES Winter Meeting, WM 094-3, New York, NY, Feb. 1991.

[33] Y. Tamura et al., "Monitoring and Control Strategies of Voltage Stability based on Voltage Instability Index," *Proceedings: Bulk Power System Voltage Phenomena - Voltage Stability and Security*, EPRI Report EL-6183, Jan. 1989.

[34] A. Yokoyama and Y. Sekine, "A Static Voltage Stability Index based on Multiple Load Flow Solutions," *Proceedings: Bulk Power*

System Voltage Phenomena - Voltage Stability and Security, EPRI Report EL-6183, Jan. 1989.

[35] M. Vidyasagar, *Nonlinear Systems Analysis*, Prentice-Hall, Englewood Cliffs, NJ, 1978.

[36] M. A. Pai and P. W. Sauer, "Stability Analysis of Power Systems by Lyapunov's Direct Method," *IEEE Control Magazine*, Jan. 1989.

[37] A. R. Bergen and D. J. Hill, "A Structural Preserving Model for Power System's Stability Analysis," *IEEE Trans. Power App. and Sys.*, Vol. PAS-101, pp. 25-35, Jan. 1981.

[38] C. L. DeMarco and A. R. Bergen, "Application of Singular Perturbation Techniques to Power System Transient Analysis," I.S.C.A.S. Proc. pp. 597-601, Montreal, May 1985 (abridged version); also Electronics Research Laboratory, Memo. No. UCB/ERL M84/&, U. of CA, Berkeley (complete version).

[39] C. L. DeMarco, "A New Method of Constructing Lyapunov Functions for Power Systems," IEEE International Symposium on Circuits and Systems, Espoo, Finland, June 1988.

[40] A. Arapostathis, S. Sastry, and P. Varaiya, "Global Analysis of Swing Dynamics," IEEE Trans. Circuits and Systems, Vol. CAS-29, pp. 673-679, Oct. 1982.

[41] V. A. Venikov et al., "Estimation of Electrical Power System Steady-State Stability," *IEEE Trans. Power App. and Sys.*, Vol. PAS-94, pp. 1034-1041, May/June 1975.

[42] Y. Tamura, H. Mori, and S. Iwamoto, "Relationship between Voltage Instability and Multiple Load Flow Solutions in Electric

Power System," *IEEE Trans. Power App. and Sys.*, Vol. PAS-102, pp. 1115-1123, May 1983.

[43] H. Chiang, "Study of the Existence of Energy Functions for Power Systems with Losses," *IEEE Trans. Circuits and Systems*, pp. 1423-1429, Vol. CAS-36, no. 11, Nov. 1989.

[44] H. Chiang and J. S. Thorp, "The Closest Unstable Equilibrium Point Method for Power System Dynamic Security Assessment," *IEEE Trans. Circuits and Systems*, pp. 1187-1200, Vol. CAS-36, no. 9, Sep. 1989.

[45] C. L. DeMarco and A. R. Bergen, "A Security Measure for Random Load Disturbances in Nonlinear Power System Models," IEEE Trans. Circuits and Systems, pp. 1546-1557, Vol. CAS-34, no. 12, Dec. 1987.

[46] A. A. Fouad et al., "Direct Transient Stability Analysis Using Energy Functions: Applications to Large Power Networks," *IEEE Trans. on Power Systems*, Vol. PWRS-2, pp. 37-44, Feb. 1987.

[47] P. W. Sauer and M. A. Pai, "Power System Steady State Stability, and the Load-Flow Jacobian," *IEEE Trans. on Power Sys.*, Vol. PWRS-5, pp. 1374-1383, Nov. 1990.

[48] A. Klos and A. Kerner, "The Non-Uniqueness of Load-Flow Solutions," *Proc. PSCC* V., 3.1/8, 1975.

[49] I. Dobson and H. Chiang, "Towards a Theory of Voltage Collapse in Electric Power Systems," *System & Control Letters*, pp. 253-262, 1989.

[50] I. Dobson et al., "A Model of Voltage Collapse in Electric Power Systems," *Proc. 27th IEEE Conf. Decision and Control*, Austin, TX, Dec. 1988.

[51] Y. Tamura, K. Sakamoto, and Y. Tayama, "Voltage Instability Proximity Index (VIPI) based on Multiple Load Flow Solutions in Ill-Conditioned Power Systems," *Proc. 27 IEEE Conf. Decision and Control*, Austin, TX, Dec. 1988.

[52] Report of Working Group on a Common Format for Exchange of Solved Load Flow Data, IEEE PES Summer Meeting, San Francisco, CA, July 1972.

[53] J. S. Thorp, S. A. Naqavi, and H. D. Chiang, "More Load Flow Fractals," *Proc. of 29th IEEE Conf. on Decision and Control*, pp. 3028-3030, Honolulu, HI, Dec. 1990.

[54] J. S. Thorp and S. A. Naqavi, "Load Flow Fractals," Proc. of 28th *IEEE Conf. on Decision and Control,* pp. 1822-1827, Tampa, FL, Dec. 1989.

[55] C. L. DeMarco and T. J. Overbye, "Low Voltage Power Flow Solutions and Their Role in Exit Time Security Measures for Voltage Collapse," *Proc. of 27th IEEE Conf. on Decision and Control*, pp. 2127-2131m Austin, TX, Dec. 1988.

[56] S. Iwamoto and Y. Tamura, "A Load Flow Calculation for Ill-conditioned Power Systems," *IEEE Trans. Power App. and Sys.*, Vol. PAS-100, pp. 1736-1743, April 1981.

[57] K. Iba et al., "A Method for Finding a Pair of Multiple Load Flow Solutions in Bulk Power Systems," *IEEE Trans. on Power Systems*, Vol. PWRS-5, pp.582-591, May 1990.

[58] C. L. DeMarco, "An Optimization Scheme for Locating Power System Equilibrium Ranked by a Scalar Lyapunov Function," *Proc. of the 1980 American Control Conf.*, pp. 1264-1268, Pittsburgh, PA, June 1989.

[59] D. G. Luenberger, *Linear and Nonlinear Programming*, Addison-Wesley, Reading, MA, 1984.

[60] G. W. Stagg and A. H. El-Abiad, *Computer Methods in Power Systems Analysis*, McGraw-Hill, New York, NY, 1968.

[61] W. F. Tinney and J. M. Bright, "Adaptive Reductions for Power Flow Equivalents," *IEEE Trans. on Power Sys.*, Vol. PWRS-2, pp. 351-360, May 1987.

[62] Y. Tamura, K. Iba and S. Iwamoto, "A Method of Finding Multiple Load Flow Solutions for General Power Systems," *IEEE PES Winter Meeting*, A 80 043-0, New York, Feb. 1980.

[63] S. Deckmann et al., "Studies on Power System Load Flow Equivalencing," *IEEE Trans. on Power Sys.*, Vol. PAS-99, pp. 2301-2310, Nov/Dec 1980.

[64] S. Deckmann et al., "Numerical Testing of Power System Load Flow Equivalents," *IEEE Trans. on Power Sys.*, Vol. PAS-99, pp. 2292-2300, Nov/Dec 1980.

[65] J. B. Ward, "Equivalent Circuits for Power Flow Studies," *AIEE Trans. Power App. Sys.*, vol. 68, pp. 373-382, 1949.

[66] F. L. Alvarado and E. H. Elkonyaly, "Reduction in Power Systems," IEEE PES Summer Meeting A77 507-7, Mexico City, Mexico, July 1977.

[67] M. K. Enns, J. J. Quada, "Sparsity-Enhanced Network Reduction for Fault Studies," IEEE PES Summer Meeting, SM 489-5, Minneapolis, MN, July 1990.

[68] W. F. Tinney et al., "Sparse Vector Methods," *IEEE Trans. Power App. and Sys.*, vol. PAS-104, pp. 295-301, Feb. 1985.

[69] W. F. Tinney and J. W. Walker, "Direct Solution of Sparse Network Equations by Optimally Ordered Triangular Factorization," *Proceeding of IEEE*, Vol. 55, pp. 1801-1809, Nov. 1967.

[70] R. Betancourt, "An Efficient Heuristic Ordering Algorithm for Partial Matrix Refactorization," *IEEE Trans. on Power Sys.*, Vol. PWRS-3, pp. 1181-1187, Aug. 1988.

[71] M. G. Lauby, T. A. Mikolinnas, and N. D. Reppen, "Contingency Selection of Branch Outages causing Voltage Problems," *IEEE Trans. on Power App. and Sys.*, Vol. PAS-102, No. 12, pp. 3899-3904, Dec. 1983.

[72] J. Zaborszky, K. Whang, and K. Prasad, "Fast Contingency Evaluation using Concentric Relaxation," *IEEE Trans. on Power App. and Sys.*, Vol. PAS-99, No. 1, pp. 28-36, Jan./Feb. 1980.

[73] B. Stott and J. L. Marinho, "Linear Programming for Power System Security Applications," *IEEE Trans. on Power App. and Sys.*, Vol. PAS-98, No. 3, pp. 837-848, May 1979.

[74] V. Vittal et al., "Derivation of Stability Limits using Analytical Sensitivity of Transient Energy Margin," *IEEE Trans. on Power Systems*, Vol. PWRS-4, pp. 1363-1372, Nov. 1989.

Appendix A

This appendix contains the 118 bus system data in IEEE common data format.

BUS DATA FOLLOWS

1	1	1	1	1	2	0.95	0.0	51.0	27.0	0.0	0.0	1	0.955	15.	-50.0	0	0	0
2	2	1	1	1	0	1.00	0.0	20.0	9.0	0.0	0.0	1	1.00	0.0	0.0	0	0	0
3	3	1	1	1	0	1.00	0.0	39.0	10.0	0.0	0.0	1	1.00	0.0	0.0	0	0	0
4	4	1	1	1	2	1.00	0.0	30.0	12.0	-9.0	0.0	1	0.998	300.0	-300.0	0	0	0
5	5	0	1	1	0	1.00	0.0	0.0	0.0	0.0	0.0	0	1.00	0.0	0.0	0	0	0
6	6	1	1	1	2	0.99	0.0	52.0	22.0	0.0	0.0	1	0.990	50.0	-13.0	0	0	0
7	7	1	1	1	0	1.00	0.0	19.0	2.0	0.0	0.0	1	1.00	0.0	0.0	0	0	0
8	8	1	1	1	2	1.01	0.0	0.0	0.0	-28.0	0.0	1	1.015	300.0	-300.0	0	0	0
9	9	1	1	1	0	1.00	0.0	0.0	0.0	0.0	0.0	1	1.00	0.0	0.0	0	0	0
10	10	1	1	1	2	1.05	0.0	0.0	0.0	450.0	0.0	1	1.050	200.0	-147.0	0	0	0
11	11	1	1	1	0	1.00	0.0	70.0	23.0	0.0	0.0	1	1.00	0.0	0.0	0	0	0
12	12	1	1	1	2	1.00	0.0	47.0	10.0	0.0	0.0	1	0.990	120.0	-35.0	0	0	0
13	13	1	1	1	0	1.00	0.0	34.0	16.0	0.0	0.0	1	1.00	0.0	0.0	0	0	0
14	14	1	1	1	0	1.00	0.0	14.0	1.0	0.0	0.0	1	1.00	0.0	0.0	0	0	0
15	15	1	1	1	2	0.97	0.0	90.0	30.0	0.0	0.0	1	0.970	30.0	-10.0	0	0	0
16	16	1	1	1	0	1.00	0.0	25.0	10.0	0.0	0.0	1	1.00	0.0	0.0	0	0	0
17	17	1	1	1	0	1.00	0.0	11.0	3.0	0.0	0.0	1	1.00	0.0	0.0	0	0	0
18	18	1	1	1	2	0.97	0.0	60.0	34.0	0.0	0.0	1	0.973	50.0	-16.0	0	0	0
19	19	1	1	1	2	0.96	0.0	45.0	25.0	0.0	0.0	1	0.967	24.0	-8.0	0	0	0
20	20	1	1	1	0	1.00	0.0	18.0	3.0	0.0	0.0	1	1.00	0.0	0.0	0	0	0
21	21	1	1	1	0	1.00	0.0	14.0	8.0	0.0	0.0	1	1.00	0.0	0.0	0	0	0
22	22	1	1	1	0	1.00	0.0	10.0	5.0	0.0	0.0	1	1.00	0.0	0.0	0	0	0
23	23	1	1	1	0	1.00	0.0	7.0	3.0	0.0	0.0	1	1.00	0.0	0.0	0	0	0
24	24	1	1	1	2	0.99	0.0	0.0	0.0	-13.0	0.0	1	0.992	300.0	-300.0	0	0	0
25	25	1	1	1	2	1.05	0.0	0.0	0.0	220.0	0.0	1	1.050	140.0	-47.0	0	0	0
26	26	1	1	1	2	1.01	0.0	0.0	0.0	314.0	0.0	1	1.015	1000.0	-1000.0	0	0	0
27	27	1	1	1	2	0.97	0.0	62.0	13.0	-9.0	0.0	1	0.968	300.0	-300.0	0	0	0
28	28	1	1	1	0	1.00	0.0	17.0	7.0	0.0	0.0	1	1.00	0.0	0.0	0	0	0
29	29	1	1	1	0	1.00	0.0	24.0	4.0	0.0	0.0	1	1.00	0.0	0.0	0	0	0
30	30	1	1	1	0	1.00	0.0	0.0	0.0	0.0	0.0	1	1.00	0.0	0.0	0	0	0
31	31	1	1	1	2	0.97	0.0	43.0	27.0	0.0	0.0	1	0.967	300.0	-300.0	0	0	0
32	32	1	1	1	2	0.96	0.0	59.0	23.0	0.0	0.0	1	0.963	42.0	-14.0	0	0	0
33	33	1	1	1	0	1.00	0.0	23.0	9.0	0.0	0.0	1	1.00	0.0	0.0	0	0	0
34	34	1	1	1	2	0.98	0.0	59.0	26.0	0.0	0.0	1	0.984	24.0	-8.0	0	0	0

35	35	1	1	1	0	1.00	0.0	33.0	9.0	0.0	0.0	1	1.00	0.0	0.0	0	0	0
36	36	1	1	1	2	0.98	0.0	31.0	17.0	0.0	0.0	1	0.980	24.0	-8.0	0	0	0
37	37	1	1	1	0	1.00	0.0	0.0	0.0	0.0	0.0	1	1.00	0.0	0.0	0	0	0
38	38	1	1	1	0	1.00	0.0	0.0	0.0	0.0	0.0	1	1.00	0.0	0.0	0	0	0
39	39	1	1	1	0	1.00	0.0	27.0	11.0	0.0	0.0	1	1.00	0.0	0.0	0	0	0
40	40	1	1	1	2	0.97	0.0	20.0	23.0	-46.0	0.0	1	0.970	300.0	-300.0	0	0	0
41	41	1	1	1	0	1.00	0.0	37.0	10.0	0.0	0.0	1	1.00	0.0	0.0	0	0	0
42	42	1	1	1	2	0.98	0.0	37.0	23.0	-59.0	0.0	1	0.985	300.0	-300.0	0	0	0
43	43	1	1	1	0	1.00	0.0	18.0	7.0	0.0	0.0	1	1.00	0.0	0.0	0	0	0
44	44	1	1	1	0	1.00	0.0	16.0	8.0	0.0	0.0	1	1.00	0.0	0.0	0	0	0
45	45	1	1	1	0	1.00	0.0	53.0	22.0	0.0	0.0	1	1.00	0.0	0.0	0	0	0
46	46	1	1	1	2	1.00	0.0	28.0	10.0	19.0	0.0	1	1.005	100.0	-100.0	0	0	0
47	47	1	1	1	0	1.00	0.0	34.0	0.0	0.0	0.0	1	1.00	0.0	0.0	0	0	0
48	48	1	1	1	0	1.00	0.0	20.0	11.0	0.0	0.0	1	1.00	0.0	0.0	0	0	0
49	49	1	1	1	2	1.02	0.0	87.0	30.0	204.0	0.0	1	1.025	210.0	-85.0	0	0	0
50	50	1	1	1	0	1.00	0.0	17.0	4.0	0.0	0.0	1	1.00	0.0	0.0	0	0	0
51	51	1	1	1	0	1.00	0.0	17.0	8.0	0.0	0.0	1	1.00	0.0	0.0	0	0	0
52	52	1	1	1	0	1.00	0.0	18.0	5.0	0.0	0.0	1	1.00	0.0	0.0	0	0	0
53	53	1	1	1	0	1.00	0.0	23.0	11.0	0.0	0.0	1	1.00	0.0	0.0	0	0	0
54	54	1	1	1	2	0.95	0.0	113.0	32.0	48.0	0.0	1	0.955	300.0	-300.0	0	0	0
55	55	1	1	1	2	0.95	0.0	63.0	22.0	0.0	0.0	1	0.952	23.0	-8.0	0	0	0
56	56	1	1	1	2	0.95	0.0	84.0	18.0	0.0	0.0	1	0.954	15.0	-8.0	0	0	0
57	57	1	1	1	0	1.00	0.0	12.0	3.0	0.0	0.0	1	1.00	0.0	0.0	0	0	0
58	58	1	1	1	0	1.00	0.0	12.0	3.0	0.0	0.0	1	1.00	0.0	0.0	0	0	0
59	59	1	1	1	2	0.98	0.0	277.0	113.0	155.0	0.0	1	0.985	180.0	-60.0	0	0	0
60	60	1	1	1	0	1.00	0.0	78.0	3.0	0.0	0.0	1	1.00	0.0	0.0	0	0	0
61	61	1	1	1	2	0.99	0.0	0.0	0.0	160.0	0.0	1	0.995	300.0	-100.0	0	0	0
62	62	1	1	1	2	1.00	0.0	77.0	14.0	0.0	0.0	1	0.998	20.0	-20.0	0	0	0
63	63	1	1	1	0	1.00	0.0	0.0	0.0	0.0	0.0	1	1.00	0.0	0.0	0	0	0
64	64	1	1	1	0	1.00	0.0	0.0	0.0	0.0	0.0	1	1.00	0.0	0.0	0	0	0
65	65	1	1	1	2	1.00	0.0	0.0	0.0	391.0	0.0	1	1.005	200.0	-67.0	0	0	0
66	66	1	1	1	2	1.05	0.0	39.0	18.0	392.0	0.0	1	1.050	200.0	-67.0	0	0	0
67	67	1	1	1	0	1.00	0.0	28.0	7.0	0.0	0.0	1	1.00	0.0	0.0	0	0	0
68	68	1	1	1	0	1.00	0.0	0.0	0.0	0.0	0.0	1	1.00	0.0	0.0	0	0	0
69	69	1	2	1	3	1.03	0.0	0.0	0.0	516.4	0.0	1	1.035	9999.0	-9999.0	0	0	0
70	70	1	1	1	2	0.98	0.0	66.0	20.0	0.0	0.0	1	0.984	32.0	-10.0	0	0	0
71	71	1	1	1	0	1.000	0.0	0.0	0.0	0.0	0.0	1	1.000	0.0	0.0	0	0	0
72	72	1	1	1	2	0.980	0.0	0.0	0.0	-12.0	0.0	1	0.980	100.0	-100.0	0	0	0
73	73	1	1	1	2	0.991	0.0	0.0	0.0	-6.0	0.0	1	0.991	100.0	-100.0	0	0	0
74	74	1	1	1	2	0.958	0.0	68.0	27.0	0.0	0.0	1	0.958	9.0	-6.0	0	0	0
75	75	1	1	1	0	1.000	0.0	47.0	11.0	0.0	0.0	1	1.000	0.0	0.0	0	0	0

76	76	1	1	1	2	0.943	0.0	68.0	36.0	0.0	0.0	1	0.943	23.0	-8.0	0	0	0
77	77	1	1	1	2	1.006	0.0	61.0	28.0	0.0	0.0	1	1.006	70.0	-20.0	0	0	0
78	78	1	1	1	0	1.000	0.0	71.0	26.0	0.0	0.0	1	1.000	0.0	0.0	0	0	0
79	79	1	1	1	0	1.000	0.0	39.0	32.0	0.0	0.0	1	1.000	0.0	0.0	0	0	0
80	80	1	1	1	2	1.040	0.0	130.0	26.0	477.0	0.0	1	1.040	280.0	-165.0	0	0	0
81	81	1	1	1	0	1.000	0.0	0.0	0.0	0.0	0.0	1	1.000	0.0	0.0	0	0	0
82	82	1	1	1	0	1.000	0.0	54.0	27.0	0.0	0.0	1	1.000	0.0	0.0	0	0	0
83	83	1	1	1	0	1.000	0.0	11.0	7.0	0.0	0.0	1	1.000	0.0	0.0	0	0	0
84	84	1	1	1	0	1.000	0.0	11.0	7.0	0.0	0.0	1	1.000	0.0	0.0	0	0	0
85	85	1	1	1	2	0.985	0.0	24.0	15.0	0.0	0.0	1	0.985	23.0	-8.0	0	0	0
86	86	1	1	1	0	1.000	0.0	21.0	10.0	0.0	0.0	1	1.000	0.0	0.0	0	0	0
87	87	1	1	1	2	1.015	0.0	0.0	0.0	4.0	0.0	1	1.015	1000.0	-100.0	0	0	0
88	88	1	1	1	0	1.000	0.0	48.0	10.0	0.0	0.0	1	1.000	0.0	0.0	0	0	0
89	89	1	1	1	2	1.005	0.0	0.0	0.0	607.0	0.0	1	1.005	300.0	-210.0	0	0	0
90	90	1	1	1	2	0.985	0.0	78.0	42.0	-85.0	0.0	1	0.985	300.0	-300.0	0	0	0
91	91	1	1	1	2	0.980	0.0	0.0	0.0	-10.0	0.0	1	0.980	100.0	-100.0	0	0	0
92	92	1	1	1	2	0.990	0.0	65.0	10.0	0.0	0.0	1	0.990	9.0	-3.0	0	0	0
93	93	1	1	1	0	1.000	0.0	12.0	7.0	0.0	0.0	1	1.000	0.0	0.0	0	0	0
94	94	1	1	1	0	1.000	0.0	30.0	16.0	0.0	0.0	1	1.000	0.0	0.0	0	0	0
95	95	1	1	1	0	1.000	0.0	42.0	31.0	0.0	0.0	1	1.000	0.0	0.0	0	0	0
96	96	1	1	1	0	1.000	0.0	38.0	15.0	0.0	0.0	1	1.000	0.0	0.0	0	0	0
97	97	1	1	1	0	1.000	0.0	15.0	9.0	0.0	0.0	1	1.000	0.0	0.0	0	0	0
98	98	1	1	1	0	1.000	0.0	34.0	8.0	0.0	0.0	1	1.000	0.0	0.0	0	0	0
99	99	1	1	1	2	1.010	0.0	0.0	0.0	-42.0	0.0	1	1.010	100.0	-100.0	0	0	0
100	100	1	1	1	2	1.017	0.0	37.0	18.0	252.0	0.0	1	1.017	155.0	50.0	0	0	0
101	101	1	1	1	0	1.000	0.0	22.0	15.0	0.0	0.0	1	1.000	0.0	0.0	0	0	0
102	102	1	1	1	0	1.000	0.0	5.0	3.0	0.0	0.0	1	1.000	0.0	0.0	0	0	0
103	103	1	1	1	2	1.010	0.0	23.0	16.0	40.0	0.0	1	1.010	40.0	-15.0	0	0	0
104	104	1	1	1	2	0.971	0.0	38.0	25.0	0.0	0.0	1	1.000	23.0	-8.0	0	0	0
105	105	1	1	1	2	0.965	0.0	31.0	26.0	0.0	0.0	1	1.000	23.0	-8.0	0	0	0
106	106	1	1	1	0	1.000	0.0	43.0	16.0	0.0	0.0	1	1.000	0.0	0.0	0	0	0
107	107	1	1	1	2	0.952	0.0	28.0	12.0	-22.0	0.0	1	0.952	200.0	-200.0	0	0	0
108	108	1	1	1	0	1.000	0.0	2.0	1.0	0.0	0.0	1	1.000	0.0	0.0	0	0	0
109	109	1	1	1	0	1.000	0.0	8.0	3.0	0.0	0.0	1	1.000	0.0	0.0	0	0	0
110	110	1	1	1	2	0.973	0.0	39.0	30.0	0.0	0.0	1	0.973	23.0	-8.0	0	0	0
111	111	1	1	1	2	0.980	0.0	0.0	0.0	36.0	0.0	1	0.980	1000.0	-100.0	0	0	0
112	112	1	1	1	2	0.975	0.0	25.0	13.0	-43.0	0.0	1	0.975	1000.0	-100.0	0	0	0
113	113	1	1	1	2	0.993	0.0	0.0	0.0	-6.0	0.0	1	0.993	200.0	-100.0	0	0	0
114	114	1	1	1	0	1.000	0.0	8.0	3.0	0.0	0.0	1	1.000	0.0	0.0	0	0	0
115	115	1	1	1	0	1.000	0.0	22.0	7.0	0.0	0.0	1	1.000	0.0	0.0	0	0	0
116	116	1	1	1	2	1.005	0.0	0.0	0.0	-184.0	0.0	1	1.005	1000.0	-1000.0	0	0	0

```
117 117 1 1 1 0 1.000 0.0 20.0  8.0   0.0 0.0 1 1.000   0.0   0.0 0 0 0
118 118 1 1 1 0 1.000 0.0 33.0 15.0   0.0 0.0 1 1.000   0.0   0.0 0 0 0
-999
BRANCH DATA FOLLOWS
  1   2   1 1 1 0 0.0303  0.0999  0.0127  0 0 0 0 0 1.0   0 0 0 0 0 0
  1   3   1 1 1 0 0.0129  0.0424  0.0054  0 0 0 0 0 1.0   0 0 0 0 0 0
  3   5   1 1 1 0 0.0241  0.1080  0.0142  0 0 0 0 0 1.0   0 0 0 0 0 0
  5   6   1 1 1 0 0.0119  0.0540  0.0071  0 0 0 0 0 1.0   0 0 0 0 0 0
  6   7   1 1 1 0 0.0046  0.0208  0.0027  0 0 0 0 0 1.0   0 0 0 0 0 0
  8   9   1 1 1 0 0.0024  0.0305  0.5810  0 0 0 0 0 1.0   0 0 0 0 0 0
  8   5   1 1 1 0 0.0000  0.0267  0.0000  0 0 0 0 0 0.985 0 0 0 0 0 0
  9   10  1 1 1 0 0.0026  0.0322  0.6150  0 0 0 0 0 1.0   0 0 0 0 0 0
  4   11  1 1 1 0 0.0209  0.0688  0.0087  0 0 0 0 0 1.0   0 0 0 0 0 0
  5   11  1 1 1 0 0.0203  0.0682  0.0087  0 0 0 0 0 1.0   0 0 0 0 0 0
 11   12  1 1 1 0 0.0059  0.0196  0.0025  0 0 0 0 0 1.0   0 0 0 0 0 0
  2   12  1 1 1 0 0.0187  0.0616  0.0079  0 0 0 0 0 1.0   0 0 0 0 0 0
  3   12  1 1 1 0 0.0484  0.1600  0.0203  0 0 0 0 0 1.0   0 0 0 0 0 0
  7   12  1 1 1 0 0.0086  0.0340  0.0044  0 0 0 0 0 1.0   0 0 0 0 0 0
 11   13  1 1 1 0 0.0225  0.0731  0.0094  0 0 0 0 0 1.0   0 0 0 0 0 0
 12   14  1 1 1 0 0.0215  0.0707  0.0091  0 0 0 0 0 1.0   0 0 0 0 0 0
 13   15  1 1 1 0 0.0744  0.2444  0.0313  0 0 0 0 0 1.0   0 0 0 0 0 0
 14   15  1 1 1 0 0.0595  0.1950  0.0251  0 0 0 0 0 1.0   0 0 0 0 0 0
 12   16  1 1 1 0 0.0212  0.0834  0.0107  0 0 0 0 0 1.0   0 0 0 0 0 0
 15   17  1 1 1 0 0.0132  0.0437  0.0222  0 0 0 0 0 1.0   0 0 0 0 0 0
 16   17  1 1 1 0 0.0454  0.1801  0.0233  0 0 0 0 0 1.0   0 0 0 0 0 0
 17   18  1 1 1 0 0.0123  0.0505  0.0065  0 0 0 0 0 1.0   0 0 0 0 0 0
 18   19  1 1 1 0 0.0112  0.0493  0.0057  0 0 0 0 0 1.0   0 0 0 0 0 0
 19   20  1 1 1 0 0.0252  0.1170  0.0149  0 0 0 0 0 1.0   0 0 0 0 0 0
 15   19  1 1 1 0 0.0120  0.0394  0.0050  0 0 0 0 0 1.0   0 0 0 0 0 0
 20   21  1 1 1 0 0.0183  0.0849  0.0108  0 0 0 0 0 1.0   0 0 0 0 0 0
 21   22  1 1 1 0 0.0209  0.0970  0.0123  0 0 0 0 0 1.0   0 0 0 0 0 0
 22   23  1 1 1 0 0.0342  0.1590  0.0202  0 0 0 0 0 1.0   0 0 0 0 0 0
 23   24  1 1 1 0 0.0135  0.0492  0.0249  0 0 0 0 0 1.0   0 0 0 0 0 0
 23   25  1 1 1 0 0.0156  0.0800  0.0432  0 0 0 0 0 1.0   0 0 0 0 0 0
 26   25  1 1 1 0 0.0000  0.0382  0.0000  0 0 0 0 0 0.96  0 0 0 0 0 0
 25   27  1 1 1 0 0.0318  0.1630  0.0882  0 0 0 0 0 1.0   0 0 0 0 0 0
 27   28  1 1 1 0 0.0191  0.0855  0.0108  0 0 0 0 0 1.0   0 0 0 0 0 0
 28   29  1 1 1 0 0.0237  0.0943  0.0119  0 0 0 0 0 1.0   0 0 0 0 0 0
 30   17  1 1 1 0 0.0000  0.0388  0.0000  0 0 0 0 0 0.96  0 0 0 0 0 0
  8   30  1 1 1 0 0.0043  0.0504  0.2570  0 0 0 0 0 1.0   0 0 0 0 0 0
 26   30  1 1 1 0 0.0080  0.0860  0.4540  0 0 0 0 0 1.0   0 0 0 0 0 0
```

17	31	1	1	1	0	0.0474	0.1563	0.0199	0 0 0 0 0	1.0	0 0 0 0 0 0
29	31	1	1	1	0	0.0108	0.0331	0.0042	0 0 0 0 0	1.0	0 0 0 0 0 0
23	32	1	1	1	0	0.0317	0.1153	0.0587	0 0 0 0 0	1.0	0 0 0 0 0 0
31	32	1	1	1	0	0.0298	0.0985	0.0126	0 0 0 0 0	1.0	0 0 0 0 0 0
27	32	1	1	1	0	0.0229	0.0755	0.0096	0 0 0 0 0	1.0	0 0 0 0 0 0
15	33	1	1	1	0	0.0380	0.1244	0.0160	0 0 0 0 0	1.0	0 0 0 0 0 0
19	34	1	1	1	0	0.0752	0.2470	0.0316	0 0 0 0 0	1.0	0 0 0 0 0 0
35	36	1	1	1	0	0.0022	0.0102	0.0013	0 0 0 0 0	1.0	0 0 0 0 0 0
35	37	1	1	1	0	0.0110	0.0497	0.0066	0 0 0 0 0	1.0	0 0 0 0 0 0
33	37	1	1	1	0	0.0415	0.1420	0.0183	0 0 0 0 0	1.0	0 0 0 0 0 0
34	36	1	1	1	0	0.0087	0.0268	0.0028	0 0 0 0 0	1.0	0 0 0 0 0 0
34	37	1	1	1	0	0.0026	0.0094	0.0049	0 0 0 0 0	1.0	0 0 0 0 0 0
38	37	1	1	1	0	0.0000	0.0375	0.0000	0 0 0 0 0	0.935	0 0 0 0 0 0
37	39	1	1	1	0	0.0321	0.1060	0.0135	0 0 0 0 0	1.0	0 0 0 0 0 0
37	40	1	1	1	0	0.0593	0.1680	0.0210	0 0 0 0 0	1.0	0 0 0 0 0 0
30	38	1	1	1	0	0.0046	0.0540	0.2110	0 0 0 0 0	1.0	0 0 0 0 0 0
39	40	1	1	1	0	0.0184	0.0605	0.0078	0 0 0 0 0	1.0	0 0 0 0 0 0
40	41	1	1	1	0	0.0145	0.0487	0.0061	0 0 0 0 0	1.0	0 0 0 0 0 0
40	42	1	1	1	0	0.0555	0.1830	0.0233	0 0 0 0 0	1.0	0 0 0 0 0 0
41	42	1	1	1	0	0.0410	0.1350	0.0172	0 0 0 0 0	1.0	0 0 0 0 0 0
43	44	1	1	1	0	0.0608	0.2454	0.0303	0 0 0 0 0	1.0	0 0 0 0 0 0
34	43	1	1	1	0	0.0413	0.1681	0.0211	0 0 0 0 0	1.0	0 0 0 0 0 0
44	45	1	1	1	0	0.0224	0.0901	0.0112	0 0 0 0 0	1.0	0 0 0 0 0 0
45	46	1	1	1	0	0.0400	0.1356	0.0166	0 0 0 0 0	1.0	0 0 0 0 0 0
46	47	1	1	1	0	0.0380	0.1270	0.0158	0 0 0 0 0	1.0	0 0 0 0 0 0
46	48	1	1	1	0	0.0601	0.1890	0.0236	0 0 0 0 0	1.0	0 0 0 0 0 0
47	49	1	1	1	0	0.0191	0.0625	0.0080	0 0 0 0 0	1.0	0 0 0 0 0 0
42	49	1	1	1	0	0.0715	0.3230	0.0430	0 0 0 0 0	1.0	0 0 0 0 0 0
42	49	1	1	1	0	0.0715	0.3230	0.0430	0 0 0 0 0	1.0	0 0 0 0 0 0
45	49	1	1	1	0	0.0684	0.1860	0.0222	0 0 0 0 0	1.0	0 0 0 0 0 0
48	49	1	1	1	0	0.0179	0.0505	0.0063	0 0 0 0 0	1.0	0 0 0 0 0 0
49	50	1	1	1	0	0.0267	0.0752	0.0094	0 0 0 0 0	1.0	0 0 0 0 0 0
49	51	1	1	1	0	0.0486	0.1370	0.0171	0 0 0 0 0	1.0	0 0 0 0 0 0
51	52	1	1	1	0	0.0203	0.0588	0.0070	0 0 0 0 0	1.0	0 0 0 0 0 0
52	53	1	1	1	0	0.0405	0.1635	0.0203	0 0 0 0 0	1.0	0 0 0 0 0 0
53	54	1	1	1	0	0.0263	0.1220	0.0155	0 0 0 0 0	1.0	0 0 0 0 0 0
49	54	1	1	1	0	0.0730	0.2890	0.0369	0 0 0 0 0	1.0	0 0 0 0 0 0
49	54	1	1	1	0	0.0869	0.2910	0.0365	0 0 0 0 0	1.0	0 0 0 0 0 0
54	55	1	1	1	0	0.0169	0.0707	0.0101	0 0 0 0 0	1.0	0 0 0 0 0 0
54	56	1	1	1	0	0.0027	0.0096	0.0037	0 0 0 0 0	1.0	0 0 0 0 0 0
55	56	1	1	1	0	0.0049	0.0151	0.0019	0 0 0 0 0	1.0	0 0 0 0 0 0

56	57	1	1	1	0	0.0343	0.0966	0.0121	0 0 0 0 0 1.0 0 0 0 0 0 0
50	57	1	1	1	0	0.0474	0.1340	0.0166	0 0 0 0 0 1.0 0 0 0 0 0 0
56	58	1	1	1	0	0.0343	0.0966	0.0121	0 0 0 0 0 1.0 0 0 0 0 0 0
51	58	1	1	1	0	0.0255	0.0719	0.0089	0 0 0 0 0 1.0 0 0 0 0 0 0
54	59	1	1	1	0	0.0503	0.2293	0.0299	0 0 0 0 0 1.0 0 0 0 0 0 0
56	59	1	1	1	0	0.0825	0.2510	0.0284	0 0 0 0 0 1.0 0 0 0 0 0 0
56	59	1	1	1	0	0.0803	0.2390	0.0268	0 0 0 0 0 1.0 0 0 0 0 0 0
55	59	1	1	1	0	0.0474	0.2158	0.0282	0 0 0 0 0 1.0 0 0 0 0 0 0
59	60	1	1	1	0	0.0317	0.1450	0.0188	0 0 0 0 0 1.0 0 0 0 0 0 0
59	61	1	1	1	0	0.0328	0.1500	0.0194	0 0 0 0 0 1.0 0 0 0 0 0 0
60	61	1	1	1	0	0.0026	0.0135	0.0073	0 0 0 0 0 1.0 0 0 0 0 0 0
60	62	1	1	1	0	0.0123	0.0561	0.0073	0 0 0 0 0 1.0 0 0 0 0 0 0
61	62	1	1	1	0	0.0082	0.0376	0.0049	0 0 0 0 0 1.0 0 0 0 0 0 0
63	59	1	1	1	0	0.0000	0.0386	0.0000	0 0 0 0 0 0.96 0 0 0 0 0 0
63	64	1	1	1	0	0.0017	0.0200	0.1080	0 0 0 0 0 1.0 0 0 0 0 0 0
64	61	1	1	1	0	0.0000	0.0268	0.0000	0 0 0 0 0 0.985 0 0 0 0 0 0
38	65	1	1	1	0	0.0090	0.0986	0.5230	0 0 0 0 0 1.0 0 0 0 0 0 0
64	65	1	1	1	0	0.0027	0.0302	0.1900	0 0 0 0 0 1.0 0 0 0 0 0 0
49	66	1	1	1	0	0.0180	0.0919	0.0124	0 0 0 0 0 1.0 0 0 0 0 0 0
49	66	1	1	1	0	0.0180	0.0919	0.0124	0 0 0 0 0 1.0 0 0 0 0 0 0
62	66	1	1	1	0	0.0482	0.2180	0.0289	0 0 0 0 0 1.0 0 0 0 0 0 0
62	67	1	1	1	0	0.0258	0.1170	0.0155	0 0 0 0 0 1.0 0 0 0 0 0 0
65	66	1	1	1	0	0.0000	0.0370	0.0000	0 0 0 0 0 0.935 0 0 0 0 0 0
66	67	1	1	1	0	0.0224	0.1015	0.0134	0 0 0 0 0 1.0 0 0 0 0 0 0
65	68	1	1	1	0	0.0014	0.0160	0.3190	0 0 0 0 0 1.0 0 0 0 0 0 0
47	69	1	1	1	0	0.0844	0.2778	0.0355	0 0 0 0 0 1.0 0 0 0 0 0 0
49	69	1	1	1	0	0.0985	0.3240	0.0414	0 0 0 0 0 1.0 0 0 0 0 0 0
68	69	1	1	1	0	0.0000	0.0370	0.0000	0 0 0 0 0 0.935 0 0 0 0 0 0
69	70	1	1	1	0	0.0300	0.1270	0.0610	0 0 0 0 0 1.0 0 0 0 0 0 0
24	70	1	1	1	0	0.1022	0.4115	0.0510	0 0 0 0 0 1.0 0 0 0 0 0 0
70	71	1	1	1	0	0.00882	0.03550	0.00439	0 0 0 0 0 1.0 0 0 0 0 0 0
24	72	1	1	1	0	0.04880	0.19600	0.02440	0 0 0 0 0 1.0 0 0 0 0 0 0
71	72	1	1	1	0	0.04460	0.18000	0.02222	0 0 0 0 0 1.0 0 0 0 0 0 0
71	73	1	1	1	0	0.00866	0.04540	0.00589	0 0 0 0 0 1.0 0 0 0 0 0 0
70	74	1	1	1	0	0.04010	0.13230	0.01684	0 0 0 0 0 1.0 0 0 0 0 0 0
70	75	1	1	1	0	0.04280	0.14100	0.01800	0 0 0 0 0 1.0 0 0 0 0 0 0
69	75	1	1	1	0	0.04050	0.12200	0.06200	0 0 0 0 0 1.0 0 0 0 0 0 0
74	75	1	1	1	0	0.01230	0.04060	0.00517	0 0 0 0 0 1.0 0 0 0 0 0 0
76	77	1	1	1	0	0.04440	0.14800	0.01840	0 0 0 0 0 1.0 0 0 0 0 0 0
69	77	1	1	1	0	0.03090	0.10100	0.05190	0 0 0 0 0 1.0 0 0 0 0 0 0
75	77	1	1	1	0	0.06010	0.19990	0.02489	0 0 0 0 0 1.0 0 0 0 0 0 0

77	78	1	1	1	0	0.00376	0.01240	0.00632	0 0 0 0 0	1.0	0 0 0 0 0 0
78	79	1	1	1	0	0.00546	0.02440	0.00324	0 0 0 0 0	1.0	0 0 0 0 0 0
77	80	1	1	1	0	0.01700	0.04850	0.02360	0 0 0 0 0	1.0	0 0 0 0 0 0
77	80	1	1	1	0	0.02940	0.10500	0.01140	0 0 0 0 0	1.0	0 0 0 0 0 0
79	80	1	1	1	0	0.01560	0.07040	0.00935	0 0 0 0 0	1.0	0 0 0 0 0 0
68	81	1	1	1	0	0.00175	0.02020	0.40400	0 0 0 0 0	1.0	0 0 0 0 0 0
81	80	1	1	1	0	0.00000	0.03700	0.00000	0 0 0 0 0	0.935	0 0 0 0 0 0
77	82	1	1	1	0	0.02980	0.08530	0.04087	0 0 0 0 0	1.0	0 0 0 0 0 0
82	83	1	1	1	0	0.01120	0.03665	0.01898	0 0 0 0 0	1.0	0 0 0 0 0 0
83	84	1	1	1	0	0.06250	0.13200	0.01290	0 0 0 0 0	1.0	0 0 0 0 0 0
83	85	1	1	1	0	0.04300	0.14800	0.01740	0 0 0 0 0	1.0	0 0 0 0 0 0
84	85	1	1	1	0	0.03020	0.06410	0.00617	0 0 0 0 0	1.0	0 0 0 0 0 0
85	86	1	1	1	0	0.03500	0.12300	0.01380	0 0 0 0 0	1.0	0 0 0 0 0 0
86	87	1	1	1	0	0.02828	0.20740	0.02250	0 0 0 0 0	1.0	0 0 0 0 0 0
85	88	1	1	1	0	0.02000	0.10200	0.01380	0 0 0 0 0	1.0	0 0 0 0 0 0
85	89	1	1	1	0	0.02390	0.17300	0.02350	0 0 0 0 0	1.0	0 0 0 0 0 0
88	89	1	1	1	0	0.01390	0.07120	0.00967	0 0 0 0 0	1.0	0 0 0 0 0 0
89	90	1	1	1	0	0.05180	0.18800	0.02640	0 0 0 0 0	1.0	0 0 0 0 0 0
89	90	1	1	1	0	0.02380	0.09970	0.05300	0 0 0 0 0	1.0	0 0 0 0 0 0
91	90	1	1	1	0	0.02540	0.08360	0.01070	0 0 0 0 0	1.0	0 0 0 0 0 0
89	92	1	1	1	0	0.00990	0.05050	0.02740	0 0 0 0 0	1.0	0 0 0 0 0 0
89	92	1	1	1	0	0.03930	0.15810	0.02070	0 0 0 0 0	1.0	0 0 0 0 0 0
91	92	1	1	1	0	0.03870	0.12720	0.01634	0 0 0 0 0	1.0	0 0 0 0 0 0
92	93	1	1	1	0	0.02580	0.08480	0.01090	0 0 0 0 0	1.0	0 0 0 0 0 0
92	94	1	1	1	0	0.04810	0.15800	0.02030	0 0 0 0 0	1.0	0 0 0 0 0 0
93	94	1	1	1	0	0.02230	0.07320	0.00938	0 0 0 0 0	1.0	0 0 0 0 0 0
94	95	1	1	1	0	0.01320	0.04340	0.00555	0 0 0 0 0	1.0	0 0 0 0 0 0
80	96	1	1	1	0	0.03560	0.18200	0.02470	0 0 0 0 0	1.0	0 0 0 0 0 0
82	96	1	1	1	0	0.01620	0.05300	0.02720	0 0 0 0 0	1.0	0 0 0 0 0 0
94	96	1	1	1	0	0.02690	0.08690	0.01150	0 0 0 0 0	1.0	0 0 0 0 0 0
80	97	1	1	1	0	0.01830	0.09340	0.01270	0 0 0 0 0	1.0	0 0 0 0 0 0
80	98	1	1	1	0	0.02380	0.10800	0.01430	0 0 0 0 0	1.0	0 0 0 0 0 0
80	99	1	1	1	0	0.04540	0.20600	0.02730	0 0 0 0 0	1.0	0 0 0 0 0 0
92	100	1	1	1	0	0.06480	0.29500	0.03860	0 0 0 0 0	1.0	0 0 0 0 0 0
94	100	1	1	1	0	0.01780	0.05800	0.03020	0 0 0 0 0	1.0	0 0 0 0 0 0
95	96	1	1	1	0	0.01710	0.05470	0.00737	0 0 0 0 0	1.0	0 0 0 0 0 0
96	97	1	1	1	0	0.01730	0.08850	0.01200	0 0 0 0 0	1.0	0 0 0 0 0 0
98	100	1	1	1	0	0.03970	0.17900	0.02380	0 0 0 0 0	1.0	0 0 0 0 0 0
99	100	1	1	1	0	0.01800	0.08130	0.01080	0 0 0 0 0	1.0	0 0 0 0 0 0
100	101	1	1	1	0	0.02770	0.12620	0.01640	0 0 0 0 0	1.0	0 0 0 0 0 0
92	102	1	1	1	0	0.01230	0.05590	0.00732	0 0 0 0 0	1.0	0 0 0 0 0 0

```
  101  102  1 1 1 0 0.02460  0.11200 0.01470  0 0 0 0 0 1.0   0 0 0 0 0 0
  100  103  1 1 1 0 0.01600  0.05250 0.02680  0 0 0 0 0 1.0   0 0 0 0 0 0
  100  104  1 1 1 0 0.04510  0.20400 0.02705  0 0 0 0 0 1.0   0 0 0 0 0 0
  103  104  1 1 1 0 0.04660  0.15840 0.02035  0 0 0 0 0 1.0   0 0 0 0 0 0
  103  105  1 1 1 0 0.05350  0.16250 0.02040  0 0 0 0 0 1.0   0 0 0 0 0 0
  100  106  1 1 1 0 0.06050  0.22900 0.03100  0 0 0 0 0 1.0   0 0 0 0 0 0
  104  105  1 1 1 0 0.00994  0.03780 0.00493  0 0 0 0 0 1.0   0 0 0 0 0 0
  105  106  1 1 1 0 0.01400  0.05470 0.00717  0 0 0 0 0 1.0   0 0 0 0 0 0
  105  107  1 1 1 0 0.05300  0.18300 0.02360  0 0 0 0 0 1.0   0 0 0 0 0 0
  105  108  1 1 1 0 0.02610  0.07030 0.00922  0 0 0 0 0 1.0   0 0 0 0 0 0
  106  107  1 1 1 0 0.05300  0.18300 0.02360  0 0 0 0 0 1.0   0 0 0 0 0 0
  108  109  1 1 1 0 0.01050  0.02880 0.00380  0 0 0 0 0 1.0   0 0 0 0 0 0
  103  110  1 1 1 0 0.03906  0.18130 0.02305  0 0 0 0 0 1.0   0 0 0 0 0 0
  109  110  1 1 1 0 0.02780  0.07620 0.01010  0 0 0 0 0 1.0   0 0 0 0 0 0
  110  111  1 1 1 0 0.02200  0.07550 0.01000  0 0 0 0 0 1.0   0 0 0 0 0 0
  110  112  1 1 1 0 0.02470  0.06400 0.03100  0 0 0 0 0 1.0   0 0 0 0 0 0
   17  113  1 1 1 0 0.00913  0.03010 0.00384  0 0 0 0 0 1.0   0 0 0 0 0 0
   32  113  1 1 1 0 0.06150  0.20300 0.02590  0 0 0 0 0 1.0   0 0 0 0 0 0
   32  114  1 1 1 0 0.01350  0.06120 0.00814  0 0 0 0 0 1.0   0 0 0 0 0 0
   27  115  1 1 1 0 0.01640  0.07410 0.00986  0 0 0 0 0 1.0   0 0 0 0 0 0
  114  115  1 1 1 0 0.00230  0.01040 0.00138  0 0 0 0 0 1.0   0 0 0 0 0 0
   68  116  1 1 1 0 0.00034  0.00405 0.08200  0 0 0 0 0 1.0   0 0 0 0 0 0
   12  117  1 1 1 0 0.03290  0.14000 0.01790  0 0 0 0 0 1.0   0 0 0 0 0 0
   75  118  1 1 1 0 0.01450  0.04810 0.00599  0 0 0 0 0 1.0   0 0 0 0 0 0
   76  118  1 1 1 0 0.01640  0.05440 0.00678  0 0 0 0 0 1.0   0 0 0 0 0 0
-999
INTERCHANGE DATA FOLLOWS          4 ITEMS
 1 1 -610.07 1.0
 2 0  0   1.0
-999
TIE LINES FOLLOW                  65 ITEMS

 69  2  47  1  1
 69  2  49  1  1
 69  2  68  1  1
 69  2  70  1  1
 69  2  75  1  1
 69  2  77  1  1
-999
END OF DATA
```

This generator participation factors used in this thesis are

Gen. #	Relative Participation	Gen. #	Relative Participation
1	5	4	3
6	5	8	12
12	5	15	8
18	6	19	5
24	2	27	6
31	4	32	6
34	6	36	3
40	2	42	4
46	3	49	4
54	5	55	6
59	10	62	7
70	6	72	1
73	1	74	7
76	7	77	6
85	3	87	1
90	8	91	1
92	7	99	5
104	4	105	3
110	4	112	5
113	1		

This generator participation factors used in this thesis are

Gen. #	Relative Participation	Gen. #	Relative Participation
1	5	4	3
6	5	8	12
12	5	15	8
18	6	19	5
24	2	27	6
31	4	32	6
34	6	36	3
40	2	42	4
46	3	49	4
54	5	55	6
59	10	62	7
70	6	72	1
73	1	74	7
76	7	77	6
85	3	87	1
90	8	91	1
92	7	99	5
104	4	105	3
110	4	112	5
113	1		

Appendix B

This appendix contains a derivation of the closed form expression for calculating the two solutions of the voltage at bus i when all other bus voltages are assumed fixed. Starting with the power flow equations at each bus in rectangular coordinates:

$$P_i = \sum_{j=1}^{n} \{ e_i (e_j G_{ij} - f_j B_{ij}) + f_i (f_j G_{ij} + e_j B_{ij}) \} \quad \text{(B-1)}$$

$$Q_i = \sum_{j=1}^{n} \{ f_i (e_j G_{ij} - f_j B_{ij}) - e_i (f_j G_{ij} + e_j B_{ij}) \} \quad \text{(B-2)}$$

rearranging terms the equations can be rewritten as

$$P_i = G_{ii} (e_i^2 + f_i^2) + e_i C + f_i D \quad \text{(B-3)}$$

$$Q_i = -B_{ii} (e_i^2 + f_i^2) + f_i C - e_i D \quad \text{(B-4)}$$

where

$$C = \sum_{j=1\ j\neq i}^{n} (e_j G_{ij} - f_j B_{ij})$$

$$D = \sum_{j=1\ j\neq i}^{n} (f_j G_{ij} + e_j B_{ij})$$

Multiplying (B-3) by B_{ii} and (B-4) by G_{ii}

$$P_i B_{ii} = B_{ii} G_{ii} (e_i^2 + f_i^2) + e_i B_{ii} C + f_i B_{ii} D \quad \text{(B-5)}$$

$$Q_i G_{ii} = -B_{ii} G_{ii} (e_i^2 + f_i^2) + f_i G_{ii} C - e_i G_{ii} D \quad \text{(B-6)}$$

Summing (B-5) and (B-6) and then solving for f_i we get

$$P_i B_{ii} + Q_i G_{ii} = e_i B_{ii} C + f_i B_{ii} D + f_i G_{ii} C - e_i G_{ii} D \quad \text{(B-7)}$$

$$f_i = \alpha e_i + \beta \quad \text{(B-8)}$$

$$\alpha = \frac{G_{ii} D - B_{ii} C}{B_{ii} D + G_{ii} C}$$

$$\beta = \frac{P_i B_{ii} + Q_i G_{ii}}{B_{ii} D + G_{ii} C}$$

Substituting (B-7) into (B-3) to eliminate f_i, it can be rewritten as

$$P_i = G_{ii} \{(1 + \alpha^2) e_i^2 + 2\alpha\beta e_i + \beta^2\} + e_i C + (\alpha e_i + \beta) D \quad \text{(B-9)}$$

$$0 = G_{ii}(1 + \alpha^2) e_i^2 + (2\alpha\beta G_{ii} + C + \alpha D) e_i + (\beta^2 G_{ii} + \beta D - P_i) \quad \text{(B-10)}$$

The two voltage solutions can then be determined by solving for e_i using the quadratic formula and using (B-8) to solve for f_i.